Engineering Critical Assessment for girth welds in reeled pipeline

Development of a probabilistic methodology

S.Butter

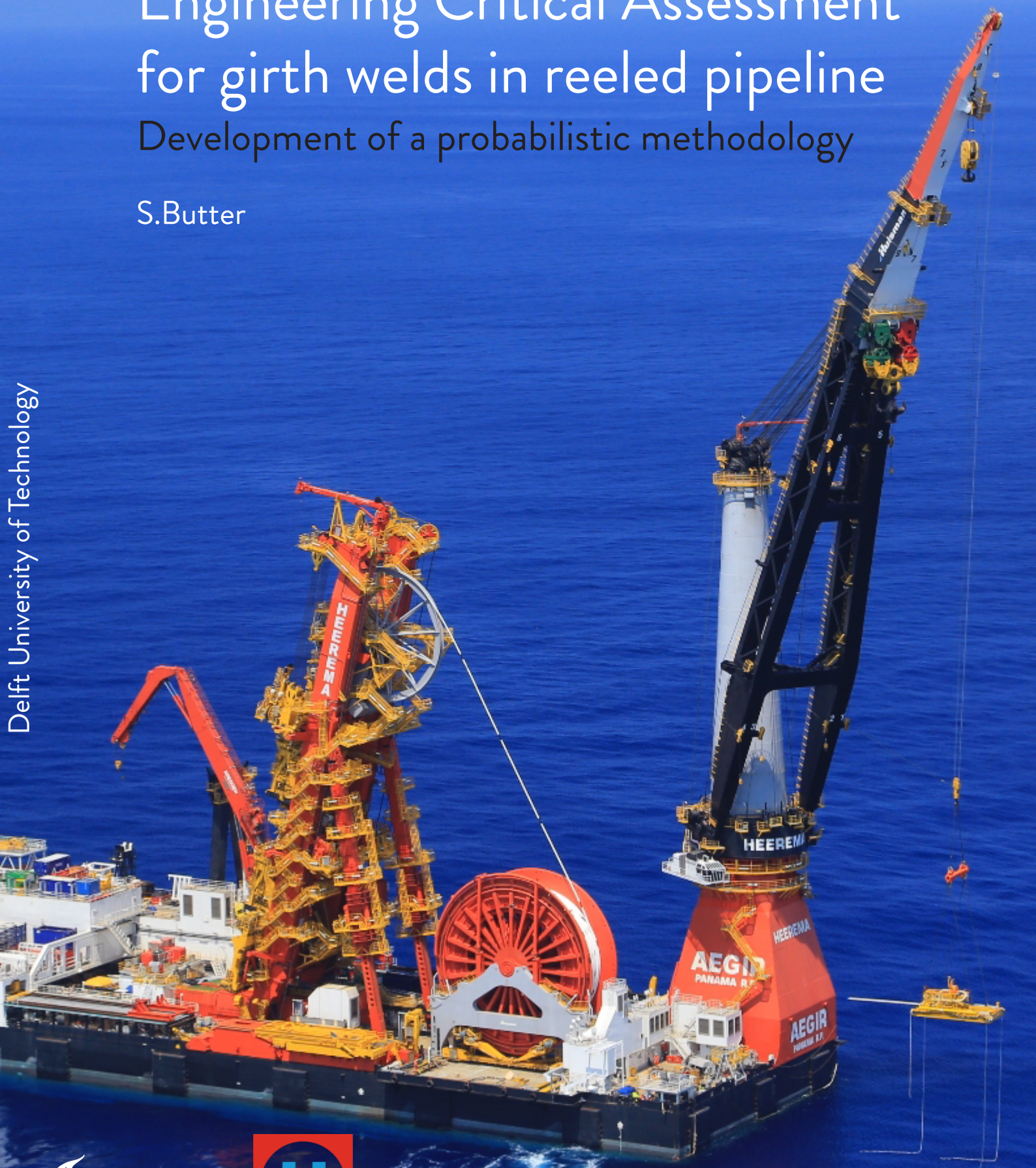

Delft University of Technology

TU Delft

MARINE CONTRACTORS

Master thesis

Development of a probabilistic ECA methodology for girth welds in reeled pipeline

by

S. Butter

to obtain the degree of Master of Science

at the Delft University of Technology,

Student number:	4080173	
Project duration:	April 1, 2017 – March 7, 2018	
Thesis committee:	Prof. Dr. Ir. S.N. Jonkman,	TU Delft, Chairman
	Ir. E.J.C. Dupuits,	TU Delft, Daily supervisor
	Dr. Ir. H. Hendrikse,	TU Delft, Offshore department
	Dr. Ir. E. Karjadi,	Heerema Marine Contractors,Senior supervisor
	Ir. T. Balder,	Heerema Marine Contractors,Daily supervisor

This thesis is under embargo and cannot be made public until 07-03-2023

An electronic version of this thesis will be available at `http://repository.tudelft.nl/`.

MARINE CONTRACTORS

TU Delft

Preface

Dear reader,

In your hands you find the thesis I have written over the course of 11 months during my graduation internship at Heerema Marine contractors. With this thesis I will obtain the title Master of Science and graduate from the Delft University of Technology.

The last couple of months have been an interesting time with it's ups and downs, but always with the support of family and friends that will help you to succeed and provide energy when its at a low. I would like to express my gratitude towards all people involved in my research at Heerema Marine Contractors and the University. In special I would like to thank Erwan and Thomas who were involved on a weekly basis and always showed interest to new findings and the eventual problems. Also I would like to thank Guy who helped me refine my thesis and think along during the research, your feedback was much appreciated.

This thesis does not only conclude my graduation research, but also my career as a student. Looking back at the past 8 years I have a great feeling of joy and pride, now it's time to make the next step.

S. Butter
Delft, March 2018

The emotional journey of creating anything great - Heerema Office poster

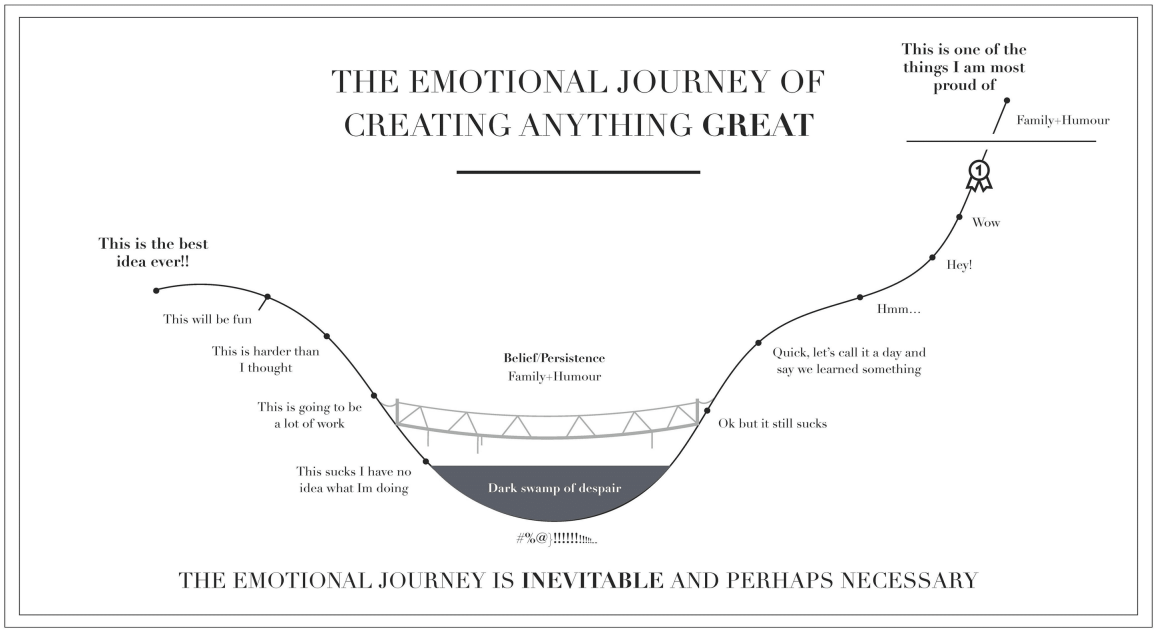

Abstract

Pipe laying projects are getting more challenging due to increasing operational depth of pipeline. The increasing depth requires more of the strength and load bearing capability of the pipeline and its girth welds. The assessment method used for checking the integrity of flaws in girth welds is called Engineering Critical Assessment (ECA) and is based on fracture mechanics (FM) formulas. A complete ECA covers both static and fatigue loading encountered over the multiple phases of the pipe laying process. The current ECA methodology for both static and fatigue load produces strict requirements that may cause unnecessary repairs of the girth welds. From within the industry it is now wondered if ECA produces (over) conservative results.

In earlier research performed within the industry it was already found that on a project specific basis the ECA for fatigue (cyclic) loading was indeed conservative (Macia et al.,2009 and Wang et al., 2015). Where normally a life safety-factor of 5 was applied which was based on engineering experience, it was found that a safety factor between 1.23 and 1.5 could already be sufficient to provide a safe design. This thesis will explore possible conservatism for the static loading ECA, the current methodology of the static ECA will be studied and a reliability based ECA methodology for external flaws under static loading will be proposed to determine the weld assessment criteria (NDT criteria). The NDT criteria are used as threshold when scanning the pipeline for defects, any flaw larger than the NDT criteria will be rejected and the section that contains the flaw will undergo repair.

The current static ECA methodology uses a worst case (deterministic) load scenario as input to determine the maximum allowable initial flaw depth (MAIF) of a girth weld which is then directly used as NDT criterion for that specific pipeline project. The proposed methodology in this research uses a reliability based approach where the probability of failure (PoF) of the pipeline/girth welds is governing in order to determine the NDT criteria. By (conservatively) assuming girth welds in a pipeline form an independent series system, the required PoF of the pipeline (10^{-4}) can be converted to the individual required PoF of a girth weld (10^{-8}). This together with stochastic input variables provides the required information to determine the NDT criterion based on the required PoF of the pipeline.

By performing a sensitivity analysis on the fracture mechanics formulas the yield strength(YS), ultimate tensile strength(UTS) and toughness were found to be the most sensitive variables towards crack growth and are therefore used as stochastic input for the two models developed in this research. In order to provide dependency between YS/UTS data points a copula is used, while the toughness is considered to be independent from the YS/UTS. The first model uses a Monte Carlo (MC) simulation and an iterative fracture mechanics solver in order to determine (per cycle) the MAIF of a girth weld. The distribution of the MAIF represents the resistance of the limit state function of model 1, while the flaw size distribution of the possible flaw present represents the loading. Solving the limit state function which is bound by the NDT criteria provides all information to construct the probability of failure curve of a single girth weld, in which the PoF versus NDT criterion can be found.

The second model uses a more implicit method of calculating the PoF of a single girth weld, since in every MC cycle already an initial flaw size is included as input together with the earlier determined stochastic variables. Each cycle determines if the flaw growth resulting from the initial flaw is stable and within predetermined limits. If a flaw is rejected (i.e. does not meet the criteria) the flaw size is stored, this together with the known number of cycles

provides the information to construct the PoF vs NDT criteria curve. By making use of importance sampling the computational time of model 2 can be sped up. Since model 2 does not have to assume/fit a distribution on the MAIF in order to determine the PoF of a girth weld, the results may turn out to be more accurate and can also be used to validate model 1.

The available data to determine the best probability density functions (PDFs) of the stochastic variables used in the reliability based approach is limited, introducing uncertainty in the accuracy of the results. However when using the limited data the two models already provide NDT criteria in the range of 5.05mm-5.20mm, while the deterministic approach dictates a NDT criteria of 4.45mm. A difference of 0.55mm-0.75mm is substantial in terms flaw assessment criteria. Experts on welding and flaw assessment within HMC estimate the impact of the increase in NDT criterion to result in one less offshore shift of 12 hours, potentially saving up to hundred of thousands of Euros.

From the research performed it may be concluded it is possible to provide NDT criteria on basis of a probabilistic ECA, it is found the current ECA for static loading on external weld flaws might indeed be conservative. Therefore using a probabilistic approach towards ECA for both static and fatigue loading can benefit future projects by reducing repairs and cost.

keywords: Engineering Critical Assessment (ECA), Optimization, Monte Carlo simulation, Flaw assessment, Probabilistic design, Copula, NDT criteria, Reeling, Importance Sampling

Contents

1 Introduction **3**

1.1 Background . . . 3

1.1.1 Company profile . . . 4

1.2 Pipe laying process . . . 4

1.3 Welding . . . 5

1.4 Types of flaws and their dimensions . . . 6

1.5 Non destructive testing . . . 8

1.6 Pipe loading and failure . . . 9

1.7 Flaw assessment . . . 10

2 Research Description **13**

2.1 Research objective . . . 13

2.2 Research question . . . 14

2.3 Scope of research . . . 14

2.4 Load case . . . 15

2.4.1 Typical pipe laying project . . . 16

2.4.2 Ichthys ECA results . . . 16

2.5 Research methodology . . . 17

2.6 Thesis structure . . . 18

3 Current methods for assessing weld flaws **19**

3.1 Engineering critical assessment . . . 19

3.1.1 Main variables . . . 20

3.1.2 ECA flowchart . . . 20

3.2 Stresses in pipeline . . . 21

3.2.1 Constructing stress-strain diagrams (Ramberg-Osgood approach) . . . 22

3.2.2 Primary and secondary stress . . . 23

3.2.3 Stress input per phase . . . 24

3.3 Assessment of fracture resistance . . . 25
3.3.1 Failure Assessment Diagram . . . 25
3.3.2 Failure assessment curve . . . 25
3.3.3 Flaw assessment point . . . 27
3.4 Assessment for fatigue . . . 29
3.4.1 Paris Law . . . 29
3.4.2 S-N curve approach . . . 30
3.5 Limitations in the current methodology . . . 31
3.6 Conservatism in current methodology . . . 31
3.6.1 Conservatism-Static Fracture Mechanics . . . 32
3.6.2 Conservatism-Fatigue assessment . . . 32
3.6.3 General conservative assumptions . . . 33
3.7 ECA software available . . . 33
3.7.1 FlawPRO . . . 34
3.7.2 Crackwise . . . 34
3.7.3 Preference . . . 34

4 Probabilistic theory and literature research 35

4.1 Probabilistic assessment . . . 35
4.2 Evaluation of the probability of failure . . . 36
4.3 Reliability analysis levels . . . 36
4.4 Research performed within the industry . . . 37
4.4.1 SN curve approach toward fatigue design . . . 38
4.4.2 Fatigue life models-FM Approach . . . 39
4.4.3 Reliability matching of SN and FM method . . . 39

5 Probabilistic model 43

5.1 Assumptions . . . 43
5.2 Aim and functionality of the models . . . 44
5.2.1 Input of models . . . 46
5.2.2 Model 1 . . . 46
5.2.3 Model 2 . . . 52

5.3 Sensitivity analysis . . . 55
5.4 Variable distributions . . . 55
5.4.1 HMC pipeline data base . . . 56
5.4.2 Bayesian Information Criterion . . . 57
5.4.3 Distributions . . . 57
5.4.4 Correlation between variables . . . 61
5.4.5 Copula . . . 62
5.4.6 Initial flaw distribution . . . 66
5.5 Fracture mechanics model verification . . . 67
5.6 Reliability of a pipeline system . . . 69
5.6.1 Type of system . . . 69
5.6.2 Probability of failure-Series system . . . 69
5.6.3 Industry standards . . . 71

6 Results **75**

6.1 Deterministic (reference) case . . . 75
6.2 Post processing . . . 76
6.2.1 Amount of girth welds . . . 77
6.2.2 Number of external flaws . . . 77
6.2.3 Post processing of model output . . . 78
6.2.4 Required PoF of single girth weld . . . 78
6.3 Model 1 results . . . 79
6.3.1 Sensitivity analysis on PoF of a girth weld . . . 81
6.4 Model 2 results . . . 85
6.4.1 Importance sampling domain . . . 85
6.5 Discussion of Results . . . 87
6.5.1 Expert opinion on new NDT criterion . . . 88

7 Conclusion and recommendations **89**

7.1 Conclusion . . . 89
7.2 Recommendations . . . 90

A Failure assessment curves **93**

A.1 Level 1-Failure assessment curve . . . 93

A.2 Level 2-Failure assessment curve . . . 94

A.3 Level 3-Failure assessment curve . . . 94

A.4 Flaw assessment point . . . 94

A.5 Fatigue assessment . . . 95

B Sensitivity analysis **97**

C Ramberg-Osgood relationship **105**

C.1 Input . . . 105

C.2 Ramberg-Osgood relation . . . 105

C.2.1 Stress-strain diagram with no Lüder plateau . . . 106

C.2.2 Stress-strain diagram with Lüder plateau . . . 106

D Copulas **107**

Bibliography **109**

List of Figures **111**

List of Tables **115**

Nomenclature

AUT	Automated ultrasonic testing
CDF	Cumulative Distribution Function
DCV	Deep water construction vessel
ECA	Engineering Critical Assessment
FAC	Failure Assessment Curve
FAD	Failure Assessment Diagram
FEA	Finite Element Method
FM	Fracture Mechanics
HAZ	Heat Affected Zone
HMC	Heerema Marine Contractors
JIP	Joint Industry Project
KDE	Kernel Density Estimation
$MAIF$	Maximum Allowable initial Flaw
MC	Monte Carlo
NDT	Non destructive testing
Pb	Primary bending stress
PDF	Probability density function
Pm	Primary membrane stress
PoF	Probability of Failure
ULS	Ultimate Limit State
UTS	Ultimate Tensile Strength
YS	Yield Strength

Part I (Chapters 1 to 4)

Introduction and literature research

1 Introduction

1.1. Background

Oil, (liquid) gas and other resources recovered from offshore oil and gas fields are transported by pipeline to and from oil platforms, ships or facilities onshore. The pipeline network forms the infrastructure needed for the successful depletion of an oil well and therefore forms a key component in the oil field design.

Offshore pipeline are constructed from a number of metal pipes which are welded together on- or offshore depending on the specific pipe-laying method in use (see section1.2). With the enormous oil spill in the Gulf of Mexico of the BP 'Deepwater Horizon' platform still fresh in mind one can imagine safety and reliability is of a high regard in the offshore space to prevent sort like disastrous events from happening. Therefore codes and methods have been developed in order to check the safety and reliability of the (mechanical) systems used in the offshore space.

This thesis will focus on the optimization/development of a method for assessing girth welds (circumferential welds) that connect two pipe sections together. Every girth welds can contain (tiny) production flaws that might form a risk to the integrity of the weld connection. Depending on the location and size of the flaw in the girth weld, unstable growth and failure under brittle rupture/plastic collapse or fatigue due to environmental and operational loading on the pipeline can occur. The consequences of girth weld failure might cause a non-functional or leaking pipeline that is potentially damaging to the environment (oil/gas leakage) and brings high cost to the operator of the pipeline.

Pipe laying projects are getting more challenging due to increasing operational depths of pipeline. The assessment method for assessing the reliability and safety of girth welds on these pipeline remains mainly unchanged. While the increasing depth requires more of the strength and load bearing capability of the pipeline and its girth welds, the current methodology is dictating strict requirements for these projects. Sometimes so strict the weld equipment is not able to fulfill these requirements. From within the industry it is now wondered if the requirements produced by the current assessment method may be too conservative, and therefore might lead to too many unnecessary repairs and higher project costs. [1] [24].

1.1.1. Company profile

This research is carried out in collaboration with Heerema Marine Contractors (HMC). Heerema Marine Contractors is a world leading marine construction company for the oil and gas industry and is specialized in design, transportation, installation and removal of all types of fixed and floating offshore structures, subsea pipelines and infrastructures in shallow and deep water. HMC owns and operates her own fleet including the world's largest semi-submersible crane vessel, a deep water crane and J-lay pipe laying vessel and a deep water construction vessel (DCV) able the lay reeled pipeline.

1.2. Pipe laying process

There are various ways of offshore pipe laying:

- J-Lay
- Reel(R)-Lay
- S-Lay

J-Lay and R-lay are used within Heerema Marine Contractors and therefore of interest for this thesis, more detail on these pipe laying methods is provided below.

1. **J-Lay** J-Lay gets its name from the shape the pipe makes from the vessel to the sea bottom during the lay operation (See figure 1.2). Using the J-lay method pipeline elements are welded together on board of the vessel in several stages, pipe elements are delivered to the vessel as single pipes or as double joints (two pipes pre-welded together onshore). It depends on the vessel in use if the pipes are than further welded together to form quad (four pipes) or hexa joints (six pipes). These pipe segments can then be placed in the vertical J-lay tower on board of the vessel where they will be connected to the already submerged pipeline. Due to the vertical tower substantial lower strains are present on the pipeline and its welds compared to the strain encountered during R-lay or S-Lay.

2. **R-Lay** During the R-lay method reels with onshore reeled pipeline can be unreeled on board of the vessel. The reels are transported from and to the vessel in order to optimize the process of replacing a reel when it runs out of pipe. Although replacing the reel on the ship can take up to one day, R-lay is considered to be faster than J-lay. The pipe segments are welded onshore before the complete pipe is reeled on the reel. Onshore welding can be more securely controlled than offshore welding which benefits weld quality. Still Welding offshore has to be performed when a new reel has to be connected to the already submerged pipeline of the previous (now empty) reel. During the reel-on and reel-off process of the pipeline high strains are encountered due to bending of the pipeline over the reel, aligner and straighteners on the vessel. (see figure 1.2).

At the (onshore and offshore) welding station each weld will be scanned by making use of Automated Ultrasonic Testing (AUT) to indicate the presence and size of flaws in the newly made girth weld. If a flaw indicated by AUT exceeds the weld requirements that is set by an industry standard, a weld assessment method or the client, a cutout of the girth weld has to be made in order to re weld and thus repair the pipe connection.

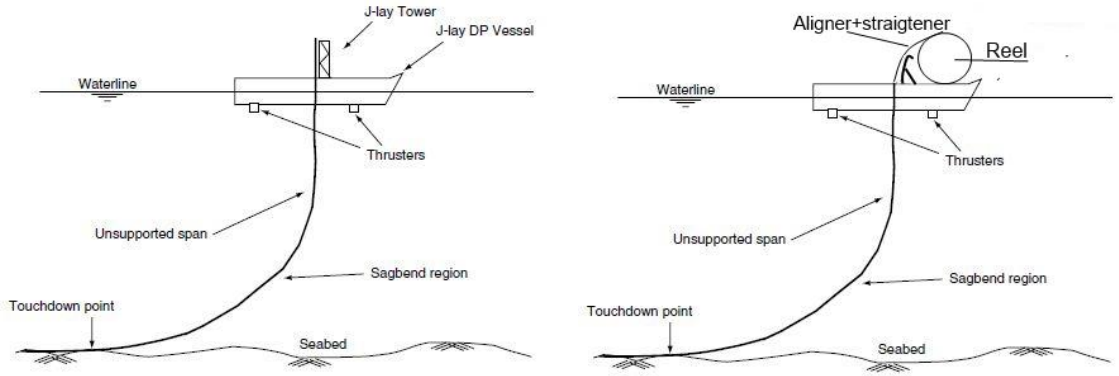

Figure 1.1: J-lay and Reel lay method in a simplified figure

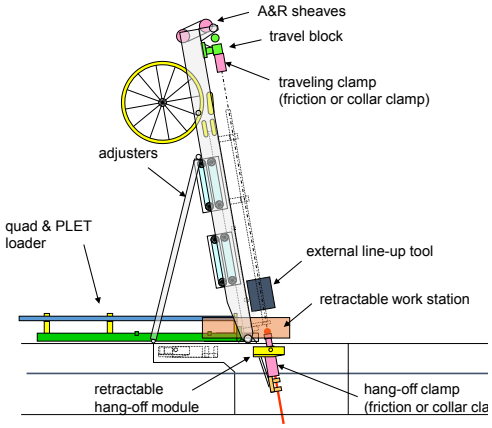

Figure 1.2: J-Lay system on board of a vessel [2]

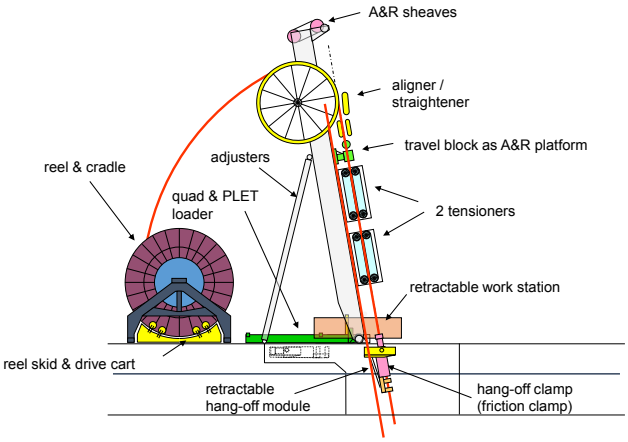

Figure 1.3: Reel lay system on board of a vessel[2]

1.3. Welding

The welding process of onshore/offshore pipeline consists out of multiple stages, the stages mentioned below both account for the J-Lay and the R-Lay method of pipe laying. Using the J-lay method leads to more welds take place on board of the vessel as opposed to R-Lay, where the only welds on board of the vessel are those that connecting the previous spooled pipe to the new spooled pipe.

Welding procedure:

1. Before two pipe sections are welded together a bevel to both pipe ends has to be made (see figure 1.4). The narrow gap created where both pipe ends come together serves as the space that will be filled up with welding material during welding and thus bonding the two pipe ends together
2. Next the pipeline sections need to be aligned, since pipe sections are not exact cylinders and their wall thicknesses are not exactly the same over their circumference aligning can be a time intensive process. The mismatch of the two pipes is called the 'hi/lo' (see figure 1.4) and influences the local bending moments at the location of the weld due to the created eccentricity ([3]). Especially for fatigue sensitive pipes the tolerance for the hi/lo is smaller compared to the hi/lo tolerance of static loaded pipe. The allowable hi/lo

tolerance is lower in order to minimize the local bending effect and thus limit fatigue damage.

3. Once the pipes are aligned the first weld layer (called the weld root) is made by the welding system. The root connects the pipe at the inner surface. Using the root as basis new weld passes are made each adding up to 3mm of material. Welding adds heat to the pipe material changing the material properties in and around the weld, the zone affected by heat is called the heat affected zone (HAZ). The last pass forms the 'Weld cap' of the weld and is located at the outer surface of the pipe (also see figure 1.6 where the root and cap are identified). The welding is done by making use of a process called narrow gap welding, the narrow gap welding system consists out two welding machines called 'bugs' which both carry a welding torch and are attached to a band on the pipeline that guides the bugs during the welding process. Each bug covers 180°of the pipe to connect both pipe elements together (see figure 1.5)

4. The weld is ready to be scanned with automated ultrasonic testing (AUT), a system that uses ultrasonic sound to detect the location and depth and dimension of possible flaws present in the girth weld (see section 1.5). Any flaw detected by AUT that is larger than specified in the weld criteria has to be checked with weld flaw assessment methods (fit-for-purpose testing), the result of this test will specify whether the weld is rejected or accepted. If the weld is accepted the pipe will go to the field coating station, where a protective coating is applied to the pipe to withstand corrosion at the sea bottom. If the flaw is not deemed fit-for-purpose and thus rejected, the girth weld will be cut out and steps 1 to 4 will have to be performed again.

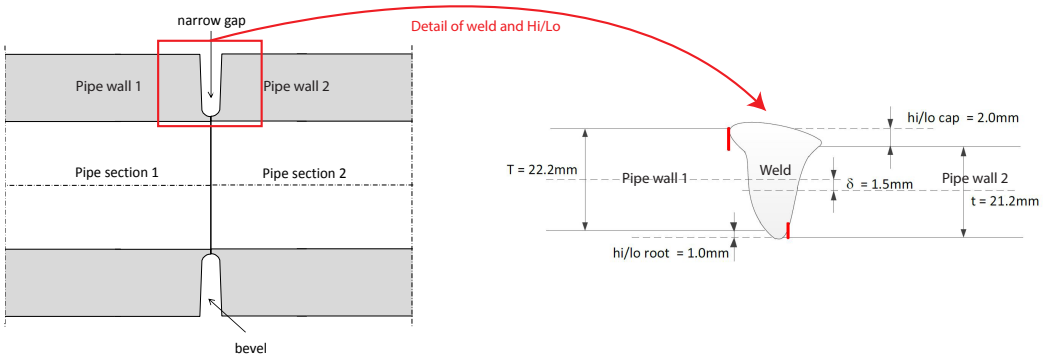

Figure 1.4: Left: Detail of the bevel on two pipe ends[2]; Right: Pipe ends welded together with a mismatch (Hi/Lo present) [2]

1.4. Types of flaws and their dimensions

Several types of (production) flaws may be present in a girth weld of a pipeline. This section will mention the types of flaws and how their dimensions are defined in literature. Depending on the size and location of a flaw, the flaw might form a risk for the pipeline system due to unstable growth till failure. Flaws that are in proximity of each other can also interact, increasing the risk of unstable crack growth [8].

In general the following types of flaws can occur in a narrow weld on different locations in the weld (see figure 1.6):

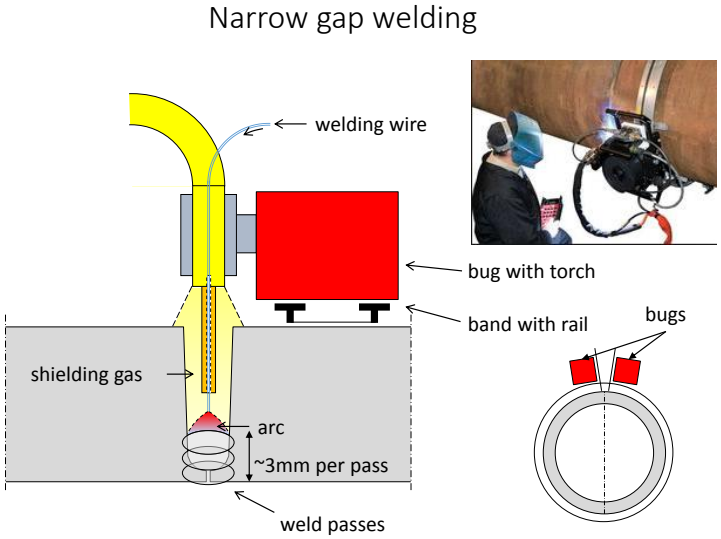

Figure 1.5: Welding system [2]

- Lack of fusion
- Porosity
- Undercut (Incomplete penetration)
- Solidification (slag inclusion)
- Inter-run fusion (incomplete fusion between weld passes)

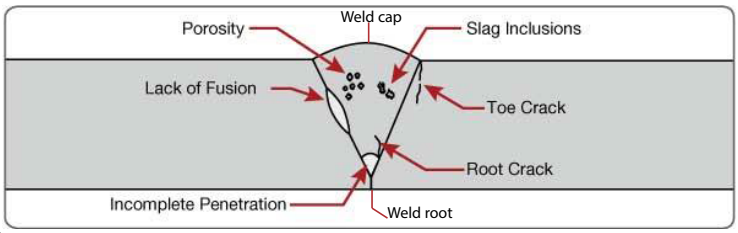

Figure 1.6: Different types of weld flaws[8]

These flaws can occur anywhere in the girth weld while the size, orientation and location with respect to the loading determines the severity of the flaw. Flaws in pipeline can be classified in four categories (figure 1.7a) [3].

- External surface breaking flaw (outer diameter)
- Internal surface breaking flaw (inner diameter)
- Embedded flaw close to outer surface
- Embedded flaw close to inner surface
- Through thickness flaw

The flaw dimensions depend on the category the flaw belongs to. For all cases, the parameter B describes the height of the section where the flaw is present.

For Through thickness flaws:

- $2a$ describes the flaw length
- B describes the section height but also the flaw height since the flaw is through thickness

For surface flaws:

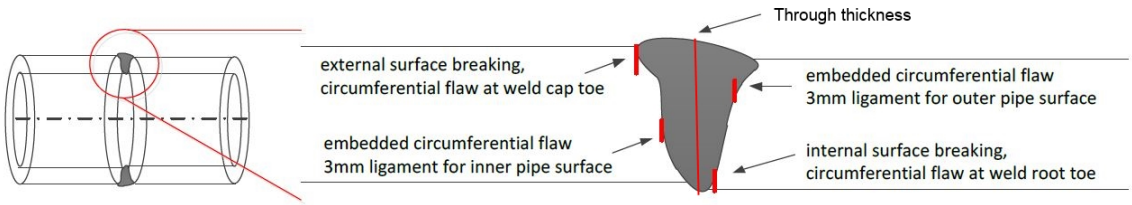

(a) Categories of weld flaws [3]

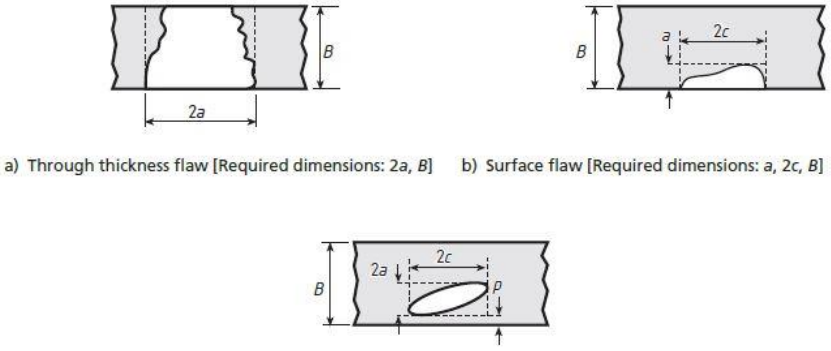

(b) Through thickness flaw, surface breaking flaw or embedded flaw [8]

Figure 1.7: Flaw categories and definition

- a describes the flaw height (i.e. depth)
- $2c$ describes the flaw length
- B describes the section height

For embedded flaws:

- $2a$ describes the flaw height
- $2c$ describes the flaw length
- p describes the ligament which is defined as the length between the surface and flaw edge.

1.5. Non destructive testing

Non destructive testing (NDT) is away of detecting flaws without having to damage the girth weld and thus influence its integrity, NDT is used to collect the following information which can be used to check the verify the integrity of a girth weld:

- Flaw length

- Flaw height
- Flaw position (along the girth weld)
- Flaw (planar) orientation with respect to the principal stress direction

There are several methods available for identifying flaws, not every method is as suitable for girth welds or finding the above mentioned properties.

- Visual inspection (surface flaws only)
- Liquid penetrant (surface flaws only)
- Magnetic particle (only for surface flaws in ferromagnetic materials)
- Eddy current (both surface flaws and embedded flaws)
- Electrical potential drop (both surface flaws and embedded flaws)
- Radiography (both surface flaws and embedded flaws)
- Ultrasonic testing (both surface flaws and embedded flaws)

AUT is most commonly used in the offshore space, this technology uses ultrasonic sound and the reflection of it within the girth weld to detect if possible flaws are present. The assessment method is able to identify the dimensional properties needed in the flaw assessment.

In order to test the weld for defects a band must be placed on the pipeline to guide the AUT machine along the girth weld. The machine will then be moved along this band while ultrasonic sound is send trough the pipe material and the girth weld. A defect can be detected by trained personal from the reflection diagram produced by the AUT machine since it will show up as a distortion in the reflected ultrasonic sound signal. The size, location and amplitude of this abnormality tells the dimensions of the flaw in the girth weld, these dimensions will be used to compare the the minimal weld requirements or as input for the girth weld assessment method to perform a fit-for-purpose assessment.

Before using AUT, the machine has to be calibrated according to the governing offshore codes and demands of the project owner. Besides calibration, the accuracy and minimal detectable flaw size of the machine has to be known in order to correct the found flaw sizes by the accuracy and know from what flaw size on flaws will not be detected anymore. It is important to check if any flaw smaller than the detectable flaw size can lead to failure for the expected load scenarios.

1.6. Pipe loading and failure

Pipelines can fail in several ways under many loading conditions, a pipeline should be able to bear the load without failure. The main loading conditions are shown in figure 1.8 and can occur anywhere in the life time of a pipeline, from the actual pipe laying process to the in-service time and removal.

Figure 1.8 shows a pipeline and its welds can fail in multiple failure modes:

- Spanning: Loads that occur on the pipeline when it 'spans' a hole/crater on the sea bottom, introducing bending loads and fatigue loads due to sea currents on the part of the pipe that spans the hole.

- Fracture/Rapture: This failure mode is of an importance not only for the pipe but also the welds, fracture or rapture occurs when loads on the pipeline/weld can not be withstand by the material of the pipe and weld.
- Fatigue: Cyclic loading on the pipe and weld weakening the material in the process, making the pipeline prone to failure
- Corrosion: Sea watter corrodes the pipe and weld material creating weak spots prone to failure.
- Buckling: High bending loads introduced during pipe installation or removal or spanning make the pipe buckle.

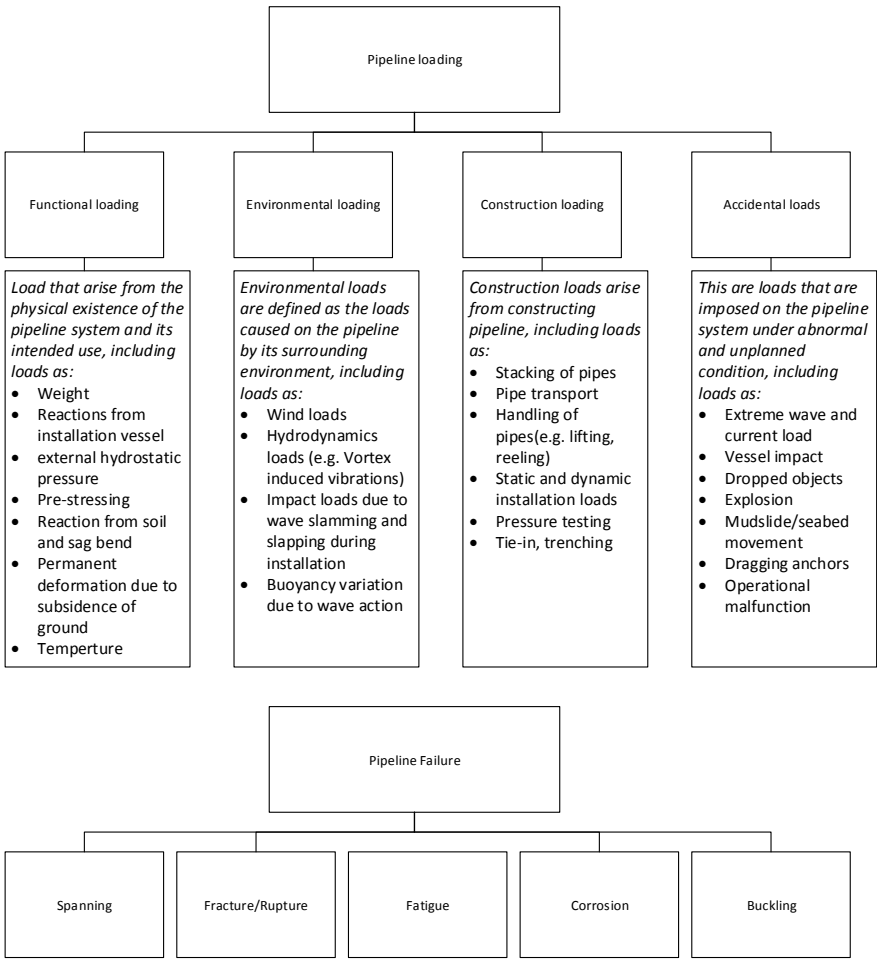

Figure 1.8: Loading on pipeline and failure scenarios

1.7. Flaw assessment

In order to assess flaws in girth welds on their safety, the 'Engineering Critical Assessment' (ECA) method is used. This method can be used on any structure containing flaws prone

to crack growth caused by static or cyclic loading on the structure. ECA is comprised of a collection of fracture mechanics formulas both applicable to static loading (e.g. strain due to reeling) and cyclic loading (e.g. currents flowing over the pipe).

For assessing fatigue failure of flaws an other method is available where use is made of the classical and proven over time stress cycle (SN) curves. This method is deemed proven by time but also conservative in its results.

Both methods will be discussed in more detail in chapter 3.

2

Research Description

This chapter will give an overview on the content and scope of this thesis. Furthermore the load case is introduced on which the probabilistic ECA methodology is tested.

2.1. Research objective

Although precise data is not available it is estimated the average day rate (operation cost per day) of an offshore construction vessel can range in the hundreds of thousands dollars, therefore any (time intensive) unnecessary repairs should be brought to a minimum.

As is mentioned in section 1.1 there is concern the current state-of-the-art methods for assessing flaws in girth welds are producing over conservative results possibly resulting in unnecessary repairs due to dictating a NDT criteria (flaw assessment criteria) that is too strict.

From within the industry it is wondered if the current methods are indeed too conservative and a less conservative model can be developed for assessing flaws in girth welds. This concern is supported by the following quotes.

> *"Variables are usually taken as deterministic values and in most of the cases, the worst case values are chosen to obtain a conservative and safe result. However, the conservatism of this approach can lead to a practical problem, that is, the required weld defect acceptance is too tight which lead to an increase number of rejected welds or the target lifetime of the weld cannot be achieved."[1]*

> *"An ECA is based on conservative data and assumptions. Therefore, it is to be expected that an ECA is conservative."* [3]

> *"The application of deterministic fracture mechanics assessment procedures to the prediction of fit-for-purpose requires the use of data that are often subject to considerable uncertainty. The use of extreme bounding values for the relevant parameters can lead, in some circumstances, to unacceptably over-conservative predictions (i.e. too strict requirements) of structural integrity."* [8]

> *"Engineering critical assessments (ECAs) have increasingly become a routine part of pipeline design to determine tolerable flaw sizes for weld defects. These assessments are now be-*

> *ing applied to pipeline systems in deeper water with increased loadings arising from responses to thermal and pressure cycling. Often these are flowline systems in which fatigue damage is exacerbated by the presence of aggressive internal conditions. In these situations, ECAs can give 'alarming' results, indicating that only very small flaws would be acceptable. In some cases, applying the same methodology to in-service pipelines would suggest that the pipeline should have failed a long time ago, whereas in reality they have not"* [9]

It is expected a less conservative method will lead to a more efficient and optimized pipe laying procedure with less unnecessary repairs needed, thus saving time and cost within the project. Within the industry accepted BS7910:2013 code, and research conducted on one of the pipe line of Exxon mobile [[17]] a strong indicator is present part of the conservatism may be overcome by approaching the assessment of flaws in girth welds in a probabilistic manner e.g. assessing the flaws on basis of stochastic variables instead of worst case (deterministic) values.[8][24]

2.2. Research question

Aiming for a less conservative methodology the following research question can be stated:

> "How to determine the NDT criteria for flaws in girth welds based on a probabilistic analysis of a complete pipeline?"

Raising the following support questions:

- *When should a flaw be repaired?*
- *What factors influences flaw size and growth?*
- *How to use a probabilistic analysis to determined probability of failure of a girth weld/pipeline?*
- *How to quantify acceptable reliability of a pipeline?*
- *How does flaw size influence reliability of a pipeline?*

2.3. Scope of research

The goal of the research conducted in this master thesis is to develop a methodology that is able to determine the flaw assessment criteria on basis of a probabilistic analysis of the pipeline. The scope of the research performed in this thesis will be on reel-lay operations, this method of pipe laying is considered to be more challenging than J-lay as high strains occur in the pipe due too large radius of the reel introducing high strains in the pipe and on the girth welds (see section 1.2).

While quite some research has already been performed on the cyclic (fatigue) loading aspect of ECA (see sources [17] and [24]) possible conservatism in the static load regime is not explored. Also in the first phase a proportional part of the flaw growth takes place under a static load regime (section 2.4.2) which indicates flaw growth under static loading has a large contributions in the overall process of flaw growth. Therefore the first cycle of phase one forms an interesting case to explore possible conservatism in the ECA during static loading

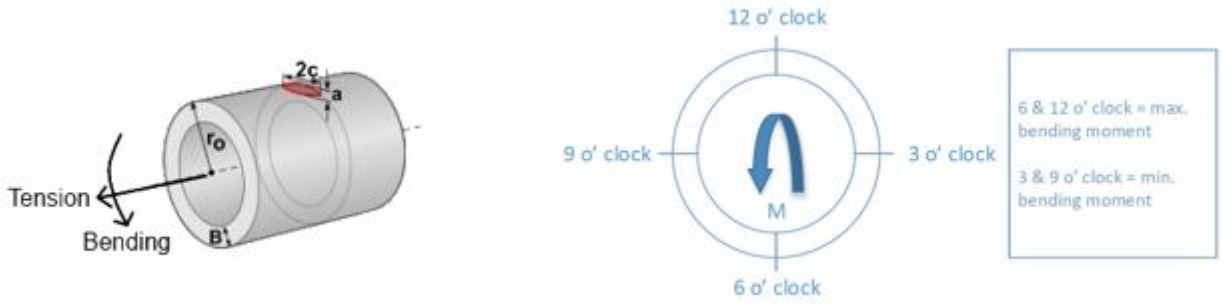

Figure 2.1: Clarification of loading on the pipeline and the critical loading positions

on pipeline (see figure 3.3 in section 3.1.2).

During the first phase the pipe is spooled off, aligned and straightened before entering the water (see figure 1.3). The first cycle (spooling-off) is used to provide the basis for the model development with a focus on external flaws. Any cycles following up the first cycle (e.g. aligning/straightening of the pipe) will make use of the same methodology and fracture mechanics model.

During this research the focus is put on external surface breaking flaws, located at the 12 o' clock position in the pipe (see figure 2.1). While flaws can grow in the radial direction ('a' in figure 2.1) as well as the circumferential direction ('2c' in figure 2.1) during this research flaw length '2c' is assumed to be fixed. The 12 o'clock position is chosen since the flaw will experience the highest bending moment at that location during the reeling process. This assumption is conservative since in reality the pipeline will twist during the reeling process and therefore the most critical flaw in the girth weld will not necessarily be at the most critical location (being the 12'o clock position).

This scope is defined to simplify the already complex relation between material, loading and flaw size in order to provide a proper basis to start on the probabilistic ECA model.

2.4. Load case

As is mentioned in section 1.2 reel lay is considered as the more challenging way of pipe laying due to the high strains endured during the reel on en reel off phase. Therefore a load case resembling this challenging procedure was found in the Ichthys project [18] HMC carried out in the coastal waters of Australia. Within the Ichthys project three pipeline diameters where installed:

- 6" Outer diameter pipeline
- 8" outer diameter pipeline
- 12" Outer diameter pipeline

All three diameters are installed by making use of the R-lay method, regarding the load case chosen for the in this report conducted research the focus will be on the installation of 8" pipeline. For the both the 6" and 8" pipeline an ECA can be conducted by making use of the fracture mechanics FAD method (level 2) as mentioned in above section. For the larger 12" pipeline an ECA is conducted on basis of finite element analysis.

The Ichthys load case can be considered challenging due to the use of three contingency

reeling cycles that should be taken in to account, this brings the total amount of reeling cycles for installing the pipeline to five. The drawback of this load case being is the lack of a full stress histogram for fatigue calculation of the pipeline, only peak stresses encountered during pipe laying and the operational phase are provided.

Several assumptions are made within the Ichthys project regarding ECA:

- The weld is over-matched
- Embedded flaws will be treated as surface flaws
- The 12 O'clock (extrados) position is more critical than the 6 o'clock (intrados) position on the pipeline, and thus is taken as the critical flaw location.
- Neubers approach is used to determine stress from the stress-strain diagram.

During the research it appeared that much of the data from Ichthys was not sufficient enough to base the probabilistic approach on, therefore it has been decided to use comparable material data from other projects as Lucius and Kaombo, however the assumptions made for the Ichthys project are kept the same for this research. Using different data than provided for Ichthys does not influence results, however it does result in output that is not comparable any more to the ECA results mentioned below in section 2.4.2.

2.4.1. Typical pipe laying project

It can be assumed that a typical pipe laying project using R-Lay uses up to three reel drums to complete the project [4]. Knowing the dimensions of the reel used for reeling, the amount of reeves around the reel drum and the total amount of layers can be calculated per reel drum. The reel dimensions of the Aegir (R-lay vessel of HMC) are specified in table 2.1. Each layer

Table 2.1: Reel dimensions on the Aegir (R-lay vessel of HMC)

Reel diameter [min]	Reel diameter [max]	Reel width
16000mm	22000mm	6500mm

of pipe added the reel diameter will increase up until the maximum allowable reel diameter of 22 meter is reached. From the dimensions of the 8" pipe and the reel it can be calculated that 30 reeves per layer are possible. As mentioned above the radius of the reel will increase per pipe layer, and therefor more pipe can be spooled per layer. Taking in to consideration the max allowable reel diameter 15 layers of pipeline can be spooled. This bring the total amount of pipe on the reel to 2247 pipe, the total amount of pipe in a typical project will three times as much (6741 pipe).
In section 6.1 a new deterministic case will be presented based on the current (deterministic) ECA methods using the data gathered from the project mentioned above. This new case will be used during this thesis to compare the probabilistic ECA methodology to.

2.4.2. Ichthys ECA results

In figure 2.2 are the ECA calculation of the Ichthys project done by HMC. The calculations are performed on a 8" pipeline with an initial flaw present of 5.5mmx9.5mm. Per calculations it is indicated in which phase the ECA calculations are performed e.g. during phase one of Ichthys five ECA calculations are performed in order to determine total crack growth during the reeling process. From this it can be concluded that close to 41% of the total crack growth occurring takes place in phase 1 (reeling of the pipeline). Taking in to consideration that both phases 2 and 3 cover by far the largest lifespan of the pipeline(+/-30 years compared to +/- 12hours in phase 1) 41% is quite substantial. Therefore a methodology which is able to

	Flaw			Flaw growth		Final crack		
	a (mm)	2c (mm)	offset (mm)	a (mm)	2c (mm)	a (mm)	2c (mm)	
Initial flaw	5.5	9.5	-	-	-	-	-	
Cycle 1 drum	5.5	9.5	-	0.14	0.28	5.64	9.78	
Cycle 2 aligner	5.64	9.78	-	0.15	0.3	5.79	10.08	
Cycle 3 aligner	5.79	10.08	-	0.16	0.32	5.95	10.4	Phase 1
Cycle 4 drum	5.95	10.4	-	0.18	0.36	6.13	10.76	
Cycle 5 aligner	6.13	10.76	-	0.2	0.4	6.33	11.16	
Fatigue installation	6.33	11.16	-	0.3545	9.144	6.6845	20.304	Phase 2
Fracture installation	6.6845	20.304	Safe					
Fatigue operation	6.6845	20.304	-	0.8588	12.519	7.5433	32.823	Phase 3
Fracture end of operation	7.5433	32.823	Safe					Phase 4

Figure 2.2: ECA calculations of the Ichthys 8" pipeline [13]

provide less conservative weld flaw acceptance criteria for static loading ECA could benefit this first phase of the pipe laying processes.

2.5. Research methodology

In order to develop a probabilistic methodology the current assessment methods will be analyzed and the parameters governing the methods will be identified. Possible alternatives to the current method will be investigated and research will be conducted to the availability of data of relevant parameters.

Once the current method is understood a realistic load case should be identified on which the new methodology can be tested.

Causes of possible conservatism in the current methodology will be identified and methods to overcome this conservatism will be investigated as well. To test the methodology the fracture mechanics formulas needed for ECA will be programmed in Matlab, the probabilistic methods will be later included in this model.

The results produced by the probabilistic method will be analyzed on relevance and impact on the results will be compared to the deterministic approach. Conclusions and recommendations based on the results will be provided on possibly moving to less conservative ECA methods. For a graphical overview of the research methodology see figure 2.3.

2.6. Thesis structure

This section will provide detail on the structure of the thesis and the work flow. The structure of this thesis is split up in three parts as shown in the list below.

- Part 1: Introduction and literature research (Chapters 1 to 4)
  - Ch 1: Chapter one provides an introduction towards the pipe laying operations, welding and non destructive testing, and pipe/girth weld loading
  - Ch 2: Chapter two provides the research objective and scope and methodology
  - Ch 3: Chapter three provides detail on engineering critical assessment
  - Ch 4: Chapter four will go in on literature research and theory required in order to develop the model
- Part 2: Data collection and problem modeling (Chapter 5)
  - Ch 5: Chapter five discusses the development of the models used in this research
- Part 3: Results processing & Discussion, conclusion and recommendations(Chapters 6 and 7)
  - Ch 6: Chapter six discusses and interprets the results following from the models developed in chapter 5
  - Ch 7: Chapter seven concludes and discusses the complete research of this thesis

In the figure 2.3 the work flow of the research performed in this thesis is shown. The chapters where the results and findings of each step during the research can be found is mentioned in the work flow diagram. The model has been in development over the course of the whole research, new findings and input have been included when necessary.

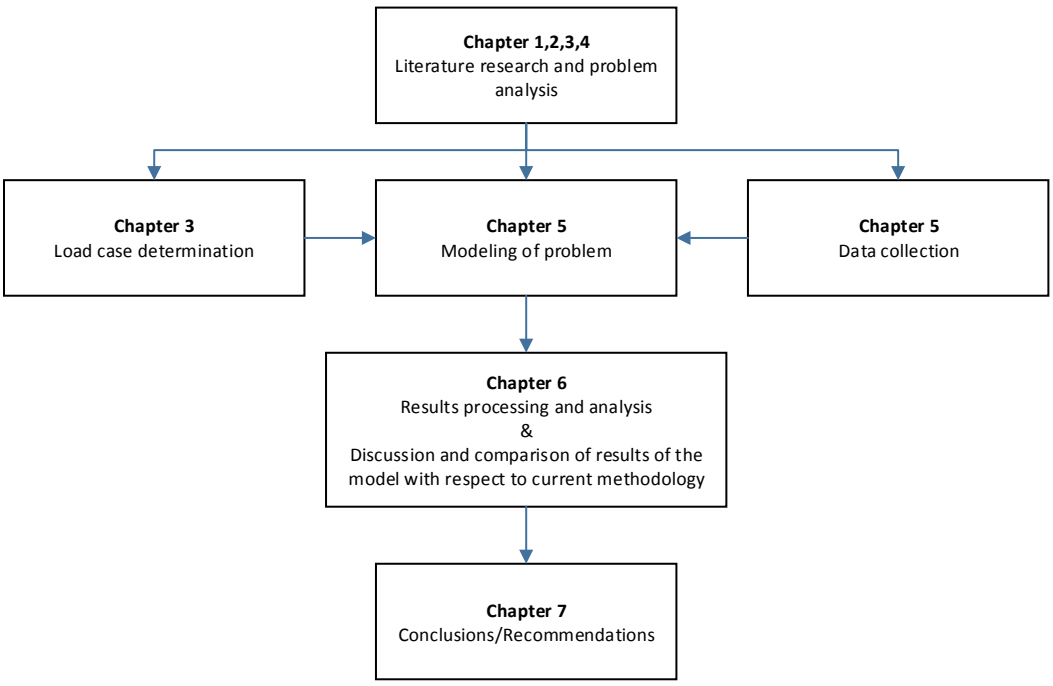

Figure 2.3: Work flow of research and model development

3

Current methods for assessing weld flaws

The assessment of the girth welds in offshore pipeline is necessary and indicate if flaws in the girth weld are prone to (critical) unstable flaw growth. Failure of a flaw can happen under plastic collapse,(brittle)fracture or fatigue and will damage the pipeline in a whole. This chapter will zoom in on how weld flaws can be assessed in order to provide a save girth weld. The assessment method for flaws in girth welds is called Engineering critical Assessment (ECA) and exists out of a collection of the general fracture mechanics (FM) formulas describing (fatigue) crack propagation due to static and cyclic loading of the environment on the pipeline. Engineering critical assessment is not only applicable to pipeline but to any structure prone to failure due to the presence of flaws.

The ECA protocol as it is used today is represented in the figure below 3.1.

Figure 3.1: The ECA protocol as used today,[Source:Liza Lecarme, HMC]

3.1. Engineering critical assessment

Engineering Critical Assessment is the name given to the collection of fracture mechanics formulas able to calculating crack growth in structures. The outcome of an ECA will verify if an initial flaw size will be safe under (brittle)fracture, plastic collapse or fatigue during the required service life of the pipeline.

An ECA can be used for the following applications:

1. To calculate the maximum allowable initial flaw size (MAIF), the MAIF is used as guideline for the NDT criteria. A flaw found during NDT of the pipeline will be checked against this criteria, flaws larger the the MAIF are rejected and the pipe will need a repair. Flaws smaller than the MAIF are regarded safe and the pipe laying process can continue. This

type of ECA is done early on in the project since it will influence expected weld quality, production rates and workability [3].

2. Determine if an existing flaw is safe or will propagate to a through thickness crack under expected maximum loading and/or repeated load cycles (e.g. lifetime extension, accidental larger flaw size, unforeseen longer contingency time). This is a fit-for-purpose application of ECA and specifies if a individual flaw considering the specific conditions is allowed.

.

3.1.1. Main variables

ECA interrelates three main variables, generally speaking it is possible to calculate one of the variables as long the other two are know.

The main variable (groups) are listed below:

- *Loading (static and cyclic):* Static loading is considered as the loading following from straining the pipe during the pipe laying process (reeling/un-reeling). Cyclic loading is the loading introduced by for example the current flowing of the piping, exciting the pipe and thus fatiguing the weld and the materials. Cyclic loading is uncertain as one can not know the loading on the pipe during its life time in advance, cyclic loading used as input for ECA therefore follows from simulation software.
- *Material properties (e.g. Toughness, Yield strength etc.)*: These are the governing variables indicating the material properties such like yield strength (YS), ultimate tensile strength (UTS) and the toughness. These properties follow from test reports of the pipeline(material) provided by the pipeline manufacturer.
- *Initial flaw size (e.g. from NDT or weld requirements)*:The flaw size (when used as an input) follows from non destructive testing of the weld or is given by pre-determined weld criteria (for example maximum quality that can be delivered by the welding equipment).

In the case of performing and ECA during pipe laying the loading on the pipe and materials properties of the pipe are know, enabling calculation of the MAIF.

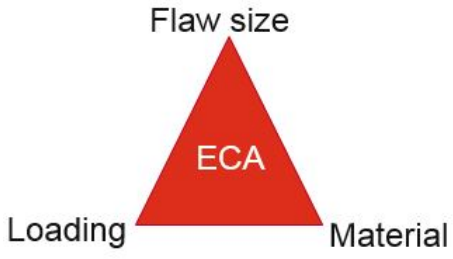

Figure 3.2: ECA and the main dependent variables

3.1.2. ECA flowchart

In general an ECA consists out of multiple ECA calculations performed within a single project, for each phase of the pipe laying project different loading occurs possibly increasing the flaw. In a typical reel laying process the following phases are present (see figure 3.3):

1. Pre-Installation
2. Installation
3. In-service
4. End of life

During each phase the FM formulas are used to calculate the increased flaw size following from an initial flaw size, this processes is show in more detail in figure 3.4). The left hand side of the figure is representing phase 1 and 2 of figure 3.2 and the companying load and material conditions, while the right hand side of the figure represents the last two phases (3 and 4) of the ECA.

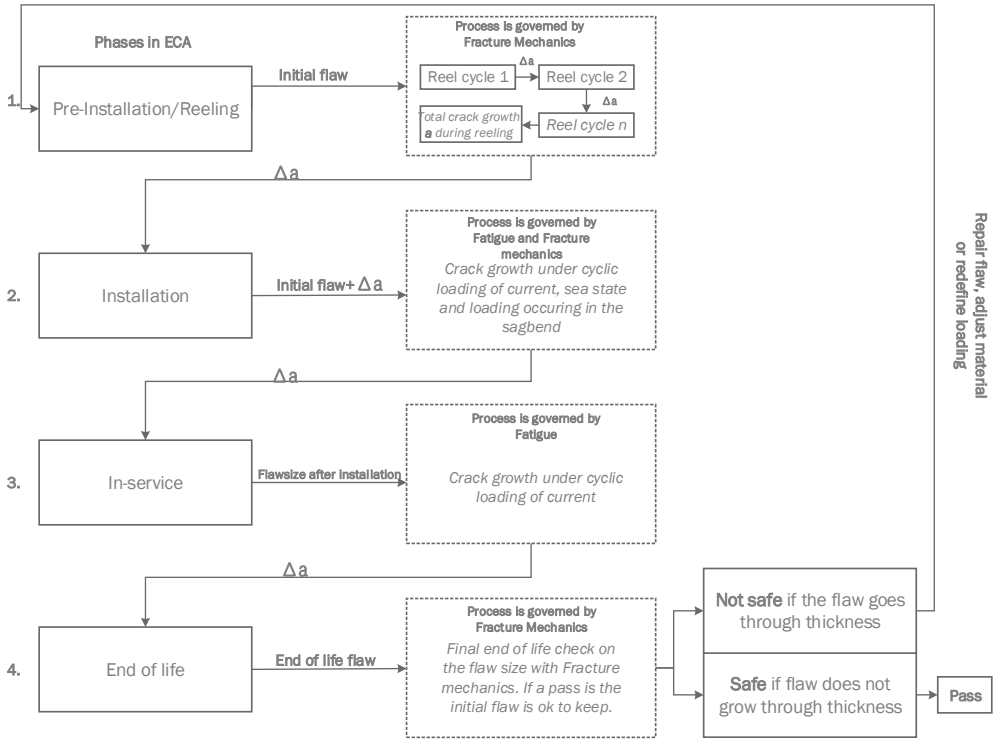

Figure 3.3: Overview of the phases in ECA in a typical Reel lay project

As can be seen in figure 3.3 each phase contributes to flaw growth, If the flaw is still within acceptable bounds after the four phases the flaw is accepted and the weld and pipe will not undergo repair. A flaw that is unstable (will not stop growing under a certain load) will grow through thicknesses (crack depth equals wall thickness of the pipe) and is regarded as unsafe and in need of repair.

3.2. Stresses in pipeline

In this section a way to construct a stress-strain diagram from the yield strength and ultimate tensile strength will be explained by making use of the Ramberg-Osgood approach, further more Neubers approach will be applied to derive the primary and secondary stress on the pipeline.

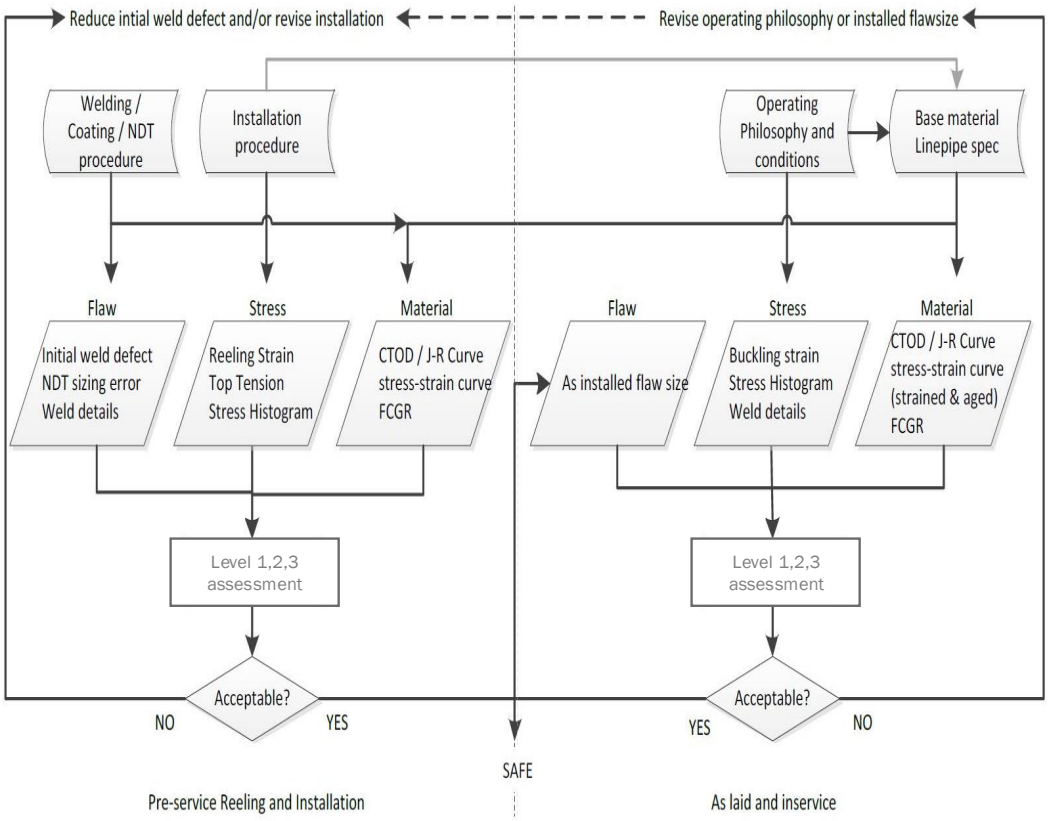

Figure 3.4: Flow diagram of a typical ECA process [3]

3.2.1. Constructing stress-strain diagrams (Ramberg-Osgood approach)

When only the yield strength(YS) and ultimate tensile strength (UTS) of a material is provided instead of the complete stress-strain measurement data, the Ramberg-Osgood approach can be used to construct a stress strain curve of that material[8], [5]. This relationship is later on used in the model described in 5, where the YS and UTS are randomly chosen and the stress strain curve needs to be constructed. The stress strain curve that is constructed for the first cycle in phase one will also include the elastic (linear) stress strain data. Once the pipe has been strained more than the allowable elastic strain the material is plastically deformed (strain hardened) and can not elastically deform anymore. Therefore the cycles following the first cycle do not include the elastic strain part anymore (this is also true for the other phases). To use the Ramberg-Osgood at least the following information of the material should be known.

Inputs for the Ramberg-Osgood method:

- (true)Yield strength σ_y
- (true)Ultimate tensile strength σ_{UTS}
- Young's modulus E
- Length of Lüders plateau (in case of strain hardening)
- Maximum strain (strain at ultimate tensile strength)

In case a Lüders plateau is present the strain at yield strength is equal to the the strain of the

Lüders plateau, if no Lüders plateau is modeled the strain at yield strength is set to 0.5%. See appendix C for the Ramberg-Osgood formulas. In figure 3.5a the stress strain curve including the Lüders plateau is shown (applicable for example phase 1/cycle 1), in figure 3.5b the stress strain hardened of an strain hardened material is shown (phase 1/cycle 2 and on).

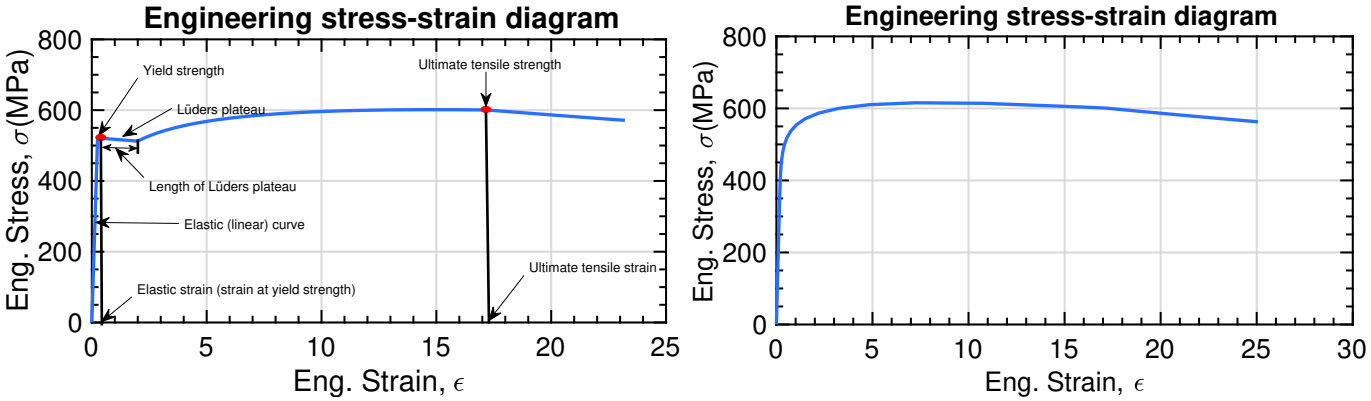

(a) Stress-strain curve including Lüders plateau

(b) Stress-strain curve of strain hardened material

Figure 3.5: Two stress-strain curves produced with Ramber-Osgood method

3.2.2. Primary and secondary stress

The BS7910 code describes primary and secondary stresses used in the ECA as follows:

Primary stress (P)

Primary stresses are stresses that can, if sufficiently high, contribute to plastic collapse of the pipe (while secondary stresses do not). They can also contribute to failure by fracture, fatigue, creep or stress corrosion cracking (SCC). They include all stresses arising from internal pressure and external loads on the pipeline.. The primary stresses are divided into membrane stress (Pm), and bending stress (Pb) components as follows.

- Membrane stress (Pm) is the mean stress through the section thickness that is necessary to ensure the equilibrium of the component or structure.
- Bending stress (Pb) is the component of stress due to imposed loading that varies linearly across the section thickness. The bending stresses are in equilibrium with the local bending moment applied to the component. Bending stress is regarded as being superimposed to the primary bending stress in the ECA method.

Secondary stress (Q)

The secondary stresses, Q, are self-equilibrating stresses necessary to satisfy compatibility in the structure. An alternative description is that they can be relieved by local yielding, heat treatment, etc. Thermal and residual stresses resulting from for example welding are usually secondary, a fluctuating thermal stress however is regarded as a primary stress when conducting a fatigue assessment. Secondary stresses do not cause plastic collapse as they arise from strain/displacement limited phenomena. They do however contribute to the severity of local conditions at a crack tip, and should be multiplied by their corresponding stress concentration factor when used in crack growth calculations.

Neuber's approach

The primary membrane stress (nominal stress) follows from the strain applied to the pipeline and can be found by making use of the stress-strain diagram of the pipeline material, to calculate the primary bending stress (Pb) Neuber's approach can be used [6]. The Neuber's approach corrects the nominal stress (Pm) to account for local stress concentration factors appearing due to misalignment of the pipe introducing more stress (Pb). Since Pb is regarded as being superimposed on Pm subtracting the nominal stress Pm from the result obtained by Neuber's approach, results in Pb. A graphical representation of this principle can be found in figure 3.6.

Neubers approach:

$$\epsilon_{loc} * \sigma_{loc} = \epsilon_{nom} * \sigma_{nom} * SCF^2 \tag{3.1}$$

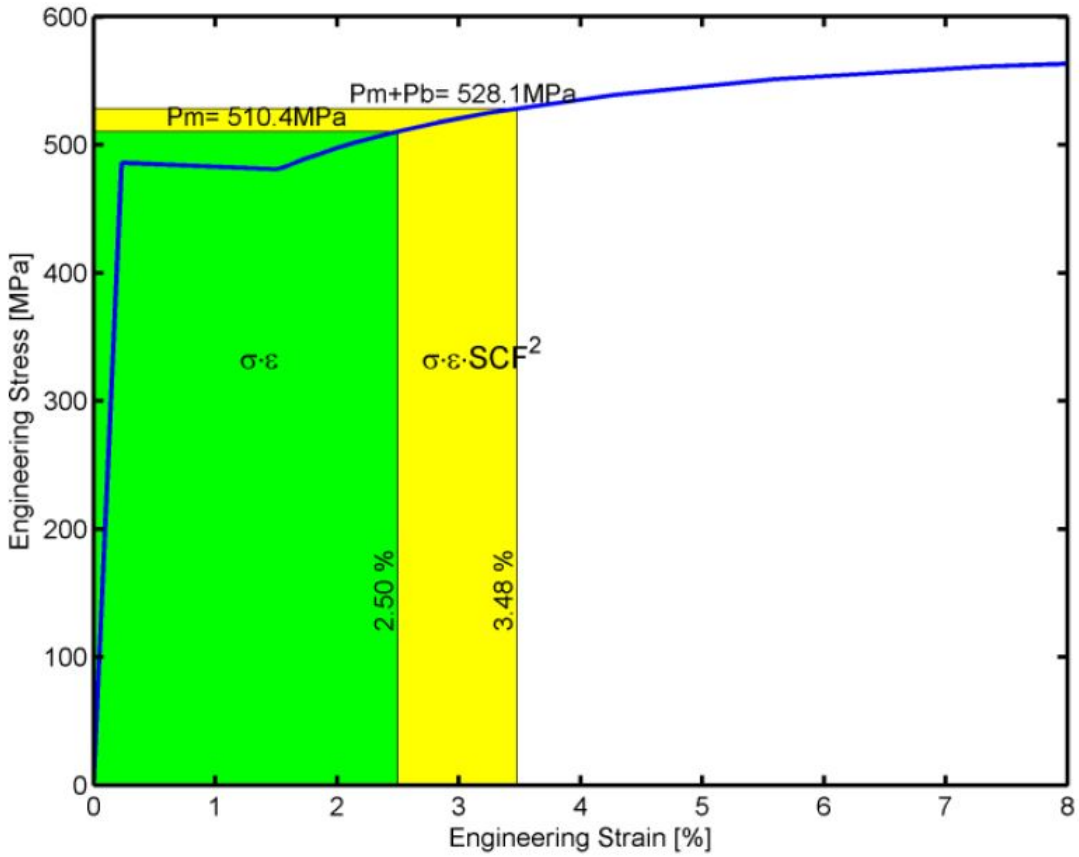

Figure 3.6: Neuber's approach applied to obtain Pb

3.2.3. Stress input per phase

Pre-installation phase

The stress input for the pre-installation phase follows from the stress-strain diagram of the pipe material and Neubers approach for the assumed stress concentration factor due to misalignment at the girth weld. The strain can be calculated and the corresponding stress is then found in the stress strain diagram.

Strain of the pipe on the reel:

$$\epsilon_{nom} = \frac{pipe\ outer\ diameter}{reel\ diameter + pipe\ outer\ diameter(inc.coating)} \tag{3.2}$$

Installation phase

Installation stress shall be determined from maximum expected dynamic top tension level, software used for simulating pipelaying forces will be used to determine cyclic loading due to current.

Operation stress input

The operational stress analysis shall consider all forms of loading the pipeline will experience during operation including:

- Extreme loading conditions (e.g. 100 year storm and extreme loading combinations)
- Vortex induced vibrations (cyclic loading)
- long term operating conditions (e.g. temperature variation, shut-down and start up)

3.3. Assessment of fracture resistance

This section will focus on the global methodology of ECA which is described for pipeline in [8] and [19]. The ECA methodology can be split up in an assessment for fracture resistance (static loading) and fatigue fracture resistance (cyclic loading). In a complete project the contribution in crack growth in each phase adds up to the total crack growth. Furthermore a distinction can be made in the ECA between the failure assessment curve, which describes the general behavior of the pipeline material under loading,

3.3.1. Failure Assessment Diagram

The ECA method and its output is visualized in the failure assessment diagram (FAD), on the Y-axis and X-axis of the FAD are K_r and $L_r$respectively . The K_r ratio defines the tearing resistance of the flaw in the material, while the ratio L_r defines the resistance against plastic collapse of the section of the pipeline containing the flaw.

The FAD contains a failure assessment curve (FAC) that depends on the pipe material and divides the FAD in an acceptable and unacceptable area (see figure 3.7) on basis of the physical limits of the pipe material. In the same figure the flaw being assessed is represented by a single assessment point or a locus of assessment point (this depends on the definition of toughness). A flaw is then assessed on basis of the locations of its assessment point/locus in the FAD, if a single assessment point or any point of the assessment locus falls on or in the FAC the flaw is considered to be safe and thus will not grow through thickness (depth of the flaw equals pipe thickness). When a single assessment point or the complete assessment locus falls outside of the FAC the flaw is regarded unacceptable.

3.3.2. Failure assessment curve

As mentioned above in section 3.3.1 the failure assessment curve defines the acceptance area on the FAD. The area below the FAC is regarded the accepted area while the area above the FAC is the unsafe area implying a crack will endure unstable growth which means the weld

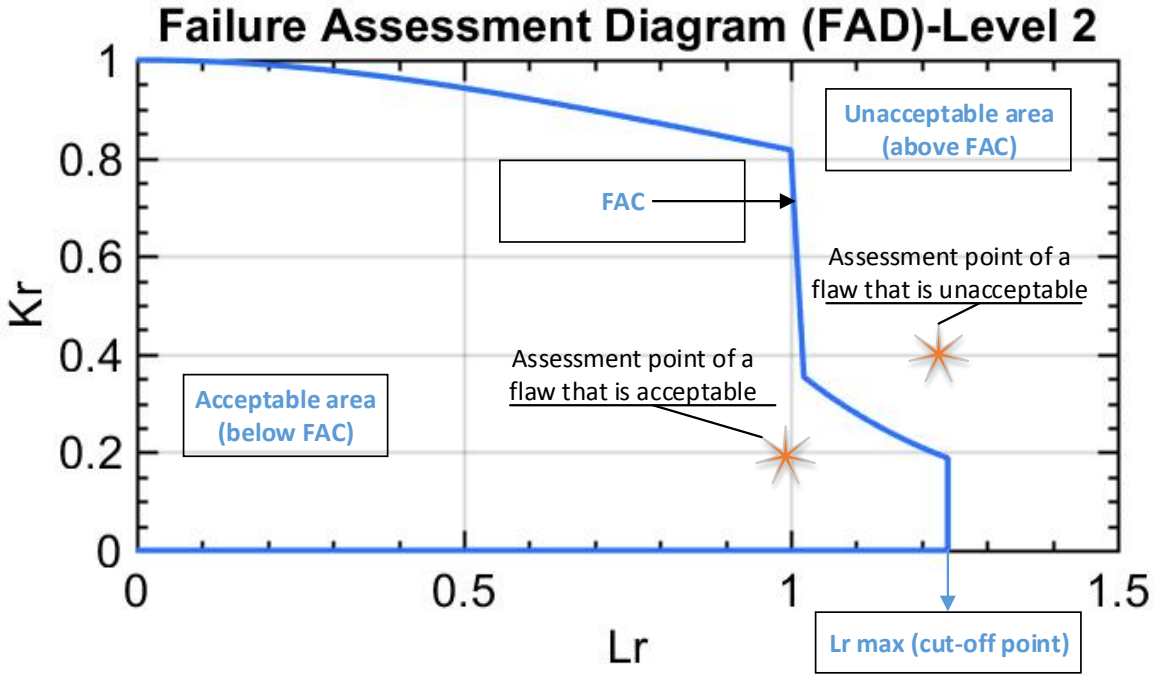

Figure 3.7: Clarification of assessing flaws using the FAD

will fail (see figure 3.7). The failure assessment curve is defined by the level of assessment used in the ECA. The FACs of the three assessment levels are defined in this section.

Level of assessment

An ECA can be performed on three different levels, each with an increase in accuracy and complexity of the method with when choosing a higher level ECA.

Each failure assessment curve is described in the form of:

$$K_r = f(L_r) \tag{3.3}$$

The failure assessment line runs up to the ”cut-off value’ Lr_{max}, the cutoff value indicates the boundary at which plastic collapse of the section containing the flaw is the governing failure mode.

Lr_{max} is defined as:

$$Lr_{max} = \frac{\sigma_Y + \sigma_{UTS}}{2 * \sigma_Y} \tag{3.4}$$

The levels of assessment available are:

- *Level 1:* Most simple method, this method does not require detailed stress-strain data for determining the failure assessment diagram of the pipeline material. The inputs that is necessary are the material properties: E (Youngs modulus), σ_Y(yield strength) and σ_{UTS}(ultimate tensile strength).
- *Level 2:* Most common method, this method requires detailed stress-strain data of the pipeline material to determine the failure assessment curve and is suitable for all metals regardless off their stress-strain behavior.

- *Level 3:* Most complex and material specific method, this method uses the loading,material and geometry of the pipeline to analyze flaw size and growth. This level is based on finite element methods (FEM)

For the specific FAC formulas see Appendix A.

3.3.3. Flaw assessment point

To assessment of a flaw is done by calculating the the L_r and K_r coordinates corresponding to the flaw and plotting it on the FAD. If the assessment points falls within the FAC the flaw is assessed to be safe and will not fail under that assessed loading and vice versa (see figure 3.7). Both the value of K_r and L_r strongly depend on the flaw dimensions, material properties and loading on the flaw size. As has been mentioned in section 3.3.1, the K_r and L_r indicate Brittle failure and plastic collapse respectively, this implies a flaw with an assessment point falling above and left of the FAC fails under brittle failure, while a flaw with an assessment point falling right and above the FAC fails under plastic collapse.

Using R-Lay during the first phase high strains are present introducing loads that plastically deform the pipe materials, this shows in the FAD with assessment points located in the high L_r regions close to the cut-off value L_{r_max}. For clarification on how to assess flaws using the failure assessment diagram see figure 3.7.

Calculating the L_r value of a flaw

The load ratio (or resistance against plastic collapse) is determined from the primary loads acting on the component the flaw is located in. The load ratio is defined as:

$$L_{r_{ass}} = \frac{\sigma_{ref}}{\sigma_Y} \tag{3.5}$$

Where:
σ_{ref}: The reference stress also referred to as the applied load
σ_Y: The rigid plastic limit load depending on flaw size a and the yield strength also called the limit load. In the context of fracture assessment σ_Y is equal to the yield strength of the material.

Reference stress σ_{ref} is depended on the the geometry of the component and the primary membrane and primary bending stress in the pipeline.

Calculating the K_r value of a flaw

The fracture ratio or (resistance against fracture) $K_{r_{ass}}$ is defined as:

$$K_{r_{ass}} = \frac{K_I^p + K_I^s}{K_{mat}} + \rho \tag{3.6}$$

or as:

$$K_{r_{ass}} = \frac{K_I^p + V * K_I^s}{K_{mat}} \tag{3.7}$$

Where:
K_I^p:Is the stress intensity factor at the current crack size due to the primary loads alone

K_I^S:Is the stress intensity factor at the current crack size due to the secondary loads acting alone
ρ:Parameter described by function of both the primary and secondary loads and account for plasticity interaction effects.
V:Parameter described by function of both the primary and secondary loads and account for plasticity interaction effects.
K_{mat}:Is the fracture toughness taking account of any ductile tearing following initiation. During the research it was found that using formula 3.6 allows for less flaw growth and therefore is more conservative than formula 3.7. This got confirmed by TWI (The welding institute) who state that from own research it also appears using formula 3.7 is less conservative and indicators are there to only allow the use of formula 3.7 in their updated software release of Crackwise. Therefore during this research the K_r value of the assessment point is calculated with correction factor V.

Ductile tearing/JR-Curve

As has been mentioned above the location of an assessment point of a flaw depends on the loading, material properties and dimensions of the flaw. A single coordinate (defined as (L_r,K_r)) is obtained when a flaw is assessed assuming the toughness of the material is fixed. In reality the toughness of a material increases when the flaw increases in size under the load. This increase in toughness in generally represented in the J-R curve (see figure 3.8). This increase in toughness is accounted for during the ECA by assessing multiple flaw sizes,

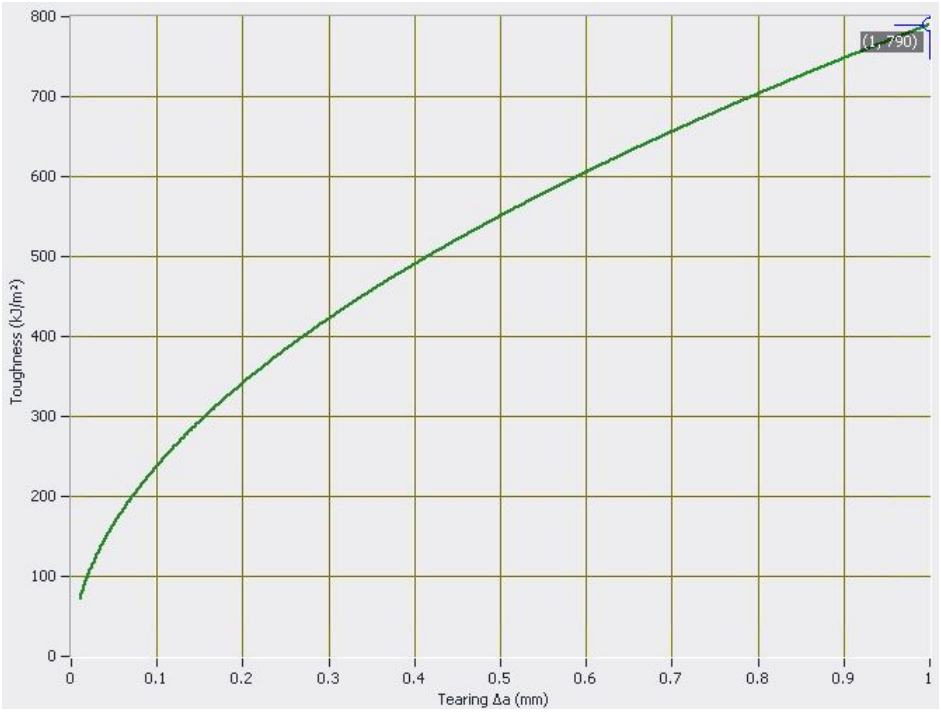

Figure 3.8: J-R curve, on the x-axis increasing flaw depth and on thy y-axis the toughness

starting from an initial flaw size and increasing by a 'δ a' and thus increasing toughness each step. By doing so a locus of assessment points will form on the FAD, if on of the points forming the locus will fall in or on the FAC the flaw is said to be stable while the initial flaw size itself increased by the total 'δ a' corresponding to the locus point (first) intersecting with the FAC. See figure 3.9 for a graphical representation of a flaw with an initial flaw size of 4mmx25mm growing to a stable flaw size of 4.5mmx25mm

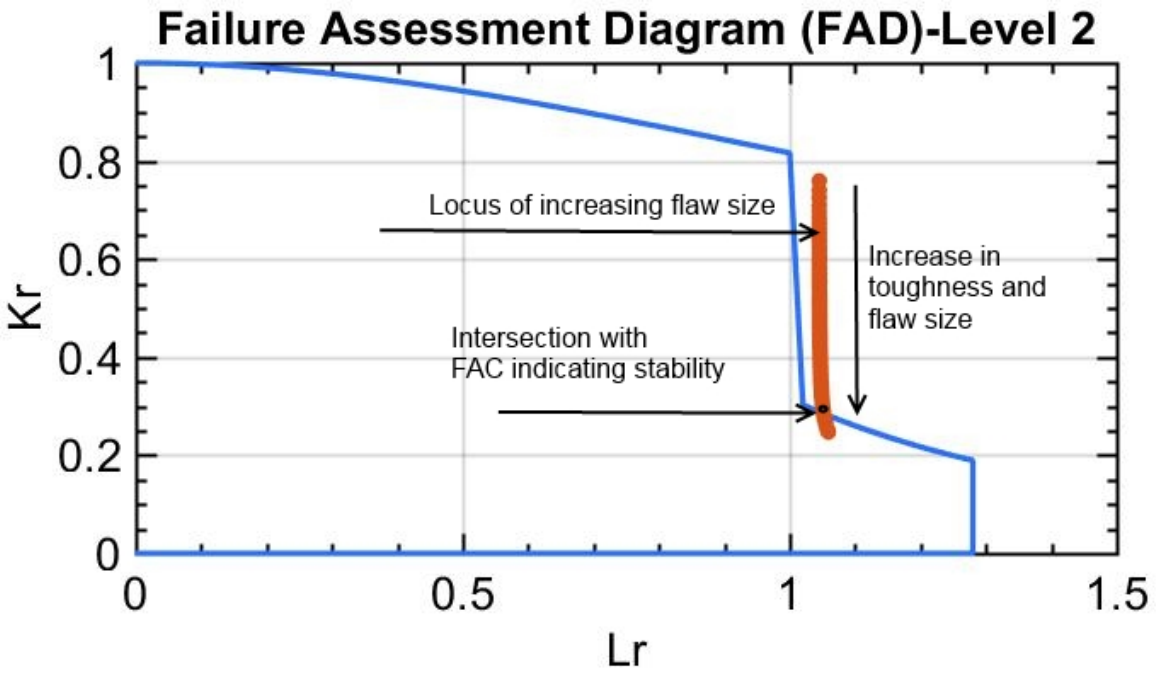

Figure 3.9: Locus on the FAD of a flaw starting at an initial flaw size of 4mmx25mm, and reaching a stable flaw size of 4.5mmx25mm

3.4. Assessment for fatigue

Besides flaw growth due to static loading also flaw growth due to cyclic loading is possible. Cyclic loading causes fatigue of the pipe material which possibly increases crack growth.

3.4.1. Paris Law

Paris law relates the stress intensity (Δ K) caused by the cyclic loading on the crack to the increase in crack size per cycle (da/dN).The crack growth law is determined experimentally, and might be generated specifically for an ECA. However the overall relationship between da/dN and Δ K is normally observed to be a sigmoidal curve in a log(dA/dN) vs log(Δ K). There is a central portion in this curve for which it is reasonable to assume a linear relation ship. This linear relationship is called *Paris Law* (formula A.18) and indicated as zone II in figure 3.10(a), two or more linear lines can be used for increased precision of the middle part of the curve as can be seen in 3.10(b) .

As shown in area I of figure 3.10(a) threshold value ΔK_0 indicates a threshold where if the stress intensity (ΔK) of the cyclic loading falls below this threshold crack growth in insignificant. On the other side in the area indicated by III the stress intensity factor of the cyclic loading approaches the physical limit of the material K_C at which not the flaw will grow but the material will fail. It is sufficient to assume that the central portion applies for all values of ΔK from ΔK_0 up to failure [8]. For a graphical representation of the full process see figure 3.11.

Safety factor

As will be further investigated in 3.6.2 currently a safety factor of 5 is used in order to design or assess for a safe pipe design, this safety factor expresses the ratio between the design life and the service (planned) life of the pipeline.

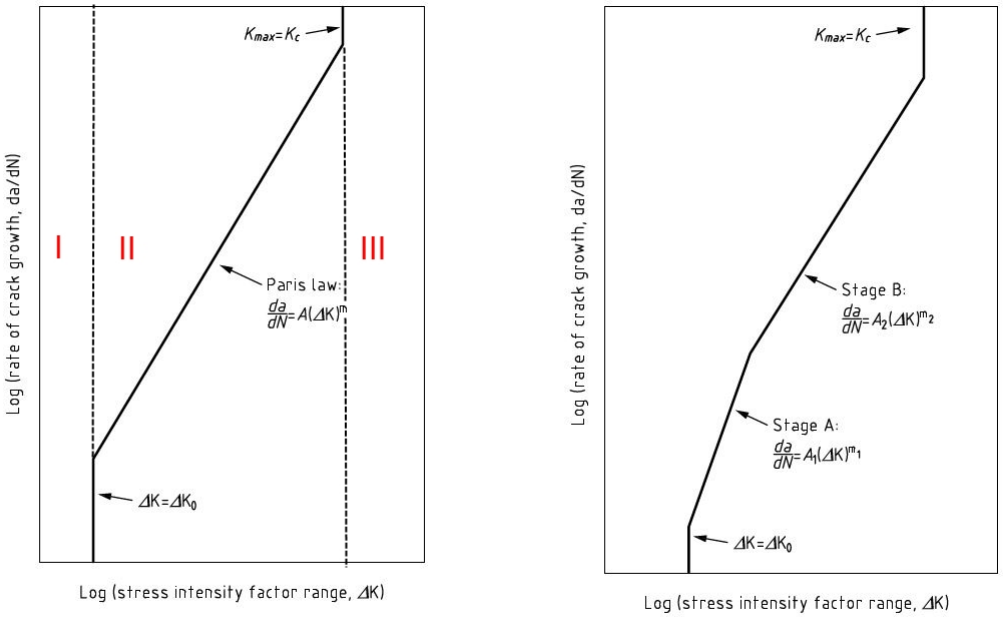

a) Simple Paris law crack growth relationship b) Two stage crack growth relationship

Figure 3.10: Paris law [8]

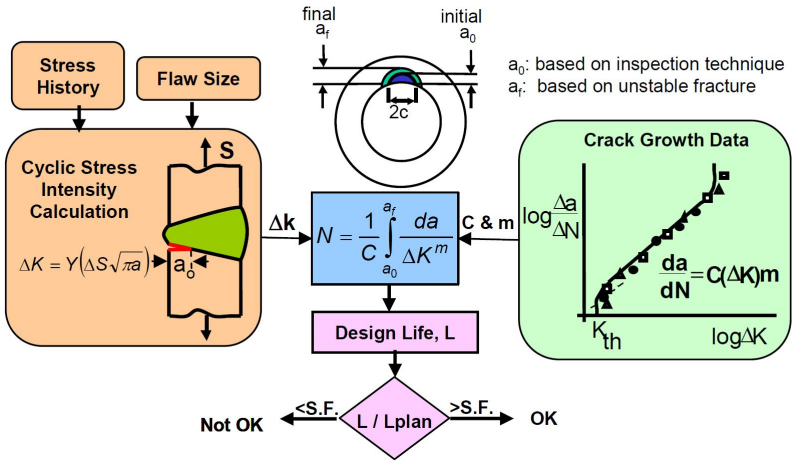

Figure 3.11: Graphical overview of the fracture mechanics fatigue approach, figure found in [17], also defining the safety factor as the ratio of design life over planned life.

3.4.2. S-N curve approach

An alternative on the Paris law is assessing flaw growth by means of a S-N Curve. A S-N curve is a graphical representation of the amount of cycles a material can withstand at a certain stress level (see figure 3.12). To assess flaws for fatigue using the S-N curve approach, use is made of S-N curve quality categories. In total 10 quality categories are available, where each increase in quality level implies less cycles at the same stress range. A flaw is accepted if its required quality category is equal or lower to its actual quality that is measured through tests.

The required quality for the flaw follows from the (cyclic) service loading that is expected on the flaw. By making use of Miners' damage rule for cyclic loading the stress range S can be calculated which then can be used to determine a quality category from the S-N diagram. The actual quality of the flaw depends on the flaw dimensions, flaw location, geometry of the weld and the loading on the flaw. The first step in the process of finding the actual quality is

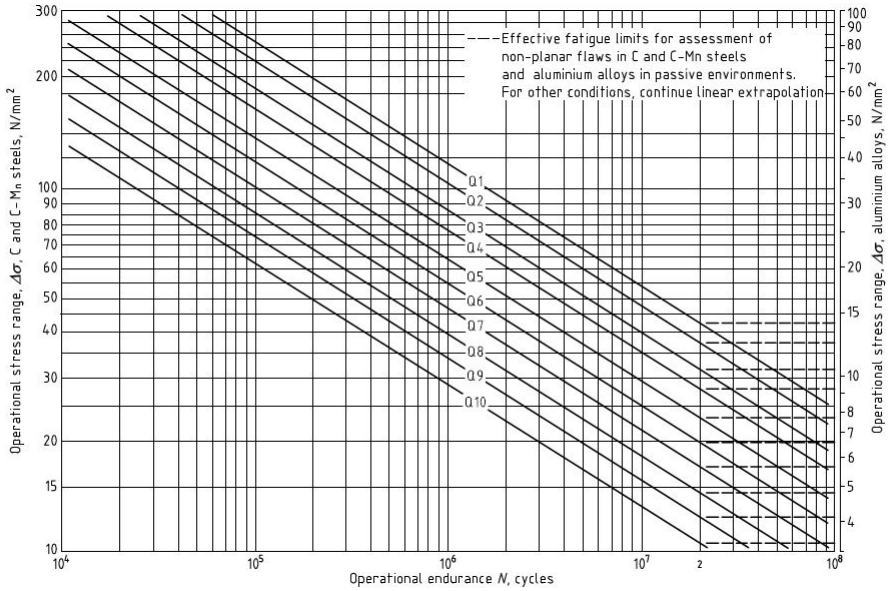

Figure 3.12: S-N Curve with quality categories [8]

converting the flaw dimensions to initial flaw parameters ($\bar{a}_i$). Also a tolerable maximum flaw height ($\bar{a}_{max}$) to which fatigue growth is permitted should be specified. Multiple figures are available to find the initial flaw parameters $\bar{a}_i$ and $\bar{a}_{max}$, which are linked to the measured flaw parameters, these figures differ per flaw type. Once $\bar{a}_i$ and $\bar{a}_{max}$ are determined the corresponding stress range can be found from another figure also depending on flaw type. This stress range can than again be linked to a quality level. All figures are based on experimental data.

Both quality levels now can be compared to each other, if the actual quality level is higher or equal to the required quality level the flaw is considered safe. For a grahical overview please see figure 3.13.

3.5. Limitations in the current methodology

The results of ECA depend on the definition of load, material properties and flaw size dimension used in the assessment. These variables are usually taken as deterministic values and in most of the cases, the worst case values are chosen to obtain a conservative and safe result. Currently it is questioned by the industry if the deterministic results are not over conservative resulting in:

- The (by method) determined weld defect acceptance criteria are too tight, which leads to an increased number of rejected welds that need unnecessary repairs
- The target lifetime of the pipeline cannot be achieved due to a MAIF provided by the ECA that is too small to produce with the welding equipment

At the end of the service life time of the pipe, the crack should still be able to withstand maximum expected loading to facilitate safe removal of the pipeline.

3.6. Conservatism in current methodology

There is concern from the industry the current method is conservative in its approach. This concern is based on the use of conservative input of loading and material properties during

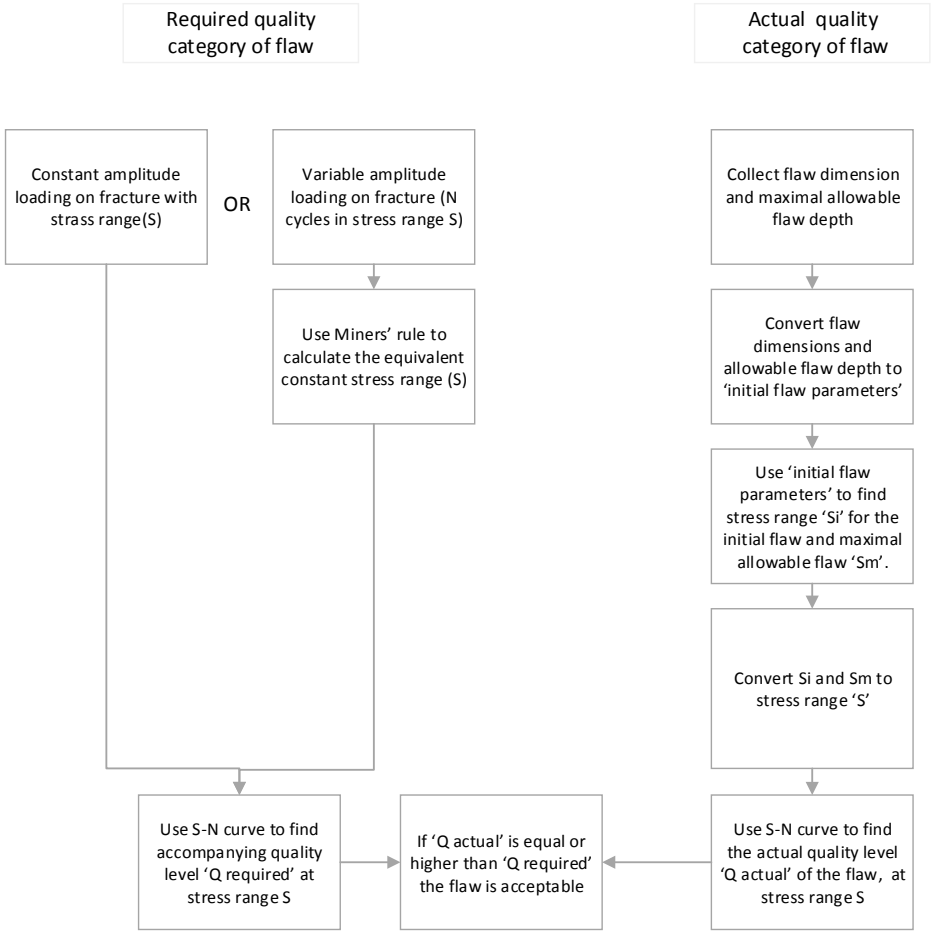

Figure 3.13: Overview of the S-N approach

the static FM calculations and a safety factor of 5 that is used during the fatigue assessment. Both aspects will be explained below.

3.6.1. Conservatism-Static Fracture Mechanics

The conservatism during the static FM analysis comes from using conservative values e.g. during the first phase of reel lay the upper bound stress train diagram is used, using the upper-bound implies using a higher yield strength in the analysis. Furthermore a low strain hardening (which is the ratio of ultimate tensile strength over yield strength) of the material is assumed, causing less resistance against plastic failure and a smaller MAIF.

3.6.2. Conservatism-Fatigue assessment

During the fatigue analysis in an ECA the cyclic loading on the area containing the flaw is used as the loading input. In this input is a large uncertainty since it comes from simulating software based on in situ measurements, the simulation will provide the load profile for the total life span of the pipe. The account for unforeseen load conditions or underestimates of the simulation use is made of a safety factor defined as:

$$SF = \frac{Design\,life}{Service\,life} \tag{3.8}$$

Stating a pipeline that should be in service for 30 years is tested for a fatigue load corresponding to a life of 150 year. The safety factor of 5 is chosen on an 'engineering experience' basis, implying if previous experiments and projects have worked without failure it is ok to keep using it.

The definition of this safety factor is somewhat remarkable since it is expressed as a lifetimes ratio, while in general in a probabilistic design the safety factor is expressed as the ratio between design resistance (Rd) of the component and the expected design load (Sd) on the component (see figure 3.14). This ratio takes in to accounts the probability of an critical event taking place.

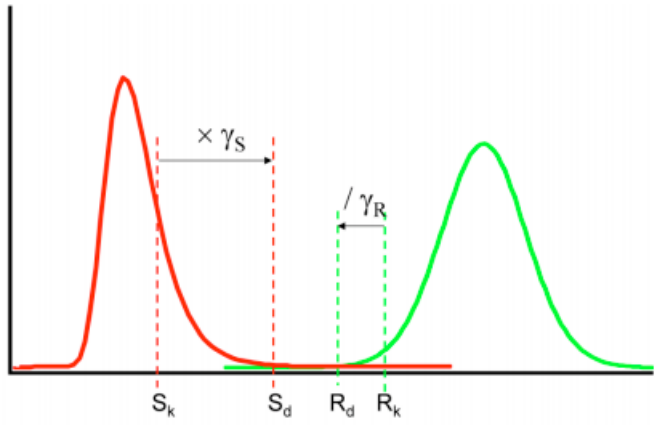

Figure 3.14: General definition of the safety factor, as the ratio between the design resistance (Rd) and design load (Sd), figure from [14]

3.6.3. General conservative assumptions

Furthermore the method uses the material properties of the parent (i.e. pipeline) material in the assessment while in general a weld is over-matched and thus stronger than the pipeline material. Also the properties of the parent pipe material are chosen to be one standard deviation away from the mean value (plus or minus depending on stress or strain based ECA)

The current practice is to assume worst case maximum installed flaw size at the worst location as input for the in-service analysis. This is very conservative since it is unlikely that the location of the maximum installed flaw size will be subjected to maximum operational fatigue loading. It is advisable to combine only likely load combination, however there is no clear guidance available and should be approached on a case by case evaluation. Also the load scenarios present at the girth weld are over conservative by assuming a worst case load at the weakest (e.g. largest flaw location).

The stress intensity solutions for flaws do not reflect the actual geometry of the flaw (e.g. a flat plate solution for stress intensity is used on an external flaws in a girth weld). Resulting in over estimates of stress concentrations and thus a smaller MAIF.

3.7. ECA software available

This section will discuss two software packages, TwI Crackwise and SwRI FlawPRO. Crackwise is widely accepted within the offshore industry space for performing ECA. FlawPRO is

the result of a join industry project (JIP) HMC participated in.

3.7.1. FlawPRO

FlawPRO is the result of a JIP where data from the participant is used as basis for the software. FlawPRO is designed with a focus on R-lay (i.e. high strain) pipe laying and is based on the level 3 (FEA) method. A database of FEA analysis within FlawPRO is available to produce the FAD. Mean reason this software is not widely used within the offshore industry is the lack of validation in projects, as a result the is not to much available data. A wide chose of analysis options is available.

Some advantages of using Level 3C FADs in engineering critical assessments (ECAs) compared to, for example, Level 2B (Material Dependent) FADs are:

- FlawPRO Level 3C FADs are more accurate since they are underpinned by a J estimation scheme unique to FlawPRO that is derived from a database of elastic-plastic finite element J analyses
- The Failure Assessment Curves that are a key component of FADs are generated in FlawPRO directly from the J estimation scheme. The FACs explicitly encapsulate not only material dependent effects related to stress-strain behavior but also the influence of flaw size, flaw geometry (embedded, surface, through-wall), pipe geometry (OD/t), and loading type (axial force, bending moment, internal pressure).
- The Lr parameter (= applied load/plastic limit load) that defines the x-axis of the FAD is calculated in FlawPRO using equations for combined axial force, bending moment, and internal pressure derived from limit load theory modified to fit accurate limit loads extracted from fully plastic FEA J solutions using an optimization technique.
- The Kr parameter (=applied stress intensity factor, K/material toughness) that defines the y-axis of the FAD is calculated in FlawPRO using weight functions that capture the effects of through-wall stress variations due to weld discontinuities and misalignment. The weight functions are derived from FEA solutions for uniform and linear stress variations.

3.7.2. Crackwise

This software package has been used many times within offshore projects and its results are validated. Within HMC this software package is the standard, and a database of results of previously done project is available. Crackwise can perform ECA on level 1 and level 2, or accepts an user defined FAD. To account for the plastic strain during reeling use is made o f the stress-strain diagram to find the primary stress encountered at the experienced (plastic) reeling strain.

3.7.3. Preference

It was found during testing results of both software packages are somewhat similar, the demo case provided by HMC ([3]) results in a final flaw size of 2.13 mm for Crackwise and 2.12mm in FlawPRo. Since most projects are done with Crackwise, and most expertise in performing ECA is with this software a preference goes to continue further research with Crackwise. It was also found Crackwise has a more user friendly interface, and is more stable in use than FlawPRO (during testing quite some unexpected errors and crashes occurred). The software package is used during this research to verify and validate the fracture mechanics model developed during this research.

4

Probabilistic theory and literature research

The current ECA methodology is mostly governed by conservative assumptions and accompanying computations (for reference see chapter 2). The use of deterministic extreme bounding values for the relevant parameters can lead to (over)conservative results, that may lead to (unnecessary) many repairs and higher project costs. An alternative approach would be to approach the ECA with reliability based assessment methods, using the probability of failure (PoF) of the system as a measurement of structural integrity. This chapter will provide the basis for designing a probabilistic method for conducting an ECA. Furthermore this chapter will provide background on the research performed within the industry on a reliability approach on ECA for fatigue. Possible elements of interest from this research for the probabilistic ECA method will be presented. The theoretical background information in this chapter has mainly been collected from [14] and [8].

4.1. Probabilistic assessment

Probabilistic (reliability) assessment of structures allows to take the uncertainty in the governing parameters in to account, and express the systems performance in term of probability of failure/reliability.

A probabilistic assessment can for example be used to take in to account the uncertainty of:

- Physical uncertainty (e.g. material properties)
- Measurement uncertainty (e.g. accuracy of NDT equipment)
- Statistical uncertainty (e.g. fit of the distribution to measured data)
- Model uncertainty (e.g. validity of assumptions)
- Human factor uncertainty (e.g. unexpected human error)

The required PoF or safety margin is very dependent on the function and consequence of failure of the system being assessed. Adequate data for all the critical variables is needed and therefore care should be taken in making assumptions and approximations.

4.2. Evaluation of the probability of failure

In its simplest format failure can be expressed as the load (S) on the system being greater than the resistance of the system (R) against this load. Mathematically this can be expressed in a limit state function (see formula 4.1).

$$Z = R - S \tag{4.1}$$

Where the system is defined safe when $Z \geq 0$ and fails when Z<0, the PoF(P_f) then is defined as $P_f = P[S > R] = P[Z < 0]$. The resistance and load effects of a system are most likely stochastic of nature and thus will vary per observation and possibly over time. In case of one-dimensional problems and simple distributions for R and S P_f can be easily calculated, often using analytical methods. However in practice multiple variables influence the limit state making it very difficult if not impossible to analytically evaluate the multidimensional integral exactly. Therefore, several methods are available to perform the reliability analysis[14].

A more general formulation for the limit state considering a structural model can be given as:

$$g(\underline{X}) = Z = 0 \tag{4.2}$$

Where $\underline{X}$ is a vector consisting of n variables each contributing to (possibly) contributing to load (S) and resistance (R) of the system, for example:

- Material properties
- Actions (loads)
- Geometrical properties
- Model uncertainties

All basic variables need to be represented by an appropriate distribution. In the case of an ECA a variable that has a negligible variation in time or space the variable can be considered as deterministic.

Now the POF (P_f) of the system can be calculated by solving the n-dimensional probability density function (pdf) of the n variables in vector $\underline{X}$ of the limit state function g($\underline{X}$).

$$P_f = \int_{g(\underline{X}<0)} f_{\underline{X}}(\underline{x}) d\underline{x} \tag{4.3}$$

With the above integral stating the PoF of a system is equal to the area (one variable) or volume of the joint probability function in the area defined by Z<0.

4.3. Reliability analysis levels

Within the reliability analysis methods distinction can be made between five levels of assessment[14]. The level of assessment required for determining the reliability of a system depends on the complexity of the system and accuracy required.

Level 0

This level is completely deterministic

Level 1

The level 1 reliability method is a semi-probabilistic method which is based on the application of partial safety factors on the variables in the deterministic formulas. Partial safety factors can be applied to in individual parameters to obtain the required level of safety without performing a full probabilistic assessment. The parameters considered attain the mean value of the parameter, which than can be multiplied by the partial safety factor γ_i (see formula 4.4 for an example). Partial safety factors are not unique and different combination are possible to obtain the required POF, they do not only depend on the POF but also on the scatter and uncertainty of the main input data.

$$F_{desing} = \gamma_i F_{mean} \tag{4.4}$$

Level 2

The level 2 reliability method is based on the first order second moment (FOSM) methods, and provides an efficient and accurate solution method in calculating the reliability/probability of failure of a system. A limit state function can be setup where the probability density functions of R and S are distributed normally. An approximate solution to the joint cumulative distribution function for any number of random variables modeled by continuous probability functions can be determined. The limit state function is linearized in the design point (i.e. where $g(\underline{X})<0$ has the highest probability density.

Level 3

The level 3 reliability method calculates the POF using analytical formulations, numerical integration or Monte Carlo simulations. Solving the problem using analytical expressions as is done during a level 2 analysis is only possible in a limited number of cases; numerical integration is only practical when the amount of samples needed is small (i.e. sample time is low). [14].

Level 4

This reliability method takes in to account (cost) consequences of failure, and risk (defined as consequence multiplied by PoF) is used as a measure of reliability. Level four calculations allow for designs to be compared on economic basis taking in to account uncertainty, cost and benefit.

4.4. Research performed within the industry

Current design of pipeline is done with use of safety factors (as has been mentioned in chapter 3), usually a factor of 10 for the SN-curve fatigue approach and a factor of 5 for the fracture mechanics (FM) fatigue approach is used. The safety factor used in the SN-curve approach is based on extensive engineering experience with this robust design methodology, where the safety factor in the fracture mechanics approach is based on engineering judgment.

While pipeline are being laid in increasing deepening waters the fatigue demand of the pipeline increases, the safety factor of 5 starts becoming onerous as flaw size calculated by the fracture mechanics methods become so small current equipment is unable to detect it.[24]

Within the industry research has been done towards lowering the safety factor used in FM design. In the paper of Macia et al. a reliability based method is developed to rationalize the

lowering of the safety factor used in FM design. The method developed compares the reliability of the SN-design to that of FM-design. The method developed by Macia et al. then is used in the Wang et al.[24], where on a project specific basis the effect of lowering the safety factor is studied. First the reliability matching method of Macia et al. is discussed then the project specific results of Wang et al. are presented.

4.4.1. SN curve approach toward fatigue design

This design model is based on the SN-curve, representing the amount of cycles till failure at a certain stress level. The curve is governed by two parameters *"A"* and *"m"* represented in formula 4.5 where N is the amount of cycles till failure occurs and S is the Stress.

$$N = A * S^m \tag{4.5}$$

Both values for *"A"* and *"m"* are both determined experimentally. Generally *"m"* is taken as deterministic value 3.0 and 3.5 for flush weld, parameter *"A"* however is variable as it represent the scatter of the fatigue data.

The limit state function for the SN-curve is represented by the Palmgren-Miner (PM) damage rule (formula 4.6. The damage limit C is distributed log-normal.

$$\sum_{i=1}^{k} \frac{n_i}{N_i} = C \tag{4.6}$$

n_i =Number of cycles in stress range occurred
N_i =Total number of cycles in stress range till failure
C =Damage occurred

In figure 4.1 the SN-curve design approach is represented, on the left hand side of the figure the actual stress (fatigue) loading is determined on the girth weld while on the right hand side the resistance (amount of cycles till failure) is determined. The design life can be calculated from the stress histogram that provides the amount of cycles over a certain amount of time, and the total amount of resistance the girth weld will offer. If the design life is a factor 10 larger than the planned life (actual operating time) the girth weld is considered safe.

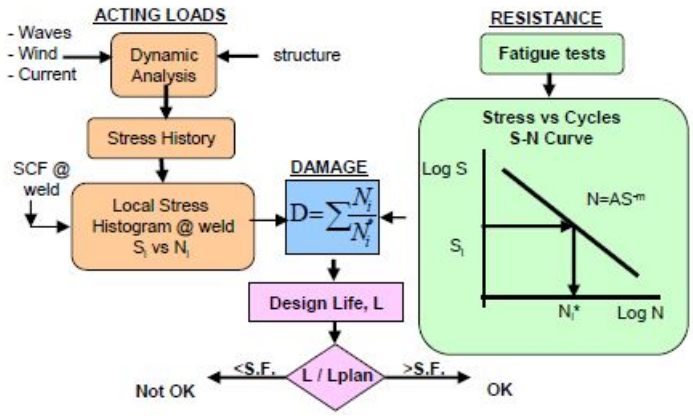

Figure 4.1: SN-curve method as described in [17]

4.4.2. Fatigue life models-FM Approach

Using this model the growth of an initial flaw can be calculated calculated during high-cycle fatigue loading till it reaches the through-thickness condition, opposed to the SN-method were crack growth can not be calculated. During this process the crack is evaluated on the possible occurring extreme loading conditions. Since this model depends on the fatigue and fracture stability of the crack the limit state function is governed by both. For a methodical overview see figure 4.2.

The acceptability of a flaw is defined as reaching a stable (sub-critical) crack size before a through thickness crack occurs during its service life. A circumferential flaw will grow under fatigue can be calculated by the Paris-Erdogan fatigue crack growth law (CGR), which is a function of stress intensity factor (K), which on its turn is depending on the local stresses range and thus the SCF and loading.

The CGR is defined by parameters C and m in the following form, both parameters are based on test data of the pipeline:

$$\frac{da}{dN} = C(\Delta K)^m \tag{4.7}$$

To evaluate the crack on the extreme loading cases use is made of the Failure assessment diagram (see chapter 3).

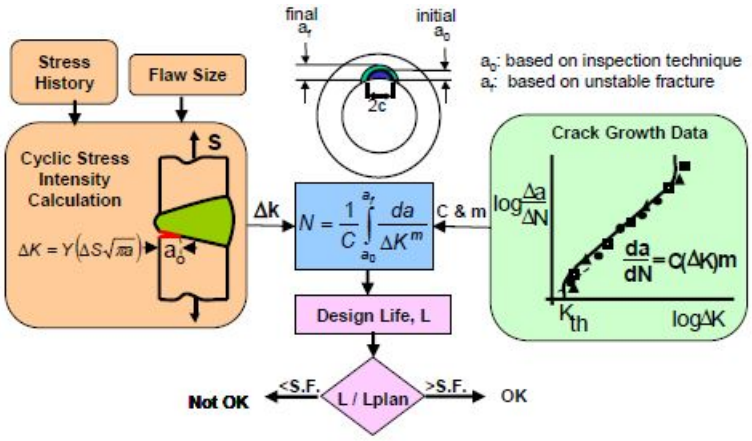

Figure 4.2: FM-Method as described in [17]

4.4.3. Reliability matching of SN and FM method

As can be seen in the paragraphs above both methods use different input, but share the same stress histogram. In the study of Macia et al. the goal is to provide rationale in choosing a right safety factor for the FM approach. The safety factor (SF) for the SN as well FM method is defined as the ratio of the design life and service life.

In the paper of Macia et al. it is tried to determine the safety factor suitable in the FM approach based on the reliability of the robust and proven over time SN-method. First the probability of failure (PoF) at a specified service life is calculated by making use of the first order reliability method.
This PoF is then used as the target reliability for the FM service life, by performing a inverse reliability calculation on the FM approach the matching service life to this reliability can be found. The design life can be calculated making use of the conventional FM analysis approach for a given initial flaw sizes. The resulting factor gives the appropriate safety factor

used for that specific design case. For a graphical representation of the reliability matching see figure 4.3.

In the study of Wang et al. it was discovered that by using the reliability approach towards determining the safety factor, an appropriate safety factor for the project in question would be between 1.23-1.5 instead of the standard factor of 5. The lower safety factor impacts design requirements and results in a less strict NDT weld flaw criteria.

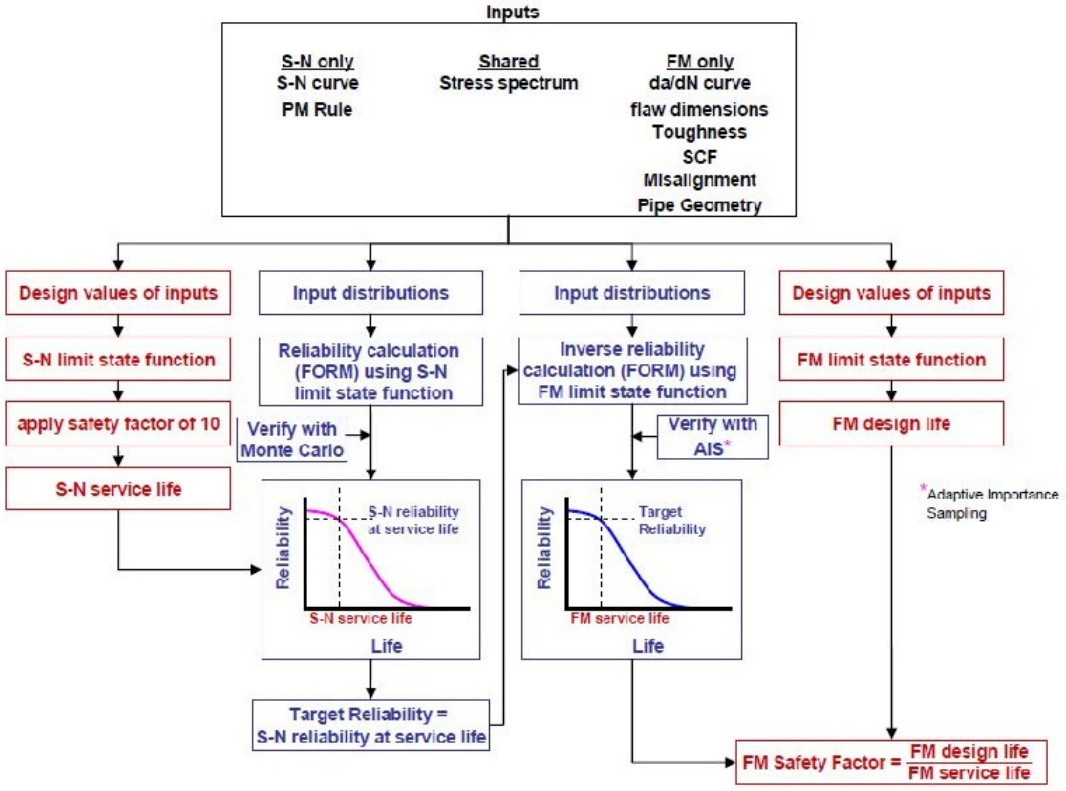

Figure 4.3: Reliability matching as described in [17]

Part II (Chapter 5)

Data collection and problem modeling

5

Probabilistic model

In this chapter it will be explained how a probabilistic approach is implemented on the static fracture mechanics ECA from chapter 3 in order to determine new NDT criteria (flaw assessment criteria). First the assumptions made to built the probabilistic model will be discussed. Next two models to determine the Probability of Failure (PoF) of a single girth weld will be explained, each model taking its own approach towards the reliability calculations and the corresponding NDT criteria. The next sections will go in on the reasoning for choosing a distribution for the stochastic variables, also the principle of using copulas is explained. The output of the models will be further discussed in chapter 6 where the results will be post processed in order to draw conclusions from the probabilistic models. In chapter 6 a sensitivity analysis will be performed to indicate the effect of the stochastic input parameters on the PoF of a pipeline and post processing of the results .

To have a clear understanding on where in the complete process of ECA the model is applied figure 5.1 can be consulted. As can be seen a probabilistic approach is applied in the first phase of the ECA process.

Further more the two definitions defined below will be used often in this chapter (and on), they are both closely related to each other since NDT criteria follows from the MAIF and in case of the deterministic ECA are assumed to be the same.

- MAIF: The MAIF is a girth weld specific value that describes the Maximum Allowable Initial Flaw size for that girth weld in order to not fail under the expected loading
- NDT criteria: Weld flaw assessment criteria which describes a flaw size used to determine if a flaw present in a girth weld is acceptable or unacceptable, the NDT is project specific. The NDT criteria is based on the outcome of the (probabilistic) ECA

5.1. Assumptions

The following assumptions are made in order to develop the models, the (likely) impact on the output is mentioned per assumptions as well:

- The models consider cycle 1 during the first phase (see figure 3.4) , this simplifies the model without compromising the research. If conservative assumptions govern the deterministic calculations this would show up in the first cycle as well

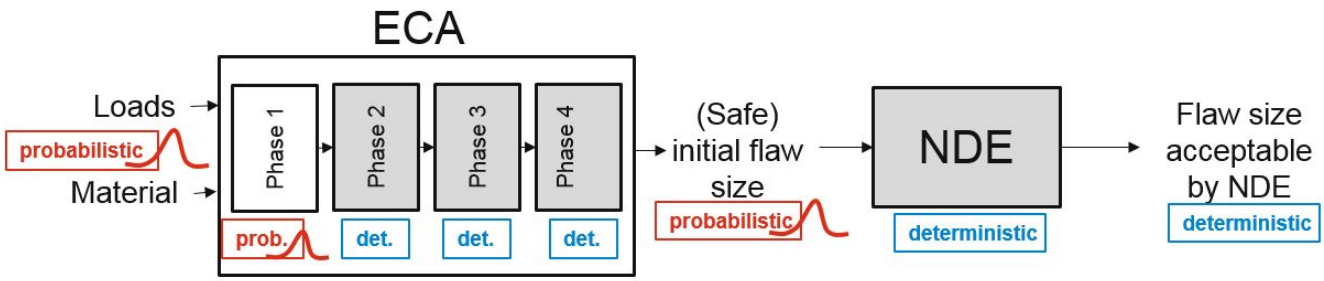

Figure 5.1: Graphical overview on where in the ECA a probabilistic approach is applied

Impact: Although conservatism can be indicated, a fully conclusive answer on the conservatism in ECA when including all cycles and phases of an ECA in the model (static+fatigue ECA)

- The allowable increase in flaw depth (a) in cycle 1/phase 1 may not be more than 0.5mm, this is to account for the further two/three cycles that follow. It is specified in the off-shore codes regarding ECA that over the total amount of cycles in phase 1 the total flaw growth my not be more than 1mm
  Impact: Flaw growth is not necessarily evenly distributed over the cycles but should add up to no more than 1mm of total growth. Therefore 0.5mm might be an over or under-estimation for the load case used. However since results of the probabilistic approach is compared to the deterministic approach (using the same boundaries), conclusions are conservatism will (likely) not change
- The crack will only grow in depth (a), flaw length (2c) is fixed
  Impact: When allowing flaw growth in the circumferential (2c) direction, the MAIF (in this research only dictated by flaw depth) will decrease
- The yield strength and ultimate tensile strength are independent of material toughness (JR-Curve)
  Impact: If a dependency does exist between the YS/UTS and JR-curve the independent draws for JR-curves might form unrealistic material properties scenarios
- The strain is assumed to be constant and is taken as the maximum expected strain (first reel layer on the drum), in reality the strain depends on the bending radius of the pipe and thus will decrease the further the pipe will be from the reel center
  Impact: Less strain will introduce less stress (crack tip driving forces), thus allowing for larger MAIFS. Therefore taking a constant maximum strain is conservative
- The flaw is located at the 12 o'clock position, where maximum strain and thus stress is applied
  Impact: It is conservative to assume the maximum weld flaw is always found at the 12 o'clock position in a girth weld. If the maximum weld flaw is located at a different position strain is expected to be less, and should allow for a larger MAIF. Therefore this assumption is conservative

5.2. Aim and functionality of the models

The scope of the research is focused on the first phase of the pipeline installation process during the first reeling cycle (see figure 3.3) and is governed by static loads (see chapter 2). The first phase of reel-lay does not include cyclic loading and therefore crack growth due to fatigue loading is not considered in the models presented below. Only the first cycle of phase 1 is sufficient to develop the probabilistic model, since the second (and potentially more) reeling cycles will make use of the same methodology to determine crack growth. Any successive cycle will only differ in the stress-strain curve (see section 3.2.1) and will take the the final flaw size of the previous cycle as initial flaw size input.

Two models will be presented in this section:

- **Model 1:** The first model is iterative of nature and iterates to the MAIF per generated random load case in each Monte Carlo (MC) cycle. The inputs of model 1 are the stochastic and deterministic variables mentioned in section 5.2.1. The output of model 1 is a dataset of MAIFS on which a distribution can be fit. By solving the limit state function where load is represented by the flaw size distribution of flaws (possibly) present in the girth weld and resistance by the MAIF distribution the probability of failure at a certain NDT criterion can be calculated. See figure 5.2 for a graphical representation of the process involved with model 1.

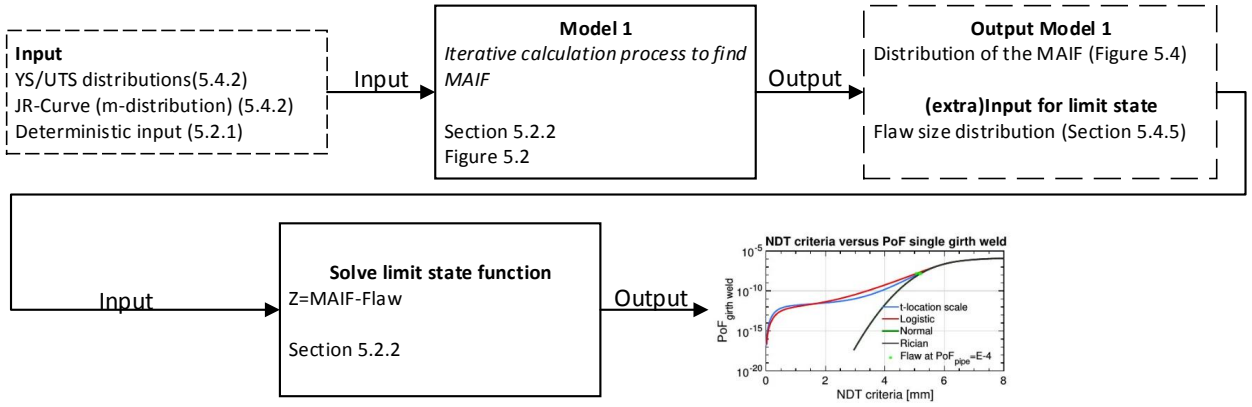

Figure 5.2: Complete functionality of model 1

- **Model 2:** The second model is a preliminary model which will directly simulate the presence of a flaw in the girth weld. Instead of iterating to the MAIF, each cycle in the Monte Carlo will check if the randomly generated flaw is safe (i.e. stable flaw growth and below 0.5mm total growth) when located in the randomly generated load case of the girth weld. The input of model 2 has one more stochastic variable than model 1 since also flaw size is now used as input. The output is a record of each flaw size that leads to failure, this output can be used to calculate the probability of failure of the girth weld at a certain flaw assessment criterion. See figure 5.3 for a graphical representation of the process involved with model 2.

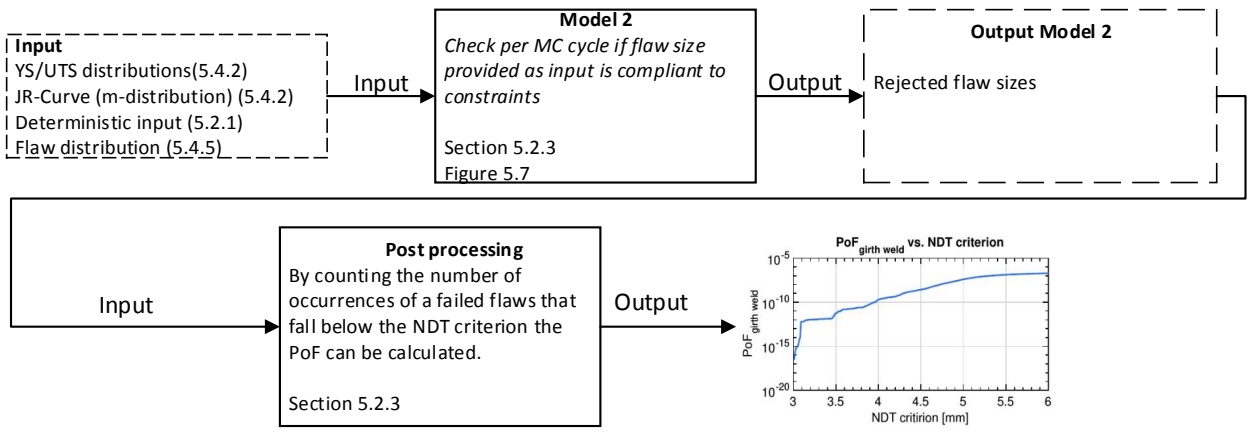

Figure 5.3: Complete functionality of model 2

5.2.1. Input of models

The input of the two probabilistic models is as follows:

- Outer diameter of pipeline (D_{outer})
- Pipe thickness (t_{pipe})
- HiLo root and cap ($HiLo_{root/cap}$)
- Weld cap length (L_{cap})
- Yield strength and Ultimate tensile strength (YS/UTS)
- Toughness (JR-curve)
- Young's modulus (E)
- Poisson ration (ν)
- Expected strain (ϵ)
- flaw angle (θ)
- Flaw width (C)
- Flaw length (2a)

Not all of these variables will be provided as a stochastic input to the probabilistic method, the variables that will be approach stochastically are determined in section 5.3.

The variables considered as stochastic are:

- Yield strength
- Ultimate tensile strength
- Toughness (JR-curve)
- Flaw size (load curve in model 1, direct input for model 2)

5.2.2. Model 1

The first model is an iterative model that will iterate to the maximum allowable initial flaw per given random load case. Repeating this iterative process in a Monte Carlo (MC) simulation where the input is generated from the probability density functions of the stochastic variables (section 5.4), a MAIF distribution will be generated as output. To solve for the probability of failure also a flaw size distribution and the possibility of occurrence of a weld flaw should be known, by solving the Z function and limiting the failure area with the NDT criteria the PoF of a single girth weld can be determined for a range of NDT criteria. The PoF can than be plotted against the NDT criteria in order to construct the Probability of failure curve.

For a graphical overview of the complete computational process of model 1 to arrive at the probability of failure curve vs NDT criterion see figure 5.2.

Model 1 can be split up in two parts as is shown in figure 5.4. The function of each part is described below:

1. *Part 1:* This is the Monte Carlo loop where a random load case is generated from the yield/ultimate tensile strength distributions together with a random JR curve. The selection of JR curve is assumed to be independent of the yield/ultimate tensile strength chosen. The selection is done from the distributions determined in section 5.4 and a copula is used (see section 5.4.5) to provide a correlation between the yield strength and ultimate tensile strength.
2. *Part 2:* This is the fracture mechanics 'core' of the model, and exists out of the formulas and boundaries of fracture mechanics (see in chapter 3) and includes the assumptions made at the start of this chapter (see 5.1). Once the MAIF is found through the iterative process it will be stored in a database and the next cycle in the Monte Carlo will start.

Once all cycles of the MC has been gone through a distribution can be fit to the MAIF data and further used in the reliability calculations as will be explained below.

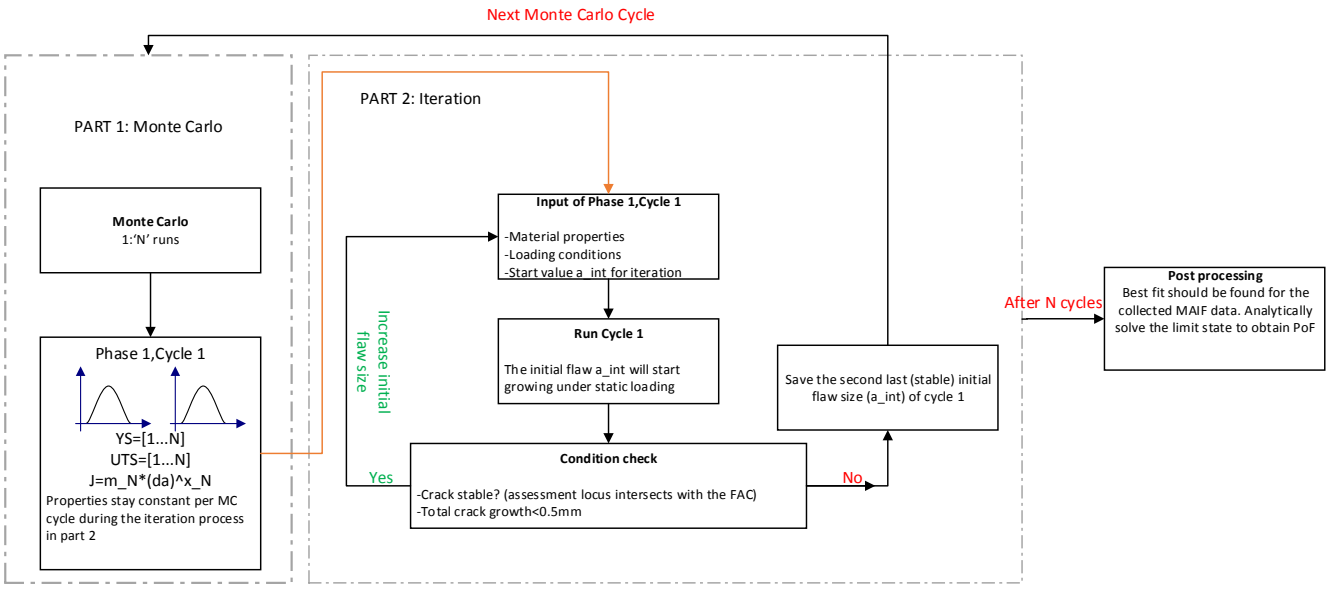

Figure 5.4: Flow chart of the iteration process to calculate the MAIF and corresponding PoF

Number of cycles needed

The output of each completed cycle in the Monte Carlo is the MAIF for the randomly picked load case in that cycle. Since the model tries to represent a real life process as close as possible a sufficient number of cycles has to be chosen in order to obtain a realistic distribution of the MAIF in order to produce consistent results. Too few cycles can result in over estimating the MAIF because load cases with a low probability of occurrence (e.g. a low toughness in combination with a high yield strength/low ultimate tensile strength) may not occur. Especially those load cases result in low MAIFs and thus should be included to determine a right distribution for the MAIF. On the other hand over estimating the amount of cycles will make the model take too much time without adding needed accuracy to the output.

An estimate on the amount of cycles required for the model to produce consistent results can be made by running the model for various amount of cycles and plotting the corresponding NDT criteria at a reference point in the PoF curve (the NDT criterion at $PoF_{pipeline} = 10^{-4}$ is taken as reference). It can be seen in the figure 5.5 the model starts to converge around 20,000 cycles in the Monte Carlo. By also including the mean value of the NDT criteria at the domain N=[20,000 120,000] it can be seen that the NDT criteria changes over the amount of cycles with respect to the mean in a range of -0.04mm to +0.01mm which is regarded as acceptable.

From figure 5.5 it can be seen that 20,000 cycles might already produce an accurate enough results, however to determine the consistency of the NDT criteria calculated, six runs are performed at both sample size 20,000 and 30,000 (yellow scatter enclosed in the rectangles of figure 5.5. It can be seen the consistency at 30,000 cycles is high, and therefore is taken as minimum required amount of samples to determine the NDT criteria with.

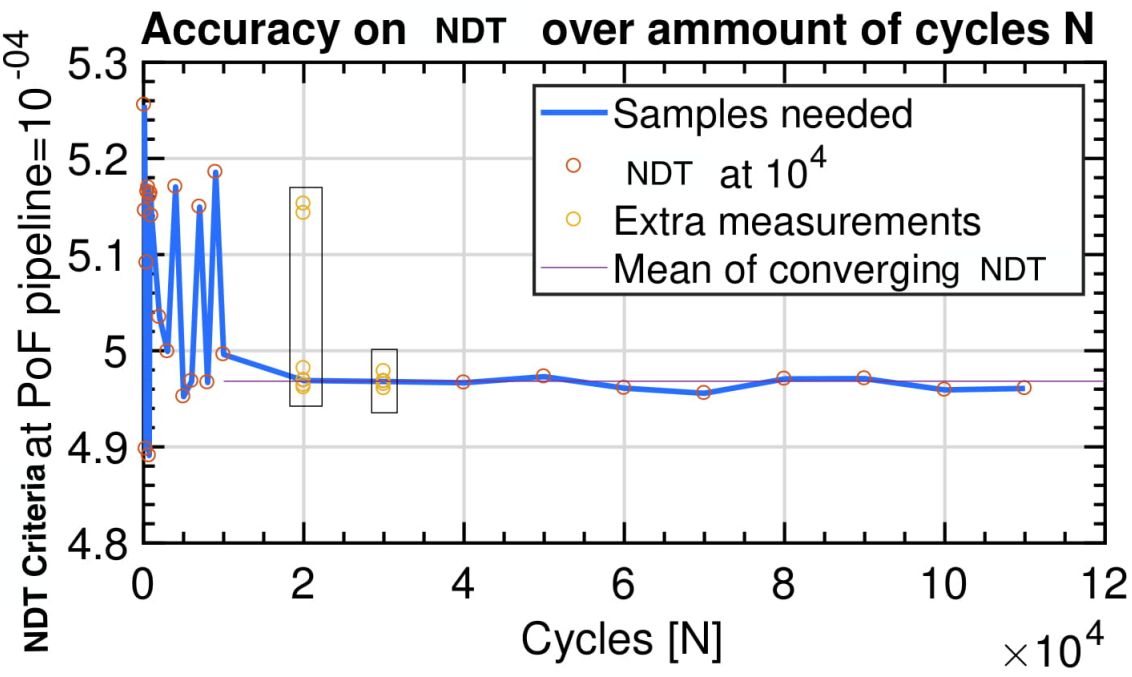

Figure 5.5: Amount of cycles on the x-axis vs NDT required on the y-axis

Table 5.1: Domains of N and the step size within the domain

Domain (Cycles 'N' used)	Step size
[100 1,000]	100
[1,000 10,000]	1000
[10,000 120,000]	10,000

Output

The output of model 1 is a database of MAIF on which a distribution can be fit that should represent the MAIF as close as possible, for a first idea on what distribution will best fit the MAIF data the histogram of the MAIF can be computed (see figure 5.6a).The analysis below is based on data following from 30,000 samples.

Already from the histogram (figure 5.6a) a symmetry can be detected, in figure 5.6b the densities of the MAIFs with respect to the complete data set are displayed. From this density plot the same symmetry can be found. Using the BIC criteria (see section 5.4.2) the top four best fitting distributions can be identified (see figure 5.6b). The best fit according to the BIC score would be the t-scale distribution with second best fit the logistic distribution and third runner up the normal distribution (as can be expected from the symmetry indicated before). The sensitivity of the distribution chosen for the MAIF on the PoF will be further explored in chapter 6.

Limit state function and Probability of failure

In order to calculate the probability of failure from model 1, a limit state function has to be formulated (Z-function). Failure in the context of ECA is considered as the occurrence of a flaw in a girth weld that exceeds the MAIF of that specific girth weld and thus indicates unstable flaw growth. Also the flaw is considered to be unacceptable if the flaw growth exceeds a maximum of 0.5mm from its initial value, even though the girth weld would not necessarily fail. This requirement follows form the offshore codes BS7910 and DNV-OS-F108 ([8][19]) which indicates that over the complete amount of cycles during phase 1 the allowable flaw growth form the initial value may not be more than 1mm.

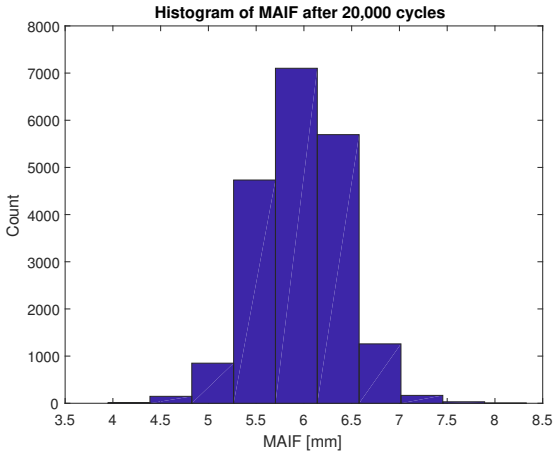

(a) Histogram of the MAIF after 30,000 cycles

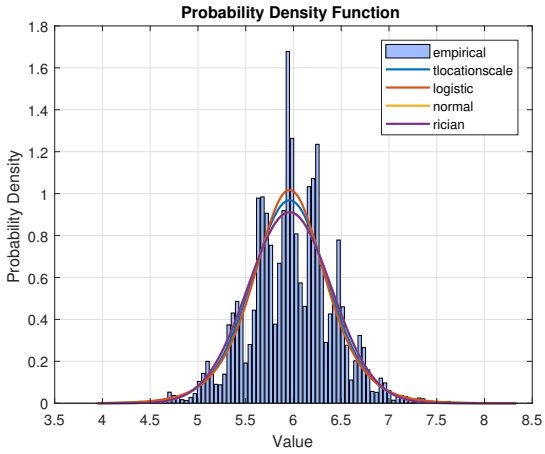

(b) Density and best PDF fits (according to BIC score) on the MAIF after 30,000 cycles

Figure 5.6: Best fit on the MAIF after 20,000 cycles

To recall from chapter 4 the probability of failure is defined as the area for which the limit state function is smaller then zero (Z<0), the Z function is defined in formula 5.1. The resistance curve in the limit state is the MAIF (see figure 5.7a), while the load curve is the flaw size of the possible defect in the girth weld (figure 5.7b).

$$
\begin{aligned}
&Z = MAIF - a_{present} \\
&Where: \\
&MAIF: \textit{The probability density function of the MAIF (resistance curve)} \\
&a_{present}: \textit{The probability density function of the weld flaw possibly present (load curve)}
\end{aligned}
\tag{5.1}
$$

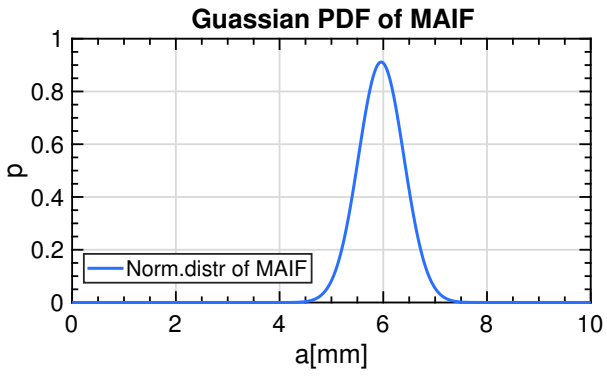

(a) A normal PDF fit to the MAIF distribution, this distribution forms the resistance curve in the limit state.

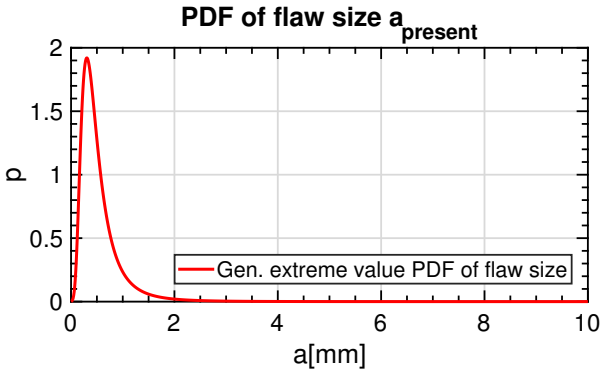

(b) A generalized extreme value distribution fit on the flaw data, this forms the load curve in the limit state.

Figure 5.7: The separate resistance (MAIF) and load (flaw size) curves

In order to visualize the PoF, both curves can be displayed in the same figure (see figure 5.8a), the right tail of the load curve will intersect the left tail of the resistance curve. This intersection is indicated by the green bar just left of 4mm in figure 5.8b. The area confined

by both tails is equal to the PoF of a girth weld since it indicates a probability of having a higher flaw size than the MAIF allows for. The failure area is restricted by the NDT criteria. The formula below (formula 5.2) can be used to calculate the total failure area (and thus the PoF of the girth weld) .

$$PoF = \int_{-\infty}^{\infty} F_{MAIF}(a) * f_{a_{present}}(a) \quad da \tag{5.2}$$

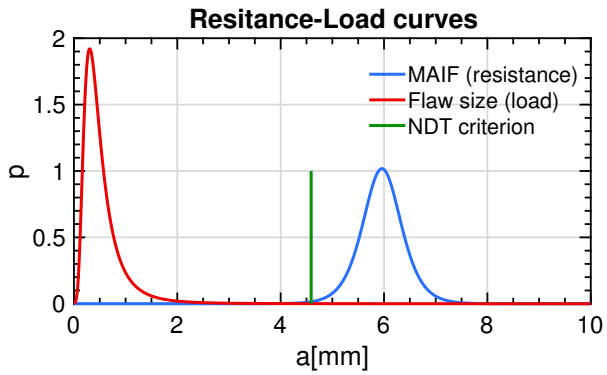

(a) The load and resistance curves including the NDT criteria

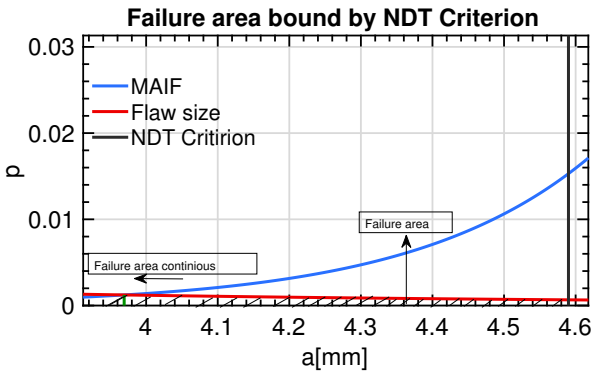

(b) Closeup of the failure area under the load en resistance curve restricted by the NDT criteria.

Figure 5.8: Resistance and load curve and the corresponding failure area

Formula 5.2 states the probability of failure can be calculated by multiplying the Cumulative Distribution Function (CDF) of the MAIF with the Probability Density Function (PDF) of the possible flaw size distribution, and taking the integral from -∞ to ∞. However the integration domain can be set to 0 for the lower boundary and the value of the NDT criterion as the upper boundary (black vertical line in figure 5.8).

This boundary can be set since a flaw can not attain a negative value (therefore the minimum value is 0) also the failure area is restricted by the NDT criteria, since any flaw found during NDT assessment which is above the NDT criteria set will be rejected and thus cannot lead to failure.

The NDT criterion accounts for all girth welds and should be set such that the area confined by the resistance/load curve and the NDT criterion is equal to the allowable probability of failure of a single girth weld. The lower the NDT criteria is set, the lower the probability of allowing a flaw size larger than the MAIF to pass as acceptable. This naturally lowers the probability of failure of a girth weld.
Therefore equation 5.2 becomes:

$$PoF = \int_{0}^{NDTcriterion} F_{MAIF}(a) * f_{a_{present}}(a) \quad da \tag{5.3}$$

By varying the NDT criterion between zero and any value higher than zero, the probability of failure of a girth weld corresponding to that range NDT criteria can be calculated. By plotting the PoF against the range of NDT criteria a probability of failure curve is created from which the PoF of a single girth weld versus the NDT criteria can be found (see chapter 6).

Algorithm for finding the MAIF and probability of failure curve model 1

The procedure to determine the MAIF and finding its corresponding PoF, using model 1:

1. Determine the amount (N) of cycles needed in the Monte Carlo

2. Create a data base with size N of the YS, UTS and JR curves

3. For each cycle the corresponding data set is given as input in the fracture mechanics formulas

4. Determine the initial flaw size 'a' to start the iteration from, the iterative process will automatically decrease or increase this value if no immediate intersection/flaw growth is found from the first iteration

5. The iterative process will check the boundary condition of having at least one intersection point with the FAD and staying within 0.5 mm flaw growth from the initial flaw size

6. If the flaw growth is within the boundary conditions the initial flaw size will be increased, and flaw growth will be checked against the boundary conditions again

7. Once the boundary conditions are met, the initial flaw size is at its maximum and now called MAIF

8. The MAIF is saved in a database which will grow to N samples (equal to the amount of cycles in the Monte Carlo)

9. Using the BIC criteria the best fit distribution can be found for the MAIF

10. Solving the Z-function Z=MAIF-$a_{present}$ the probability of failure of a single girth weld can be found corresponding to the NDT criterion set

Pros and cons of model 1

The advantage of using model 1 to assess probability of failure is the explicit calculation method to determine the probability of failure, once the MAIF are found multiple distributions on the MAIF can be tried. Also multiple distributions for the flaw size can be tried, this allows for fine tuning of (for example) the weld requirements. The explicit calculation method also allows for a good understanding of the underlying processes and provides insights on potential improvements on the model. A clear disadvantage of using model 1 is the iteration time needed to calculate the PoF, especially when moving to more than 1 cycle iteration will have to take place over multiple cycles to determine the MAIF.

Pros:

- Explicit calculation method, allows for easy/efficient adjustment of the distributions
- Offers good insight in determining the poF of a girth weld
- Currently faster than model 2 in computing the failure curve

Cons:

- Possible inaccurate fit for MAIF and thus influencing the calculated PoF of a single girth weld

5.2.3. Model 2

With the insights gained from model 1, a second model can be developed that might be able to reduce the run time for determining the PoF of a girth weld or can be used to validate model 1. Model 2 just like model 1 is built on top of the fracture mechanics formulas but does not make use of the iterative processes as in model 1 and thus does not calculate the MAIF. Model 2 uses a more implicit way of determining the PoF of a single girth weld. As input not only the material properties are provided but also a weld flaw size present in the girth weld is simulated. Per cycle the model checks if the provided weld flaw is safe by checking if the flaw will be stable (within FAD, less than 0.5mm flaw growth). The number of flaws that cause failure of the weld will be saved together with the size of the flaw and the material properties of the pipe, by knowing the total amount of runs the PoF of a single girth weld can be calculated..

For a graphical representation of the process of model 2 see figure 5.9

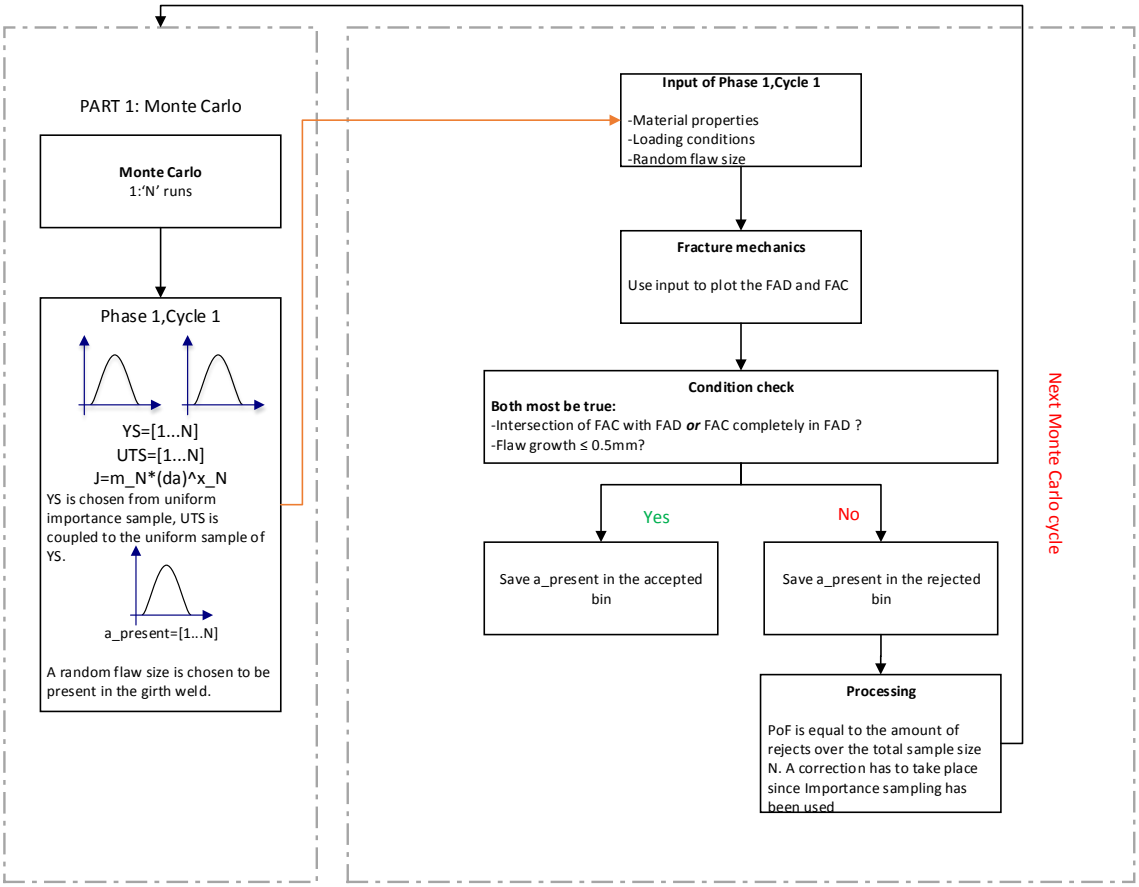

Figure 5.9: Flow chart of the process to calculate maximum allowable initial flaw size and PoF

Number of samples

A drawback of using model 2 compared to model 1 is the increased number of cycles needed in order to obtain an accurate result. This follows from the low probability of an unfavorable load case/flaw size combination to occur. Therefore more cycles are needed to produce these kind of load cases and cover the full range of probability of failure are needed.

An estimation of the total number of samples needed in order to achieve a PoF of e.g. 10^{-4}

can be done by using the following formula [14].

$$
\begin{aligned}
&V_{pf} = \frac{\sigma_{pf}}{P_f} \simeq \frac{1}{\sqrt{N * P_f}} \\
&Where: \\
&V = Coefficient\ of\ variation\ (relative\ error) \\
&N = Number\ of\ samples \\
&Pf = Probability\ of\ failure
\end{aligned}
\tag{5.4}
$$

Taking a coefficient of variation of 0.01 and a probability of failure for the pipeline system of 10^{-4} already 10^8 Monte Carlo samples are needed. With every cycle taking about 10^{-5} seconds this would mean the model has to run for ~ 41 days straight to achieve this accuracy. This is not a reasonable time domain.

Importance sampling

A method to prevent the excessive sampling time is to use importance sampling. Importance sampling is a method that can be used to reach more success (in this case failures) in less Monte Carlo cycles by using a sampling function to draw samples from, instead of the original distribution. This sampling function is chosen such that more draws will come from the (expected) failure region.

Because more draws will come from the failure area using the sampling function than when using the original distribution the PoF calculated by means of importance sampling needs correction [10].

Where normally the PoF is calculated as:

$$
PoF = \frac{N_{failure}}{N_{total}} \tag{5.5}
$$

The probability of failure using importance sampling is:

$$
\begin{aligned}
&P[N > N^*] = \frac{1}{n} * \sum_{i=1}^{n} I * [N_i > N^*] * c_i \\
&c_i = \frac{f(x)}{h(x)} \quad (correction\ coefficient) \\
&N^* = Threshold \\
&I = 1 \quad if\ [N_i > N^*]\ (Failure\ occurs) \\
&I = 0 \quad if\ [N_i < N^*]\ (No\ failure\ occurs) \\
&n = Total\ amount\ of\ samples
\end{aligned}
\tag{5.6}
$$

$c_i = \frac{f(x)}{h(x)}$ is called the correction factor and is defined as the probability density of drawing a failure from the original distribution f(x) divided by the probability density of drawing the failure from the sampling distribution. Since multiple inputs from multiple PDF are used for model 2 the correction factor should also correct for multiple importance sampled variables. For model 2 the YS,mm (variable of JR-curve), and flaw size distribution are used to generate the random input. Also it is assumed the relation between these three variables in independent. Therefore the correction factor is defined as:

$$
c_i = \frac{f(YS)}{h(YS)} x \frac{f(mm)}{h(mm)} x \frac{f(a)}{h(a)} \tag{5.7}
$$

N^* is the threshold value and can be any real value at which failure is starting to occur. In the case of engineering critical assessment the variable N^* can be set to the NDT criteria where N_i equals a flaw size present in the girth weld. This way it is possible to determine how many flaws smaller than the NDT criteria set (i.e. acceptable flaws) would still fail when using NDT criteria N^*, making it possible to calculate the PoF of a single girth weld at that specific NDT criteria. Varying the NDT criteria between 0 and a positive value creates the PoF curve just like the one created in model 1.

Validation for model 1

In contrast to model 1, model 2 simulates a girth weld including a flaw present and wont iterate to the MAIF. In model 2 for each girth weld a weld flaw is simulated and checked it meets the criteria (i.e. flaws regarded as stable within set NDT criterion), this provides a simple yes/no answers if the simulate girth weld will fail. Simulating enough girth welds provides the probability of failure of a girth weld without the need of fitting a distribution to the MAIF, this takes away an uncertainty in the calculation processes of the PoF of a girth weld.

By taking away this uncertainty in the calculations process of the PoF, one can expect that when enough samples are run for model 2 the output will be more exact than the output of model 1. Therefore model 1 can be validated by comparing the probability of failure lines to that of model 2. If any big discrepancies are shown possibly the assumed distribution for the MAIF in model 1 is not correct, and further optimization of model 1 is needed.

Algorithm for determining PoF curve model 2

1. Determine the amount (N) of cycles needed in the Monte Carlo
2. Create a data base with size N of the YS/UTS, JR curves, and random flaw size
3. For each cycle the corresponding data set is given as input in the fracture mechanics formulas
4. Calculate flaw growth of the inserted flaw size, if flaw is stable and within limits the flaw size is place in the accepted flaw size bin'. If the flaw is unstable and not within limits safe the flaw size in the unaccepted flaw size bin'
5. For all rejected flaws calculate the corresponding correction factor
6. Calculate the probability of failure for a range of NDT criteria to construct the PoF curve

Pros and Cons model 2

Pros:

- Possibly offers a more accurate computational method since the MAIF distribution is not assumed
- Possibly offers a faster computational method for the complete ECA, when importance sampling and number of samples is completely optimized.
- Model 2 can be used to validate the methods of model 1

Cons:

- Implicit method, when a new/better flaw distribution can be applied the whole model has to run again
- Multivariate importance sampling needs optimization to deliver accurate results in a reasonable time.
- Produces results for a small specified flaw size domain (the domain used for importance sampling)
- Currently 2.5x slower than model 1

5.3. Sensitivity analysis

In order to have an idea which variables in an ECA have the biggest influence on the outcome (flaw depth), a sensitivity analysis is performed using the deterministic fracture mechanics model. The most sensitive variables will have the biggest impact on the result and thus are a first choice to approach as stochastic variable. The sensitivity analysis is performed by making use of the fracture mechanics method as discussed in chapter 3. In chapter 6 a sensitivity analysis will be performed to indicate the sensitivity of the stochastic variables on the PoF of a girth weld/pipeline.

The sensitivity analysis is set up as follows:

1. For each variable in the sensitivity analysis a base value is set as reference
2. From the base value a minimum boundary and maximum boundary value is set
3. With the base value serving as the average between the minimum and maximum points are evenly distributed between the minimum and maximum boundary values, forming a vector
4. The vector now serves as input of the model, from this the influence of one variable can be measured on the Kr_{ass} and Lr_{ass} value, with the base value and corresponding Kr_{ass} and Lr_{ass} as reference
5. The change in both Kr_{ass} and Lr_{ass} can be expressed as percentual change or as actual delta in value with respect to the base value chosen at step one

The results of this method are presented in the figure below (figure 5.10). The four most sensitive parameters are presented. For the whole sensitivity analysis see appendix B. Figure 5.11 show the impact of a varying UTS on the K_r and L_r of the assessed flow. As can be seen from the flat line (no change) the UTS does not influence K_r and L_r. In figure 5.11 it can be seen that although UTS does not influence the assessment locus directly it does influence the FAC and thus the possibility and location of the locus intersecting the FAC. Therefore UTS has a direct impact on flaw growth and allowable flaw size and is regarded as a sensitive variable.

5.4. Variable distributions

Once the most sensitive parameters are indicated data has to be collected to fit the right distribution so it can be used as input for the probabilistic model. The data used in this thesis is collected from the pipeline material database of HMC. It is important to use a distribution that (closely) represents the measurement data, a misfit distribution can influence the PoF and MAIF and thus corrupt conclusion. Selection of the best fit during this research is supported by using the Bayesian information criterion.

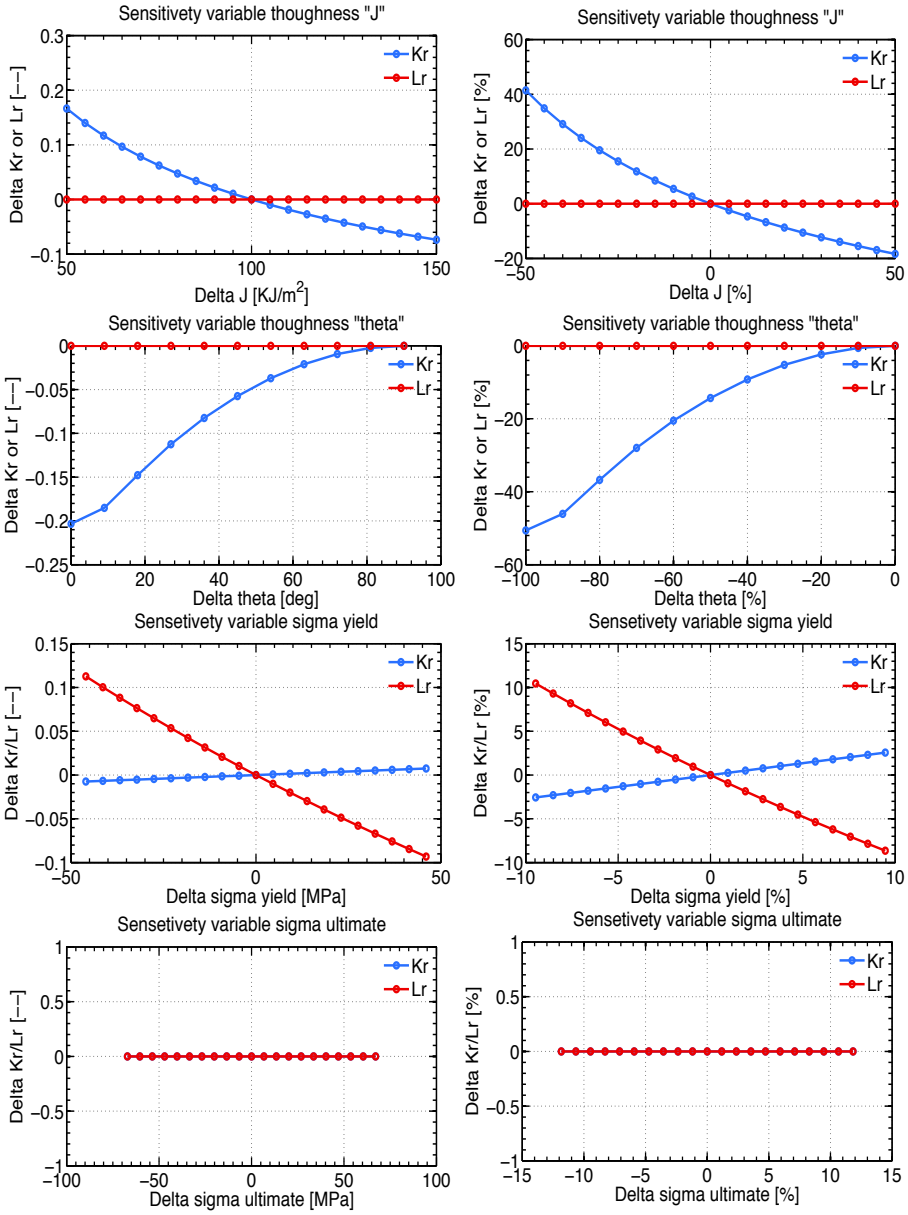

Figure 5.10: Left hand side of the figure graphs are presented with the actual change in size, where on the right hand side the percentual change is presented for a better comparison between the variables

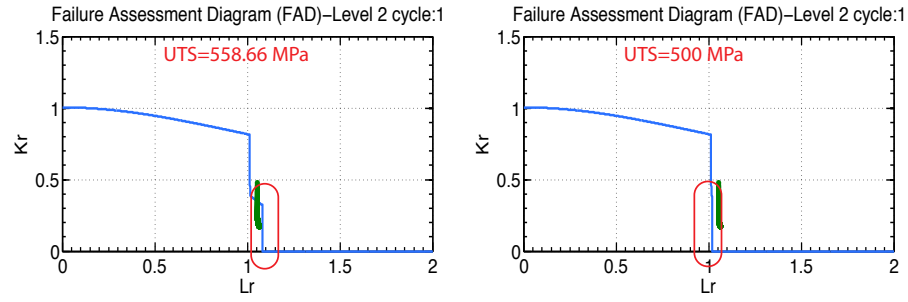

Figure 5.11: Effect of lowering the UTS on Lr_{max} and the probability of the locus intersecting the FAC (thus providing a safe weld)

5.4.1. HMC pipeline data base

The data used in this research is acquired from the HMC pipeline data base, this database consist out of a collection of pipeline data such as YS/UTS and dimensions of pipeline used

in previous projects. Since not all projects require to have the same properties measured, the number and type of data in the database is low. As has been mentioned in section 2.4 the data of Ichthys was not sufficient to base the probabilistic approach on, therefore it was chosen to work with the data of the Lucius project which uses a comparable pipeline and pipe material.

The pipeline data base of HMC for the Lucius project included to following data:

- 28 measurements for YS
- 28 measurements for UTS
- 3 JR-Curves (lower, mean and upper boundary)

While the YS/UTS are taken from the same sample and thus are coupled, the JR-curves follow from a different type of tes/sample.

5.4.2. Bayesian Information Criterion

A distribution that over/underestimates the variable or even excludes certain values might have a big impact on reliability calculations in the methodology. Therefore it is important to not only mathematically choose the right fit, but also account for the physical boundaries the variable might have for example a 'best fit' representing the flaw depth can not attain negative values. In order to quantify the goodness of fit, the Bayesian Information Criterion (BIC) can be used.

Bayesian Information Criterion

The Bayesian Information Criterion (BIC) is used to support determining the goodness of fit of a certain distribution on the data of interest. The BIC is defined as:

$$BIC = ln(n)k - 2ln(\hat{L}) \tag{5.8}$$

n=The amount of samples representing the data that should be fit
k=The number of parameters that are used to create a fit on the data
$\hat{L}$=The maximized value of the likelihood function with respect to the model fit to the data

The BIC penalizes for the amount of parameters needed in order to fit the data, preventing distributions that over-fit the data (and might not represent the 'real' distribution) to be selected as best fit. The lower the BIC score of a distribution the better it represents the data. Distributions can be compared to each other on basis of their BIC score, in general the following applies [15]:

Table 5.2: Interpretation of difference in BIC score between two distributions

Δ **BIC**	**Implication**
0 to 2	Distributions do not differ significantly
2 to 6	Distributions slightly differ
6 to 10	Significant difference in distributions
>10	Very significant difference in distributions

In section 5.4.3 multiple distributions are tried on the earlier determined variables and are compared on basis of their BIC score.

5.4.3. Distributions

Yield strength

The Yield strength(YS) data is taken from the Lucius project in pipeline data base of HMC, and is represented in the histogram in figure 5.12a. In the figure below (figure 5.12b) the histogram is converted in to its corresponding density, the distribution that are fit should get as close as possible to representing the data set.

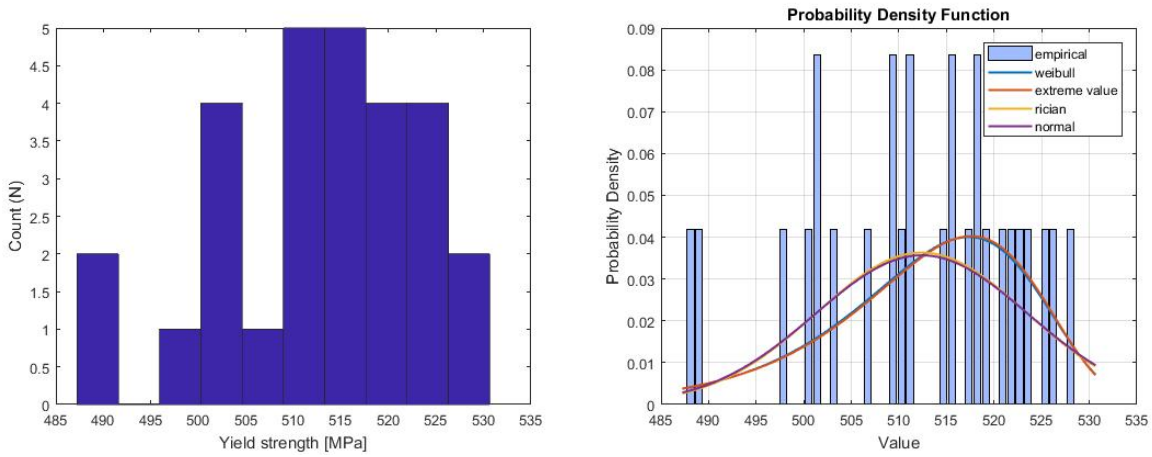

(a) Histogram of the Yield strength; total data set has the size of 28 measurements

(b) Multiple distributions fit on the density values of the yield strength

Figure 5.12: Distribution of the yield strength

From figure 5.12b it appears four distributions show a possible fit for the data based on their BIC score. If the BIC score of these four distributions are compared it can be concluded the Δ BIC is ~2 (see table 5.3. As has been been previously mentioned this implies the four distributions do not show a significant differences in fit as goes for representing the data. However a distribution should be chosen which properties (e.g. tail heaviness, symmetry etc) corresponds to process it represent. Literature suggests to use a normal,log-normal or Weibull distribution as the yield strength probability density function.[8]. Therefore as has also been suggested by the BIC score a Weibull distribution is chosen to represent the Yield strength in the development of the probabilistic model in this thesis

Table 5.3: Big scores of the top four distributions tried

Distribution fit to yield strength data	BIC score
Weibull	218.31
Extreme value	218.4
Rician	220.34
Normal	220.36

Taking a closer look to the data it should be wondered if 28 data points provide enough information to base a probability density function on, especially when the empirical density data is compared to the fits a clear mismatch is noticed . When looking at the histogram in figure 5.12a one could wonder when more data is available this histogram might turn symmetrical and a Gaussian (normal) distribution could represent the Yield strength. Even a triangular distribution with its minimum and maximum representing the minimum and maximum of the data set, and its peak located at the mean value of the data set seems to already be able to represent this (limited) amount of data. However the triangular distribution does not allow for a tail and therefore is capped(truncated) at the minimum and maximum value of the data set, therefore it would not be realistic to use.

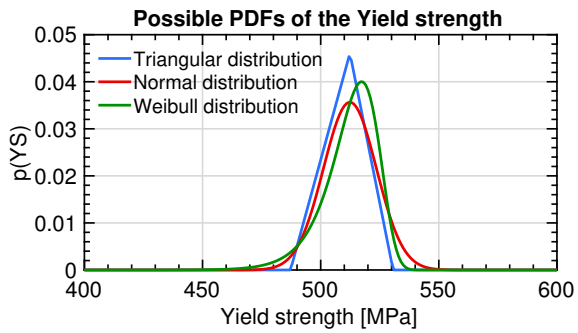

(a) Three fits tried on the yield strength data set

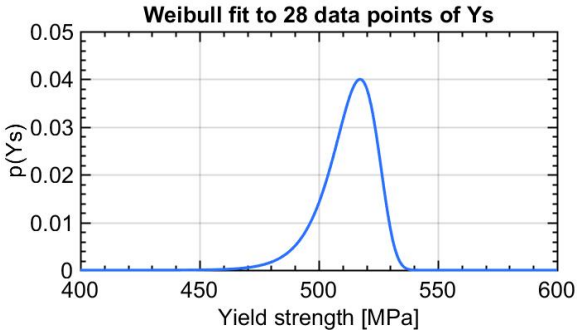

(b) Weibull distribution of the Yield strength

Figure 5.13: Probability density function of the yield strength

Ultimate tensile strength

The same argumentation used for the yield strength can be used for determining the distribution for the ultimate tensile strength. Also in this case literature suggests to use a normal,log-normal or Weibull distribution for the yield strength. [8].
The differences in BIC are negligible, the most likely distribution therefore is the Log-normal.

Table 5.4: BIC scores of the top four distributions tried

Distribution fit to ultimate tensile strength data	BIC score
Inverse Gaussian	210.17
Birnbaumsaunders	210.17
Log-normal	210.18
Gamma	210.28

It should be noted that again only 28 data points are available, and therefore a good and accurate estimation of the distribution is hard to make. In figure 5.15a it can be seen that also for the UTS a triangular and normal distribution is fit on the data, the triangular distribution it constructed with the same conditions as mentioned for the yield strength. Furthermore the log-normal and normal distribution are on top of each other, still a log-normal distribution is chosen for its property not to include values going below zero and its ability to form a tail (its non symmetrical) which is interesting if there is a need to represent a higher density of high/low UTS values.

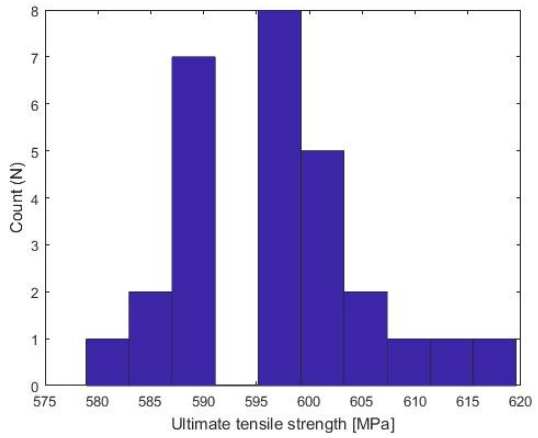

(a) Histogram of the ultimate tensile strength of a 8" pipeline total data set has the size of 28 measurements

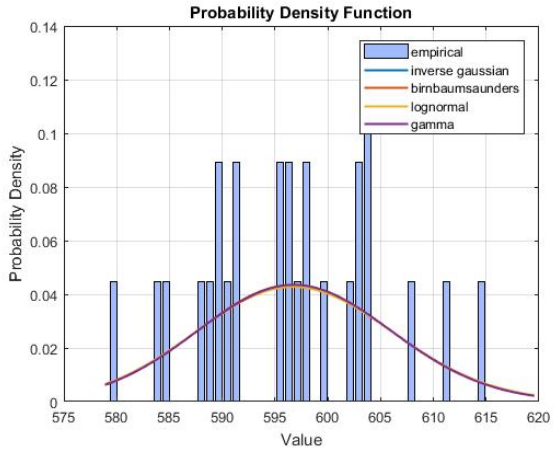

(b) Multiple distributions are fit on the density values of the yield strength

Figure 5.14: Distribution o the ultimate tensile strength

The fitted log-normal distribution to the ultimate tensile strength is presented in figure 5.15:

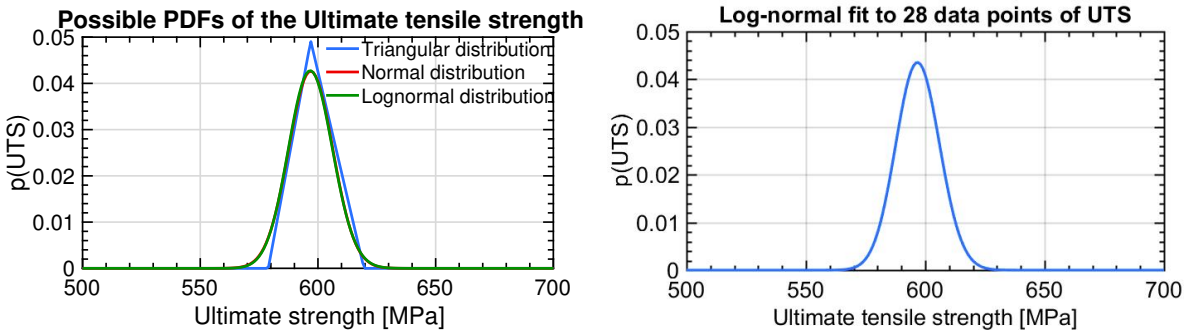

(a) Three fits tried on the yield strength data set

(b) Log-normal distribution of the ultimate tensile strength

Figure 5.15: Probability density function of the yield strength

Toughness

The toughness is described by the JR curve as has been previously explained in chapter 3. The JR curve is based on multiple material tests where a lower bound, mean and upper bound JR curve is determined (figure 5.16).

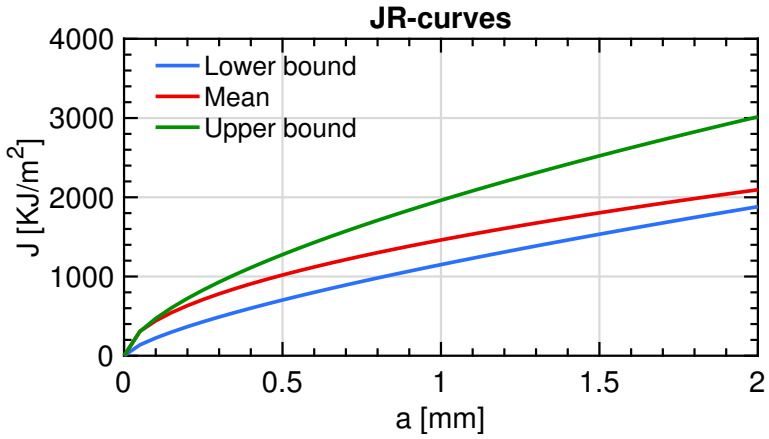

Figure 5.16: lower,mean and upper bound JR curves

All three JR curves can be described by the formula:

$$J = m * (da)^x \tag{5.9}$$

Where m and x determine the shape of the curve, and 'da' is the increase in flaw size from the initial flaw size. The variables of the three JR-curves in figure 5.16 are presented in table 5.5. The values of m and x follow from measurement data provided in the weld database of HMC [12]. Since it is assumed YS/UTS and toughness (thus the JR-Curve) are independent a

Table 5.5: Values 'm' and 'x' of the JR curves in figure 5.16

	m	x
Lower bound	1150	0.71
Mean	1461	0.52
Upper bound	1962	0.62

random pipeline material can have any JR-curve falling between the lower bound and upper bound. In order to find the curves falling in between the lower and upper bound JR-curve a way has to be found to create new 'm' and 'x' couples. To do this a scatter plot can be made of the variables m and x from table 5.5. In this case a linear regression can be applied to describe the relation between a random chosen m value and the corresponding x value

(see figure 5.17a). Note that the 'mean' JR-curve differs in shape form the upper and lower boundaries, if the mean curve would be more compliant to the shape of the outer boundaries it can be included in the interpolation in figure 5.17a and increase the accuracy of the regression. Once the relation between 'm' and 'x' is found random values of m can be chosen between 1150 and 1962 and linked through to the corresponding x values, this way new JR curves can be constructed between the lower and upper bound JR curves.

In order to draw random numbers of 'm' a normal distribution is assumed which is truncated at the lower and upper boundary with the mean equal to the 'm' value for the mean curve in table 5.5. A normal distribution is assumed since it is expected the production process of the pipeline material and pipeline itself is done under controlled circumstances, therefore it is likely the properties will vary around a mean.

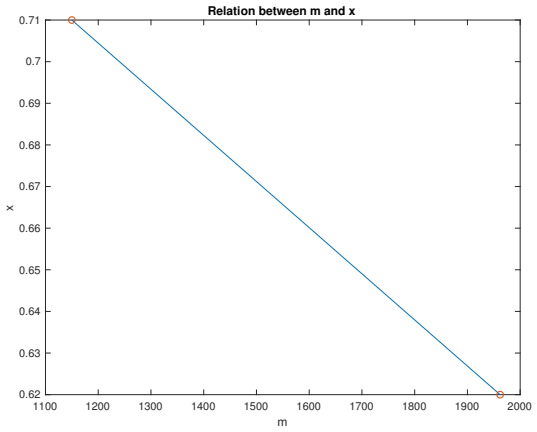

(a) Relation between m and x provided by a linear best fit

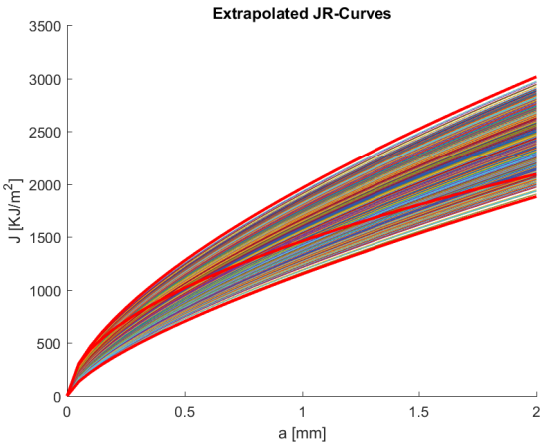

(b) 10,000 JR curves constructed between the lower and upper bound JR curves

Figure 5.17: Linear fit and construction of new JR curves

5.4.4. Correlation between variables

As explained in section 5.2 the distributions are used to draw random samples that can be used in a Monte Carlo type simulation model used in this research. One way of creating the random input can be done by creating two data sets each filled with random draws from the yield and ultimate tensile strength distributions respectively. This would be a correct procedure if there is no relation to be found between both variables (i.e. independence) what would imply the yield strength does not influence the value of the ultimate tensile strength in any way (and vice versa). However if the variables do show a relation to each other (dependency) the procedure of producing two random vectors from both distribution would not produce accurate results.

One way of showing dependence of two variables is to observe the correlation between these two variables. Correlation can be observed by plotting the measurement data in a scatter plot (see figure 5.18). From the scatter plot it can be seen there might be a linear correlation, the strength of this correlation will be determined later on in this section.

Note that correlation alone does not necessarily imply that there is a causal relationship. However both YS and UTS describe a property of the material that mainly follows from the material composition and production process of the pipeline and which is the same, therefore it can be assumed the correlation does indicate a causal relation.

To define how strong (or weak) a correlation is, the Pearson correlation coefficient between

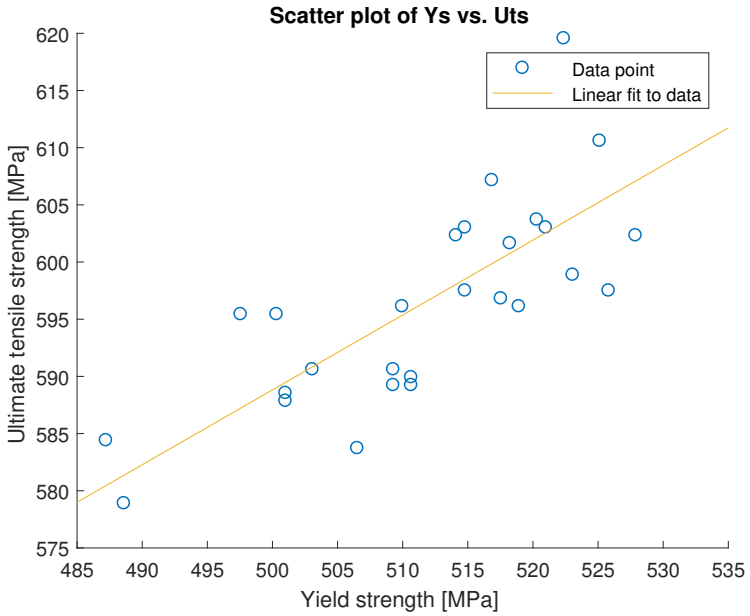

Figure 5.18: Scatter plot of the measured YS and UTS point of a 8" pipeline, the linear function is the least squares linear estimator

the two variables can be calculated. This coefficient is defined as:

$$\rho(X,Y) = \frac{Cov(X,Y)}{\sqrt{Var(X)Var(Y)}} \tag{5.10}$$

$$\rho(YS,UTS) = 0.7831$$

Where X and Y are two random variables (in this case they would be YS and UTS respectively). The value of ρ can range between -1 and +1, where -1 indicates a perfect negative linear correlation while a correlation coefficient of 1 indicates a perfect positive linear correlation. A correlation coefficient of 0 implies no (statistical) dependence between the two variables can be shown.A ρ between 0.7 and 1 indicate a strong positive linear relation, from this it can be concluded that the relation between YS and UTS is strong positively linear.[20]

5.4.5. Copula

It is clear from section 5.4.4 the yield strength and ultimate tensile strength are correlated and it would not be sufficient to simply create two independent random variables sets to use as input for the model. To create two correlated data sets use is can be made of a copula. The definition of the copula is clearly described by Kilgore and Thompson [16]: "The term "copula" refers to a function, called the dependence function, used to link two univariate distributions in such a way as to represent the bivariate dependence between the two random variables. The potential value of a copula is realized in that the copula is independent from the form of the univariate marginal distributions. Therefore, the marginal distributions can be chosen such that they provide a best fit of the univariate random variables, with the copula used to model the dependence behavior."

More formally Sklar's theorem [21] defines the copula function as:

$$F_{X,Y} = C(F_X(x), F_Y(y)) \tag{5.11}$$

Here $F_{X,Y}$ is the joint cumulative distribution function of the two marginal cumulative distribution functions $F_X(x)$ and $F_Y(y)$. C is the copula function providing the dependence structure between both marginal distributions.

Implementation

In order to use a copula the YS and UTS will have to be transformed in to uniform variables on the [01] domain. This can be done by taking the CDF of each variable using the previously defined distributions, the result of doing so is shown in figure 5.18.

To expand the uniform data set the copula that best represents the dependency has to be chosen. During this research four different types of copula where fit and assessed on their capabilities of creating a new data set for YS and UTS.

The following common copulas are tried to expand the data set:

- Gaussian Copula
- Clayton copula
- Gumbel Copula
- Student t copula

The parameters defining each copula can be calculated from the transformed uniform data set $[u, v]$. By using a copula the transformed data set $[u, v]$ can be expanded while maintaining the dependency (see figure 5.19b). Once the expanded uniform data set $[u, v]$ is found one can transform the variables to their original distributions by making use of the inverse CDF function of their original distribution.

Of the four copulas tried the Clayton copula was producing results best representing the YS/UTS dependency. For the results of the other copulas please see annex D.

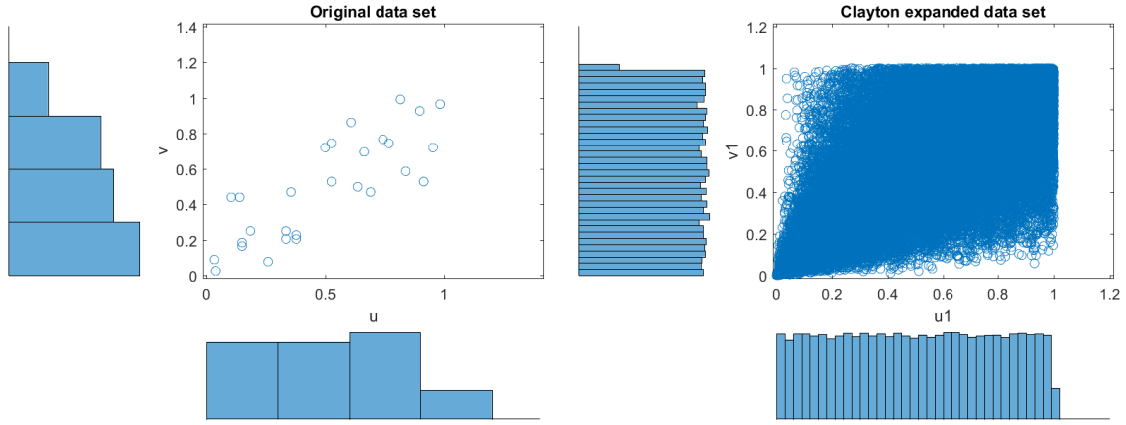

(a) Data set of YS and UTS transformed to the uniform space, u representing the transformed uniform values of YS and v the values of UTS

(b) Expanded data of u and v by using a Clayton Copula

Figure 5.19: From original uniform data set to expanded uniform data set by making use of the Clayton copula

Clayton copula

The results of using the Clayton copula to expand the data set of YS and UTS are discussed below. The expanded data set can again displayed on a scatter plot (see figure 5.20). As can be seen from the scatter plot the original data set is included in the expanded data set as the orange data points, this confirms the Clayton copula is able to reproduce the original data set. To further investigate if the Clayton copula produces a realistic expansion of the data, the expanded data set can be compared to the joint probability function of the original data set, which is computed by a bivariate kernel density estimator using a Gaussian kernel.

Kernel density estimation (KDE) is a non-parametric method of estimating the (joint) probability density function of a random variable distribution. A kernel (K) is a function that describes the influence of a data point in the data set as whole. [25][22].

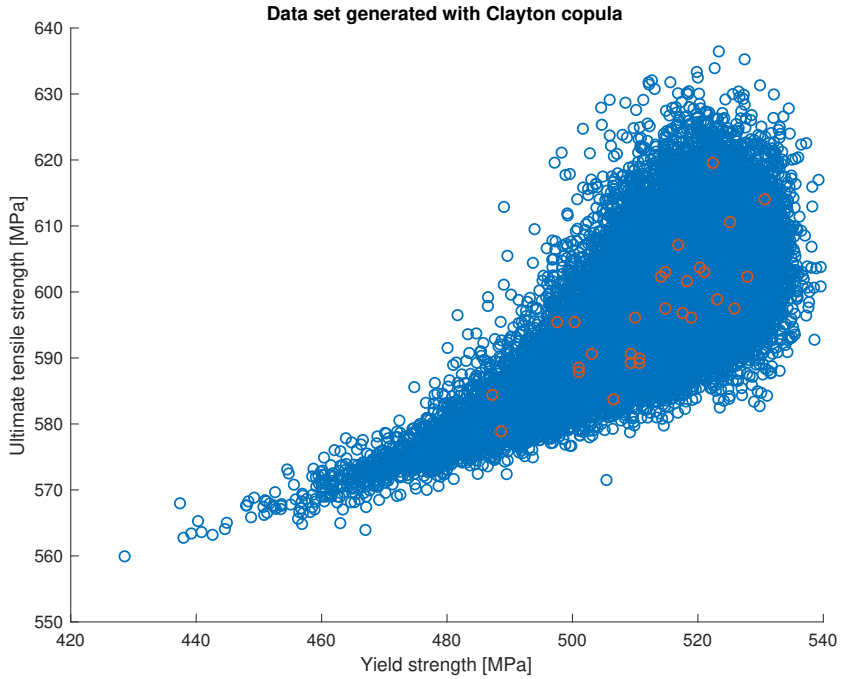

Figure 5.20: Expanded YS and UTS data by making use of the Clayton copula (blue), orange represents the measure data set

Some examples of kernels that can be used are:

- Uniform Kernel
- Gaussian kernel
- Triangular kernel

The center of a kernel will be placed above the data point, the contribution of each point can than be calculated by taking the total sum of the contributions for each point. Another important aspect of kernel density estimation is the bandwidth (h) used in the estimation, the bandwidth determines the width of the kernel. Taking the bandwidth to small might result in overestimating the probability density function, a bandwidth tot large will over-smooth the probability density function.

$$\hat{f}(x,h) = \frac{1}{nh}\sum_{i=1}^{n} K\left(\frac{x - X_i}{h}\right) \tag{5.12}$$

An example on to apply a kernel density estimation can be found in the figure below (figure 5.21) where a one-dimensional kernel density estimation is performed. Here a Gaussian kernel is placed above each data point and the contribution of each kernel results in the overlaying distribution. Performing a Gaussian kernel density estimation on the original data set of YS/UTS estimates the joint probability distribution function of both variables (figure 5.22a).

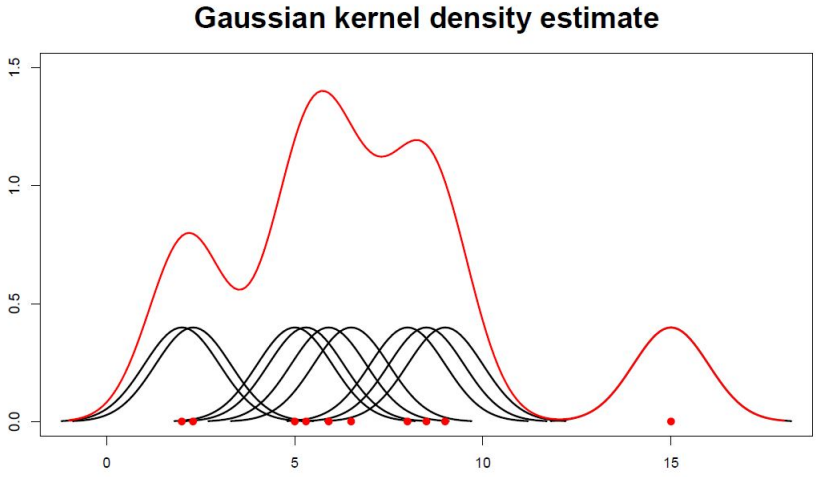

Figure 5.21: Construction of a PDF using kernel density estimation with a Gaussian kernel (figure from [23])

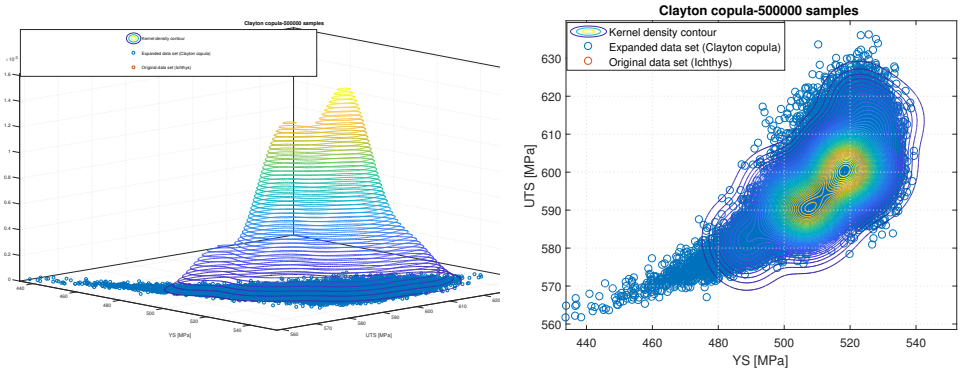

(a) Side view of the joint probability function estimated by making use of kernel density estimation

(b) Plot of the scattered data and the contour lines of the joint probability function of the original data set.

From figure 5.22b a scatter plot together with the contour lines of the joint PDF is plotted, it can be seen from the figure the Clayton copula might underestimate the number of data points in the lower regions (440MPa-460MPa) of YS and UTS. However more important are the data points representing high yield strength and high ultimate tensile strength (520MPa-540MPa), these conditions lead to failure at small initial flaw sizes. It can be seen that in this area the Clayton copula might slightly underestimate this region (since there are no data points present in a 50,000 points sample set). This on its turn might lead to overestimating the MAIF calculated in the models discussed below (as low YS/UTS lead to a higher MAIF). However the Clayton copula provided the best data compared to the other three copula tried (see appendix D).

In the tables below the generated data is compared to the original distributions determined for YS/UTS in section 5.4 to check if the generated data set falls in the range of these distributions (see table 5.6). In order to do so their cumulative distribution functions (CDF) are used for the minimum and maximum value in a expanded data set. The CDF value for the minimum value in the data set is the CDF calculated with the origin in the left tail, for the maximum value the right tail is used as origin. It can be concluded the minimum and

maximum value correspond to the far left and far right tail respectively,implying the Clayton copula is able to expand over the complete range of the distributions of YS and UTS.

Table 5.6: Data analysis of 100,000,000 data points generated by Clayton copula

	YS[MPa]	UTS[MPa]	CDF YS (origin is the left tail)	CDF UTS (origin is the right tail)
Minimum	388.41	551.01	9.5951E-08	1.5923E-07
Maximum	543.86	647.85	7.3636E-08	7.8564E-08

In section 5.4.4 the correlation coefficient of the original data set is calculated to be 0.7831, however the correlation coefficient of the expanded data set varies per generated set. It was found that the correlation coefficient varies over the sample size of the expanded data set. In figure 5.23a and figure 5.23b two histograms are provided displaying the count of varying correlation coefficient occurring over 1000 expansions of the data, for histogram 5.23a a expansion set size of 1000 is used, in histogram 5.23b a expansion set size of 100,000 points is used. It can be seen that by increasing the expansion set size the correlation coefficient falls in a smaller domain, and is more likely to correspond to the correlation coefficient of the original data set.

It was found that by restoring the default random number generator of Matlab before each new generated expanded data set the correlation coefficient per expanded data set will stay constant (see figure 5.23c).
From the histogram it can be concluded that the copula is able to reproduce the correlation coefficient of the original data set.

Last check is to verify the ratio of the yield strength to ultimate tensile strength (y/t ratio). The comparison can be found in table 5.7. The ratio of the expanded set is within reasonable (physical) limits, however the comparison to the original data set is hard since the limit amount of data in this set.

Table 5.7: y/t ratio of original and expanded data set

y/t ratio	Min.	Max.
Original data	0.8337	0.88
Expanded data	0.7654	0.9093

Remark on the use of Copula

The section above makes an effort to verify the expanded data by comparing the expanded data set to the contour of a kernel density estimation of the original data. From figure 5.22b it can be seen a good amount of the expanded data falls inside of the contour lines and the expansion happens within the physical limits of the material (table 5.6), however the validity of the density of the expanded data set is unconfirmed. Therefore it is hard to tell if certain data points in the expanded data set may be over- or underestimated during in the expansion.

Much uncertainty exists in the accuracy of the fit of the kernel density joint PDF on the original data, since the original data set is so limited in size. The same uncertainty exists for the accuracy of the expanded data set, since the copula parameters are calculated from this same limited data as well. It is strongly advised to expand and collect more measurement data in order to verify the use of copula for expanding the YS/UTS data set.

5.4.6. Initial flaw distribution

In order to determine if a failure of the girth weld occurs the possibility of a flaw present and the size of this flaw has to be known. As stated in the assumptions in the chapter and of the load case (see chapter 3) the focus lays on external flaws in which embedded flaws can

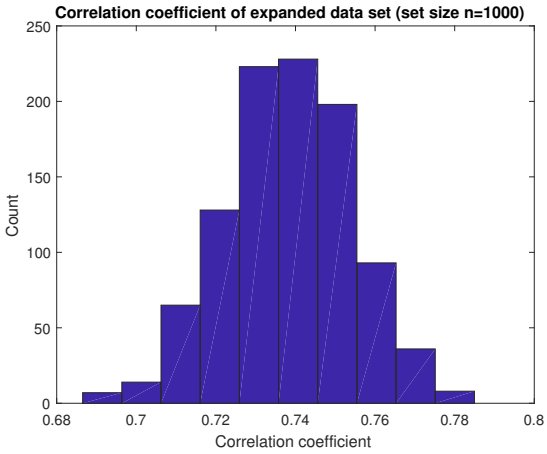

(a) Correlation coefficient of expanded data set with size 1000

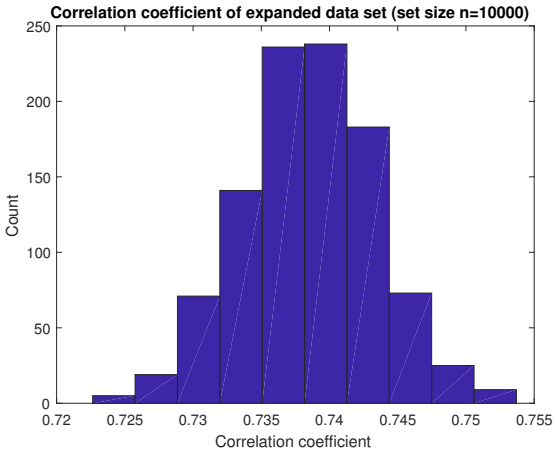

(b) Correlation coefficient of expanded data set with size 100000

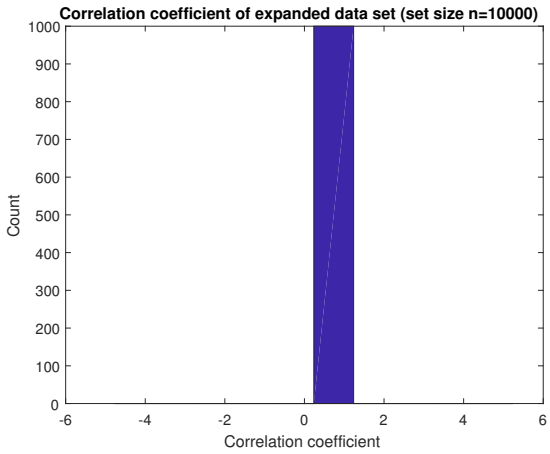

(c) Correlation coefficient of expanded data set with size 10000 with fixed random number generator

Figure 5.23: Correlation coefficient dependency on sample size and random number generator

be included. From AUT data collected during the Kaombo project the following data can be collected:

- Number of flawed girth welds
- Number of flawless girth welds
- Length (a) and width (2c) of the defects

Using the length data a distribution can be fit to the flaw size present in a girth weld (see figure 5.24). The Generalized Extreme Value distribution was found to be the best fit to this data with parameters:

5.5. Fracture mechanics model verification

Two models have been developed during this research, each of the models use a different approach in order to determine the MAIF and its accompanying probability of failure. However the probabilistic model will be built on top off the the fracture mechanics formulas as they have been discussed in chapter 3. The validation is done by running a base case in Crackwise

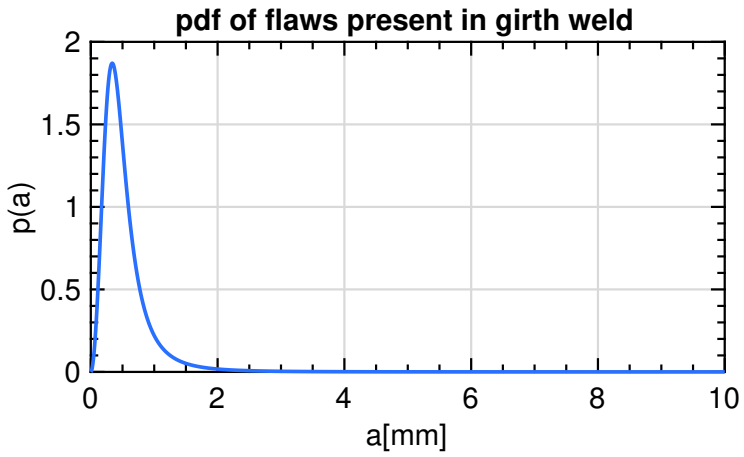

Figure 5.24: Generalized Extreme Value distribution fit on the flaw sizes found in girth welds

and the fracture mechanics model developed in this thesis. The base case used to compare both outputs can be found in table 5.8, in figure 5.25 the output of Crackwise and the model is displayed. It can be seen no concerning difference (delta) in governing fracture mechanics parameters can be found. Any discrepancy that is present is caused by the significance of Crackwise versus that of Matlab, since Matlab uses more significant numbers. Overall this does not have a concerning influence on the final results of the model, and therefore the Matlab fracture mechanics model is considered validated and can be used to further implement the probabilistic layer. Note that the probabilistic layer on top of the fracture mechanics formulas is not validated yet.

The validation of the model is based on the following input variables:

Table 5.8: Input for validation of the model

Input variable	Value
D_{outer}	219.1 mm
t_{pipe}	14.8 mm
$HiLo_{root}$	1.6 mm
YS	528.49 MPa
UTS	600.55 MPa
JR-Variable 'x'	0.53

Input variable	Value
E (Youngs modulus)	210000 MPa
ν (Poisson ratio)	0.3
Initial flaw length 'a'	1.74 mm
Initial flaw length '2c'	25 mm
θ	90 deg.
JR-Variable 'm'	530

Variable	Crackwise	Model	Delta
V	1.0866	1.0866	0
ρ	0.0163	0.0163	0
ϕ	1.0284	1.0284	0
g(90)	1.0000	1.0000	0
fθ(0)	0.4010	0.4010	0
fθ(90)	1.0000	1.0000	0
M1	1.1173	1.1173	0
M2	2.0715	2.0715	0
M3	-0.3978	-0.3978	0
Mm(90)	1.1149	1.1149	0
Mb(90)	0.9561	0.9561	0
M	1.0000	1.0000	0
fw	1.0001	1.0002	1E-04
Km	1.0000	1.0000	0
Yσp	584.9100	584.9054	0.0046
YσS	589.1900	589.1934	0.0034
YΔσP	589.1900	589.1934	0.0034
Yσ	1174.1000	1174.1000	0
Qm	528.4900	528.4900	0
Qb	0.0000	0.0000	0
KI	2760.8000	2760.8000	0
Lr_assessed	1.0067	1.0067	0
Kr_assessed	0.8827	0.8827	0
a_int	1.7400	1.7400	0
a_crack	2.2400	2.2400	0

Figure 5.25: Table of governing parameters in fracture mechanics calculations, no concerning difference between the model and Crackwise software is found

5.6. Reliability of a pipeline system

In order to interpret the output of model 1 and model 2 the the reliability of the whole pipeline system should be brought back to the reliability of a single girth weld. In this section the pipeline system will be defined and the probability of failure for the pipeline system will be defined.

5.6.1. Type of system

As has been mentioned in 2.4.1 a typical reeling project can be considered to exist out of three reel drums. The pipeline system is considered as all pipeline of the three reels connected to each other. The pipeline can be seen as a series system, this implies that one failure of a girth weld causes failure of the complete pipeline (therefore also called a weakest link system). In the figure below (figure 5.26) the pipeline system of 'n' pipes is shown, each pipe with resistance R_n and the loading on the pipeline displayed by S. The top figure shows an unbroken series system i.e. all links (girth welds) are intact and the pipeline does not fail. The bottom figure shows a broken system, in this case the girth welds between pipe 1 and pipe 2 is broken and the whole pipeline failed under load S.

5.6.2. Probability of failure-Series system

For a series system of multiple elements the failure space is defined as shown in the top formula of figure 5.27[14]]. In order for the series system to be safe each element should offer a higher resistance (R) then the loading (S) endured by that element.

The probability of failure (PoF) of a series system depends on the dependency between its

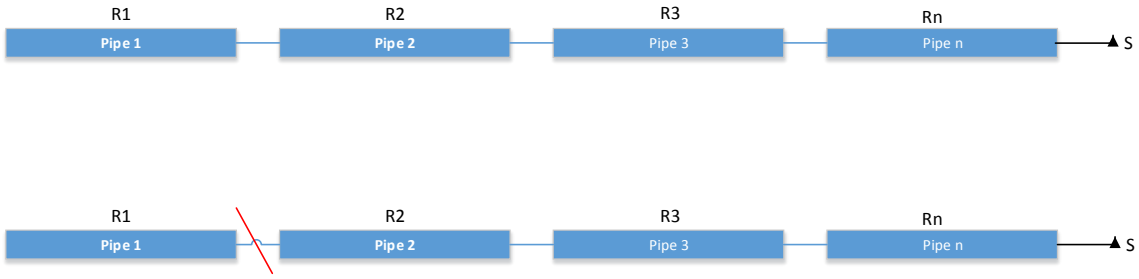

Figure 5.26: The pipeline considered as a series system; Top figure showing an unbroken system, bottom figure showing a broken system at the girth weld between pipe 1 and pipe 2.

$$R_1 < S_1 \cup R_2 < S_2 \cup R_3 < S_3 \cup \ldots \cup R_n < S_n$$

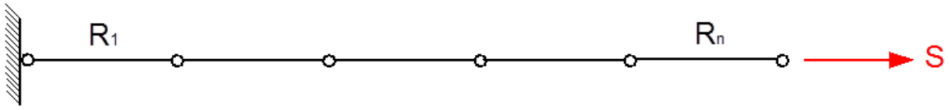

Figure 5.27: Failure space of a series system, for each element in the series system the resistance (R) should be larger than the load (S) in order not to fail[14]

elements. The three typical cases of dependency for a series system are:

- Mutually exclusive
- Independent
- Dependent

Generally speaking for a series system the fundamental boundaries (i.e. the absolute minimum and maximum) of the PoF can be defined as[14]:

$$max(P(R_i < S_i)) \leq P_f \leq \sum_{i=1}^{n} P(R_i < S_i) \tag{5.13}$$

With the lower boundary $max(P(R_i < S_i))$ being the PoF of the series system assuming mutual exclusivity between each element, and the upper boundary $\sum_{i=1}^{n} P(R_i < S_i)$ being the poF of the series system assuming a full dependency between each element.

Case	Mutually exclusive	Dependent
Correlation coefficient. ρ =	-1	1
Venn diagram	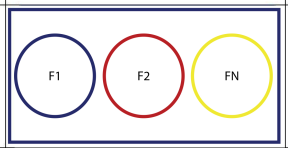	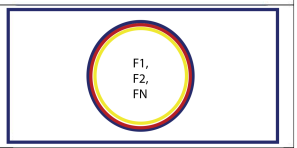
System failure probability $P(F)$	$\sum_{i=1}^{n}$ FN	max(F1,F2,FN)

Figure 5.28: Upper(mutually exclusive) and lower(Dependent) boundary of failure of a series system [14]

For a pipeline that is considered as a series system it would not be right to assume mutual exclusivity , as it would imply failure of a girth weld can not happen on multiple locations in the pipeline at the same time (as can be seen from the the non overlapping Venn diagram

in figure 5.28). The girth welds are not fully depended either, as it can be concluded not all girth welds fail once one girth weld has failed.

This leaves the option of complete independent failure of the girth welds, which is not necessarily true either since each girth weld is made with the same equipment,craftsmanship and material and therefore some form of correlation between failure of one girth weld and another can be expected. Therefore it is most plausible the PoF of the pipeline ranges between that of an independent and dependent system. Since the correlation between the girth welds is not known for now it is assumed the pipeline PoF is independent between girth welds.

5.6.3. Industry standards

The industry standard for offshore pipeline/structures is provided by DNV-OS-F101 [19] and specifies the allowable probabilities of failure depending on the consequence of failure of the component and its limit state category.

In the offshore DNV code [7] a classification list can be found that specifies the limit state categories for different failure modes in different scenarios (see figure 5.29). Since this thesis has its focus on the installation phase of a reeled pipeline in which fracture is the failure mode in consideration, the ultimate limit state is used for design and calculations.

	Ultimate limit states							*Serviceability limit states*			
	Fracture			*Instability*							
				Local buckling							
Scenario	Pressure containment	Fatigue	Fracture	System collapse	Propagating buckling	Combined loading	Global buckling	Dent	Ovalisation	Accumulated deformation	Displacement
Wall thickness design	X			X	X						
Installation		X	X	X	X	X			X		X
Free-span	(X)	X	X			X					
Trawling/3rd party	(X)					X		X			
On bottom stability	(X)	(X)	(X)			(X)		(X)	(X)		X[1]
Pipeline Walking						X					
Global Buckling	(X)	X	X			X				X	
1) Typically applied as a simplified way to avoid checking each relevant limit state											

Figure 5.29: Classification of limit states according to [7]

In figure 5.30 the annual allowable failure rates specified by the DNV offshore code are given, it is assumed Heerema performs one project per year. While multiple failure modes are possible (see figure 1.8) over all phases (from installation till end of life) it is assumed fracture is the governing failure mode. After a discussion with pipeline engineers and consulting the reeling guideline for buckling failure ([5]), in which a probabilist analysis on buckling failure during reeling is performed. It is decided an allowable failure probability of 10^{-4} for a medium safety class ULS based on one project per year is sufficient for testing the static ECA methodology for the first reeling cycle in phase one.

One could argue the allowable probability of failure of the complete pipeline follows from the individual allowable PoFs of each phase. It is strongly advised to HMC to perform more research towards the allowable probability of failure of the pipeline (per phase), as it forms an important input for the developed methodology.

Limit State Category	*Limit State*	*Safety Classes*			
		Low	*Medium*	*High*	*Very High*[4)]
SLS	All	10^{-2}	10^{-3}	10^{-3}	10^{-4}
ULS	Pressure Containment[1)]	10^{-4} to 10^{-5}	10^{-5} to 10^{-6}	10^{-6} to 10^{-7}	10^{-7} to 10^{-8}
ALS					
ULS	All other	10^{-3}	10^{-4}	10^{-5}	10^{-6}
FLS[2)]					
ALS[3)]					

1) The failure probability for the pressure containment (wall thickness design) is one to two order of magnitudes lower than the general ULS criterion given in the Table, in accordance with industry practice and reflected by the ISO requirements.

2) The failure probability will effectively be governed by the last year in operation or prior to inspection depending on the adopted inspection philosophy.

3) Nominal target failure probabilities can alternatively be one order of magnitude less (e.g. 10^{-4} per pipeline to 10^{-5} per km) for any running km if the consequences are local and caused by local factors.

4) See Appendix F Table F-2.

5) The target shall be interpret as "probability that a failure occurs in the period of one year".

Figure 5.30: Industry standard classification for several limit states and consequence classes[19]

Part III (Chapter 6 and 7)

Results processing, Discussion, Conclusions Recommendations

6

Results

In chapter 5 the theory of the probabilistic models have been discussed. This chapter will discuss and interpret the output of both models. To study the effect of using a probabilistic approach versus the deterministic approach a reference (deterministic) case is determined first. Since both models discussed in chapter 5 provide the probability of failure for a girth weld, the required PoF of the complete pipeline is brought back to that of a single girth weld. Next the output of model 1 and 2 will be discussed and a sensitivity analysis is performed to explore the effect of each stochastic variable and copula (that provides the correlation between YS and UTS) on the probability of failure of a girth weld.

6.1. Deterministic (reference) case

To determine the effect of using a probabilistic approach versus the deterministic approach on the probability of failure of a girth weld (and thus the pipeline) a deterministic reference case is created.The DNV-OS-F101 offshore code provides a method of determining this deterministic reference case([19]). The data required for the deterministic case follows from the same material tests and thus the same distributions as required for the probabilistic approach can be used.

The deterministic case takes the upper-bound stress strain curve as input, which corresponds to yield and tensile strength values from the right tail in the distribution. Both values can be found by using the formulas in 6.1. The ultimate tensile strength follows from the Yield strength and the $\frac{y}{t}$ ratio, which in this case corresponds to the highest values found in the measured data sets. A high $\frac{y}{t} ratio$ indicates a material with low strain harding capabilities, this is unfavorable since it offers less resistance against plastic collapse.

$$YS = \mu_{yield} + Z * \sigma_{yield}$$
$$UTS = YS * \frac{y}{t} \tag{6.1}$$

In order to find μ_{yield} and σ_{yield} a normal distribution is assumed to fit the yield strength data. The factor Z corresponds to the number of standard deviations that should be added to obtain the value corresponding to the 84.1% fractile while having a 95% confidence. The factor Z depends on the amount of samples available and accounts for the inaccuracy when not enough data is available to determine an accurate distribution. This can be explained by the fact a distribution will be less accurate when less samples are available and therefore needs a higher correction to give 95% confidence at the 84.1% fractile. The factor Z depending on the amount of measurements and is given in figure 6.1[19]. The JR-curve is taken as the

Number of tests, n	*Z*
3	5.01
5	2.82
10	1.93
15	1.69
20	1.57
30	1.44
50	1.32
100	1.22
∝	1.00

Table 6.1: Z factor depending on number of measurements n provided by [19]

lower bound curve (see figure 5.16).

Combining the information provided above the deterministic load case can be defined as:

Table 6.2: Mean and standard deviation yield strength

	μ_{YS}	σ_{YS}
Yield strength	512.38 MPa	11.19 MPa

The minimum $\frac{y}{t}$ found between both data sets is equal to 0.8583, with 28 samples in total the Z factor is set as 1.44. Therefore the deterministic case is:

Table 6.3: Deterministic input for ECA

Yield strength	528.49 MPa
Ultimate tensile strength	600.57 MPa
min $\frac{y}{t}$	0.8538
JR-curve	1150*$da^{0.71}$

Using the deterministic load case from table 6.3 as an input in the ECA fracture mechanics model, the MAIF following from the deterministic load case is 4.45mm (see figure 6.4). The NDT criterion in this case is equal to the MAIF.

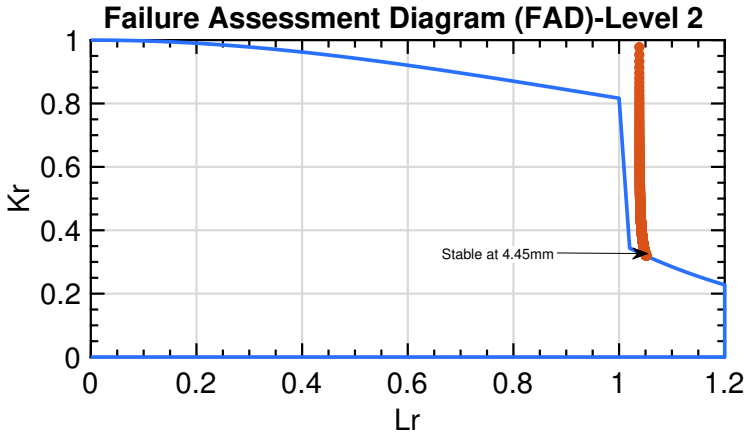

Table 6.4: FAD of the deterministic case

6.2. Post processing

This section will explain the steps taken to post processes and interpret the results produced by the models discussed in chapter 5. First the amount of girth welds taken in to consideration is calculated, next the probability of an external flaw in a girth weld is determined. This information it then used to post process the output of the models to compute the general probability of failure instead of the conditional probability of failure that is provided as

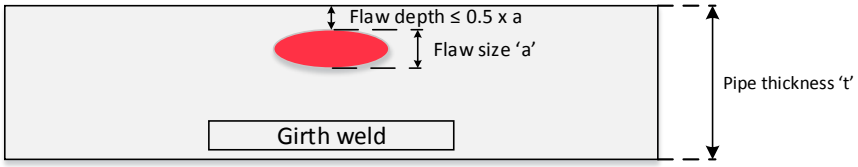

Figure 6.1: Criteria for an embedded flaw to be considered as an external surface flaw

output by the models.

6.2.1. Amount of girth welds

Since the model provides a PoF of a single girth weld, the allowable PoF of a complete pipeline should be converted to the allowable PoF of a single girth weld. To do this, first the total amount of pipe (and thus girth welds) in typical project should be known.It is assumed a typical pipe laying project uses three reels spooled with 8" pipeline equals, this equal to 6741 pipe segments in total per project (see section 2.4.1).

6.2.2. Number of external flaws

The fracture mechanics formulas implemented in the model are suitable for external flaws only, external flaws are flaws that are surface breaking on the outside of the girth weld or are located at a depth less or equal to half of the total flaw depth (see figure 6.1). Also see section 1.4 in chapter 1 for more information on classification of flaws.

The following AUT data was collected during welding operations over all weld stations on board of a pipe laying vessel (Kaombo project [11]). It is possible for the number of flaws to be larger than the amount of girth welds since multiple flaws per girth weld are possible.

Table 6.5: Weld flaw data of quad station

Quad joint welding station (793 girth welds)	#	Percentage of total
Unflawed girth welds	279	35.18%
Flawed Girth welds	514	64.82%
Total number of flaws	882	-
External flaws	7	0.79%

Table 6.6: Weld flaw data of hex station

Hex joint welding station (780 girth welds)	#	Percentage of total
Unflawed girth welds	377	48.33%
Flawed Girth welds	403	51.67%
Total number of flaws	818	-
External flaws	11	1.34%

Table 6.7: Weld flaw data of tower station

Tower welding station (832 girth welds)	#	Percentage of total
Unflawed girth welds	464	55.77%
Flawed Girth welds	368	44.23%
Total number of flaws	1063	-
External flaws	2	0.19%

Table 6.8: Weld flaw data over all welding stations

All welding station (2405 girth welds)	#	Percentage of total
Unflawed girth welds	1120	46.57%
Flawed Girth welds	1285	53.43%
Total number of flaws	2730	-
External flaws	20	0.73%

Over all welding stations the following can be concluded: Assuming that with same welding equipment and protocol equal numbers can be achieved in future projects, of all girth welds considered in the analysis 53.43% is flawed and 0.72% of those girth welds actually contains an external flaw (assuming a flawed girth weld only contains one flaw). Therefore it can be calculated that 0.39% (53.43%*0.73%) of all girth welds contains an external flaw. This percentage will be further used in section 6.2.3 to correct the probability of failure obtained from solving the limit state of model 1.

6.2.3. Post processing of model output

The models developed compute the PoF of single girth weld by calculating the enclosed area under the flaw size distribution and the MAIF distribution. Doing so is only possible when actually a flaw is present in the girth weld. In other words, the PoF of a girth weld as calculated by the model, is the PoF on condition a flaw is present (see equation 6.2).

$$PoF_{model} = P(MAIF < flaw | flaw\,present) \tag{6.2}$$

More interesting would be the probability the girth weld fails (MAIF<Flaw) and a flaw is actually present:

$$PoF_{general} = P(MAIF < flaw \cap flaw\,present) \tag{6.3}$$

To obtain the general probability of failure mentioned in formula 6.3 the following formula can be used ([14]):

$$\begin{aligned} &\frac{P(A \cap B}{P(B)} = P(A|B) \\ &P(A \cap B) = P(A|B) * P(B) \end{aligned} \tag{6.4}$$

P(B) mentioned in formula 6.4 is equal to P(Flaw Present) which is calculated in section 6.2.2 and is equal to 0.39%. Thus the probability that a girth weld fails on taking in to the account of a flaw actually being present is:

$$P(A \cap B) = P(A|B) * 0.0039 \tag{6.5}$$

Effectively this mean that the probability of failure vs NDT criteria curve (which is the output of the models) is multiplied by the probability an external flaw is present to arrive at $P(A \cap B)$ which governs the PoF of every girth weld in the pipeline.

6.2.4. Required PoF of single girth weld

As has been mentioned in section 5.6 the pipeline is considered to be a series system with each girth weld being an element of this system. The fundamental boundaries are provided in formula 6.6 , with as lower boundary the system considered with mutually exclusive elements and the upper boundary as fully dependent elements. The PoF of each element is considered

to be equal for all elements, so with 6741 girth welds (N) the fundamental boundaries are :

$$max(P(R_i < S_i)) \leq P_f \leq \sum_{i=1}^{N} P(R_i < S_i)$$
$$10^{-8} \leq P_f \leq 10^{-4} \tag{6.6}$$

Considering girth weld failure in the pipeline system is independent and using the industry standard provided in 5.6.3. The whole pipeline should provide a PoF of 10^{-4} which is defined as 'medium safety class' for its ultimate limit state (ultimate bearing capacity before failure), the PoF of a single girth weld can be determined by using formula 6.8 which is valid for independent series systems.

$$PoF_{pipeline} = 1 - (1 - PoF_{girth\ weld})^N \tag{6.7}$$

The formula in 6.7 can be rewritten to determine the required PoF of a girth weld to meet an overall PoF of the pipeline.

$$PoF_{girth\ weld} = 1 - (1 - PoF_{pipeline})^{\frac{1}{N}} \tag{6.8}$$

Now plugging in the required PoF of the pipeline and the total amount of girth welds 'N' (6741 girth welds) gives the required PoF of a single girth weld. For a PoF of the pipeline of 10^{-4}, the PoF of a single girth weld would be equal to $1.4835 * 10^{-8}$.

6.3. Model 1 results

This section will provide the results of the probabilistic analysis using Model 1. The results have been produced using the methodology discussed in section 5.2.2. Solving the integral provided in 5.2.2 and correcting it as mentioned in section 6.2.3 the PoF vs NDT criterion graph can be created, on the vertical axis the PoF of a girth weld is found, on the horizontal axis the corresponding NDT criterion to reach the corresponding probability of failure is indicated. The total run time to obtain the results of model 1 was 3,5 hours.

Model 1 is run with the following input/constraints (as has been discussed in chapter 5) :

- Weibull distributed Yield strength
- Log-normal distributed Ultimate tensile strength
- Clayton copula to provide the dependency between YS/UTS
- Normal distributed 'm' coefficient for constructing the JR-curve
- Flaw length '2c' of 25mm
- Generalized extreme value distribution of flaw size
- 30,000 Monte Carlo cycles

In figure 6.2 the probability of failure curves versus the NDT criterion of a single girth weld are plotted. Each curve uses a different probability density function (PDF) to represent the MAIF, the four best fits (according to the BIC score) are plotted. On the failure curves a single point is indicated that represent the required PoF and NDT criterion of a girth weld to achieve

the required PoF of the pipeline (10^{-4}) (see section 6.2.4).

In table 6.9 the required NDT values to achieve a PoF of 10^{-4} for the whole pipeline are stated. It can be seen in figure 6.2 that all four PDFs have close to the same results for NDT values larger than 5mm. However when lower Probabilities of failure of the girth weld (and thus pipeline) should be achieved the type of distribution used for the MAIF will start to have impact on the PoF of the girth weld, for example the Normal/Rician distributions will in the case of a lower required PoF of the pipeline allow for substantially larger NDT criterion than the t-Location and logistic distribution.

This shape difference origins from the probability density located in the far left tails of the MAIF distributions (this part of the tail is dominant in the PoF calculations, see section 5.2.2). While the t-Location scale/Logistic PDF still have a small density located in their PDF at the smaller MAIFS (left tail of the distribution), the Normal/Rician does not (see figure 6.3). From the method used for calculating the PoF a smaller area results in a lower PoF, as can be seen in figure 6.2. In general the t-location scale and Logistic distribution are more fit for representing 'outliers' since their tails are heavier. As can be seen from figure 6.3a all four (best

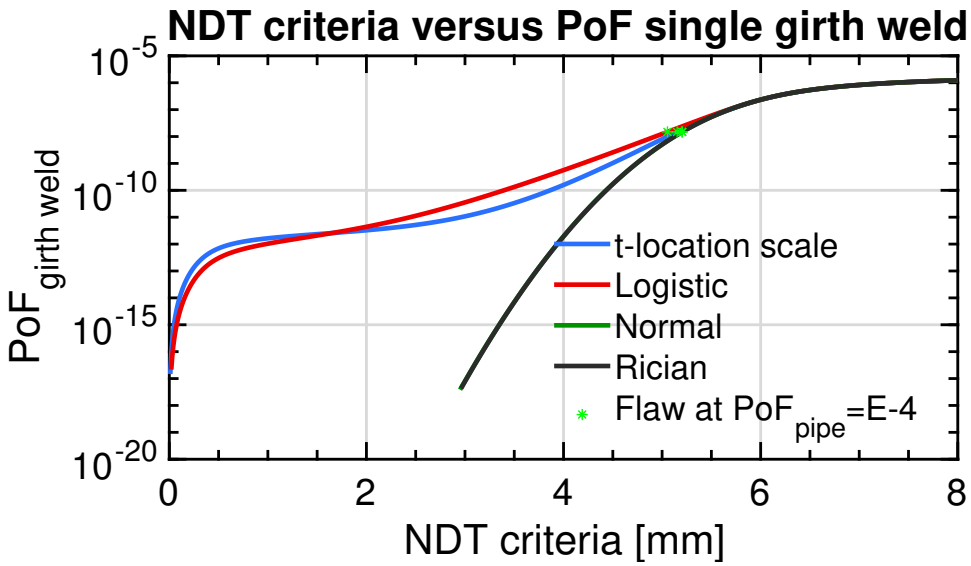

Figure 6.2: Probability of failure curves vs. NDT of a single girth weld

fitting) distribution for the MAIF are symmetrical around their mean and look very similar to each other. Since the distributions used as the input of model 1 are based on very limited data, and the toughness (which has high impact on flaw growth) is assumed to be normally distributed one can expect the MAIF to be normally distributed as well, however the Logistic PDF (which is very close to the normal distribution) is chosen to represent the MAIF due to its heavier tails and will be further used in the sensitivity analysis in section 6.3.1. A heavier tail is preferred to increase the density of at smaller MAIFS, this might be a conservative assumptions since it might overestimate the actual area in the left tail.

Comparing the deterministic NDT value (4.45mm) to the NDT value calculated with the reliability methods of model 1 (table 6.9) a difference of ~ 0.60mm-0.75mm between the deterministic and probabilistic NDT value can be noticed. From this it can be concluded that for the first cycle in phase 1 the deterministic static ECA might indeed bee conservative, and potential is there to increase the NDT criteria.

Table 6.9: Required NDT to achieve $PoF_{pipeline} = 10^{-4}$

Distribution	$NDTcriterion@PoF_{pipeline} = 10^{-4}$
t-Location scale	5.15 mm
Logistic	5.05 mm
Normal	5.20 mm
Rician	5.20 mm

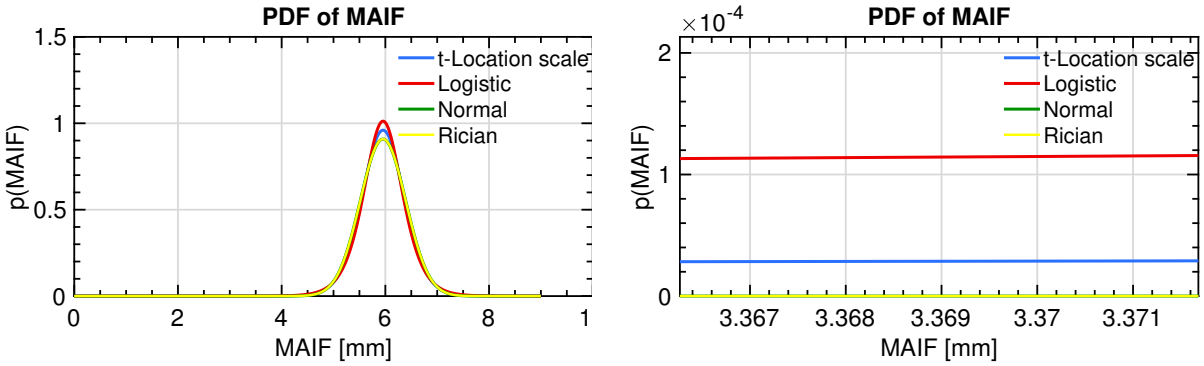

(a) PDFs of the MAIF

(b) Closeup of the density in the left tails, no density is present for the Normal/Rician

Figure 6.3: PDFs of the MAIF (left figure), and a close up of the density in the tail (right figure)

6.3.1. Sensitivity analysis on PoF of a girth weld

Multiple choices have been made on the type of distributions and copula to use in order to construct the probabilistic model. This section will perform a sensitivity analysis towards the effect of these decisions on the acceptable probability of failure of a girth weld.

The influence of the following items will be analyzed on their effect on the PoF of a girth weld:

- Type of distribution for the yield strength
- Type of copula
- Type of distribution of the 'm' coefficient
- Type of distribution of the MAIF (discussed in section 6.3)

In order to determine the sensitivity of the above mentioned variables for each variable 30,000 cycles are run while keeping the other variables unchanged. The Logistic distributions is used to represent the MAIF in the limit state function.

In figure 6.7 the PoF curves from the sensitivity analysis are shown.

Copula sensitivity

The first three curves show the impact of using a different copula, the figure shows that the Gumbel copula and the Clayton copula produce (almost) identical PoF curves. This can be explained when looking at the histogram of the MAIF produced by both copulas (figure 6.4a and 6.4b). As can be seen the histogram of the Gumbel copula covers some larger MAIFS than the Clayton copula, however for calculating the PoF the left tail of the MAIF distribution is of interest. Also it can be seen the PDFS of the MAIF almost fall on top of each other (figure 6.4c.Since the flaw distribution curve is the same, the PoF curves in figure 6.7 fall on to each

other.

The same analysis can be performed to explain the difference between the Gaussian and the Clayton copula, when using the Gaussian copula the MAIF distribution will have less density in the left tail, hence the PoF of a girth weld will be lower and a larger MAIF can be achieved for the same probability of failure of the pipeline. The density in the tails of the MAIF PDF is determined by the number of occurrences of that MAIF in a total sample set. Since the toughness is kept random with the same parameters for each copula variation it can be concluded the Gaussian copula produces less high yield/ultimate tensile strength samples (which result in low MAIFS) than the Clayton/Gumbel copula.

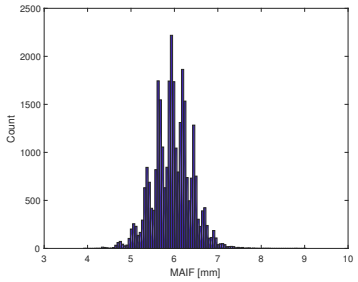

(a) Histogram of the Clayton copula

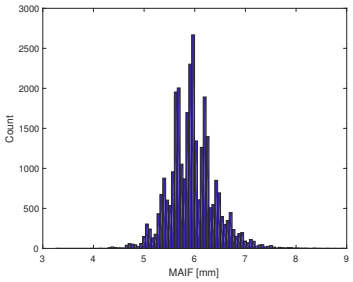

(b) Histogram of the Gumbel copula

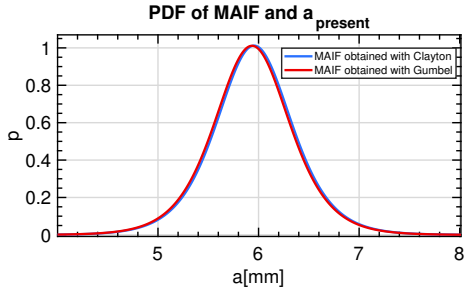

(c) PDFs of the MAIF resulting from the Clayton and Gumbel copula

Figure 6.4: Similar results for the MAIF using the Clayton or Gumbel copula

Yield strength sensitivity

In order to test the sensitivity of the yield strength on the PoF of a girth weld the distribution is changed from a Weibull distribution to a Normal distribution (see figure 6.5). From the figure it is clear when using a Normal distribution the probability of drawing a high yield (>530MPa) strength is higher than when using the Weibull distribution. A higher yield strength on its turn results in lower MAIFS, using a normal distribution thus results in higher probabilities of low(er) MAIFS during the Monte Carlo. This effect is clear when looking at 6.7 where the curve for the normal distributed yield strength has a higher failure probability per girth weld for lower NDT criterion than the curve for the Weibull distributed (standard) yield strength.

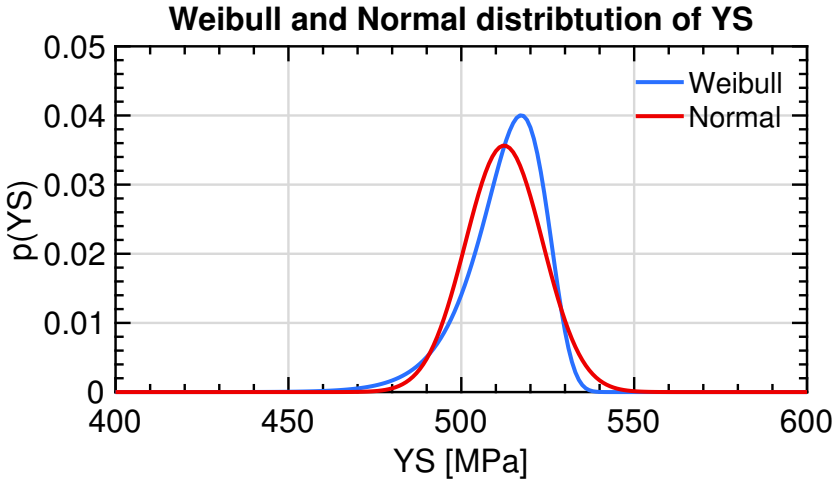

Figure 6.5: Weibull distribution and normal distribution fit on the yield strength data

Toughness sensitivity

The distribution of the toughness is the most sensitive towards the PoF of a girth weld, when the assumed normal distribution of the variable 'm' is changed in to a uniform distribution a clear shift in PoF can be noticed. This can be easily explained by the fact lower toughnesses will occur more often which result in lower PoF of the girth weld (see figure6.6).

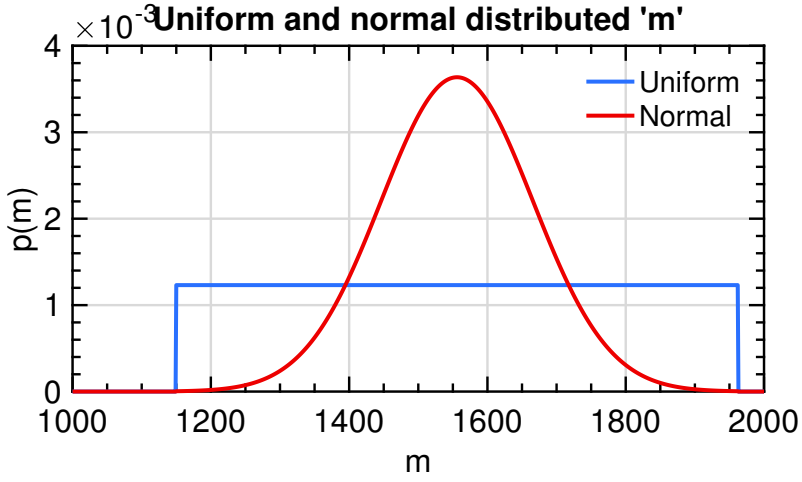

Figure 6.6: Uniform distribution and normal distribution used to draw variable 'm' used for constructing the JR-curve

Table 6.10: Required MAIF to achieve $PoF_{pipeline} = 10^{-4}$

Sensitive variable	NDT criterion @ PoF pipeline=E-4
Clayton copula (standard case)	5.05 mm
Gumbel copula	5.02 mm
Gaussian copula	5.15 mm
Normal distributed YS	4.90 mm
Uniform distributed 'm'	3.97 mm

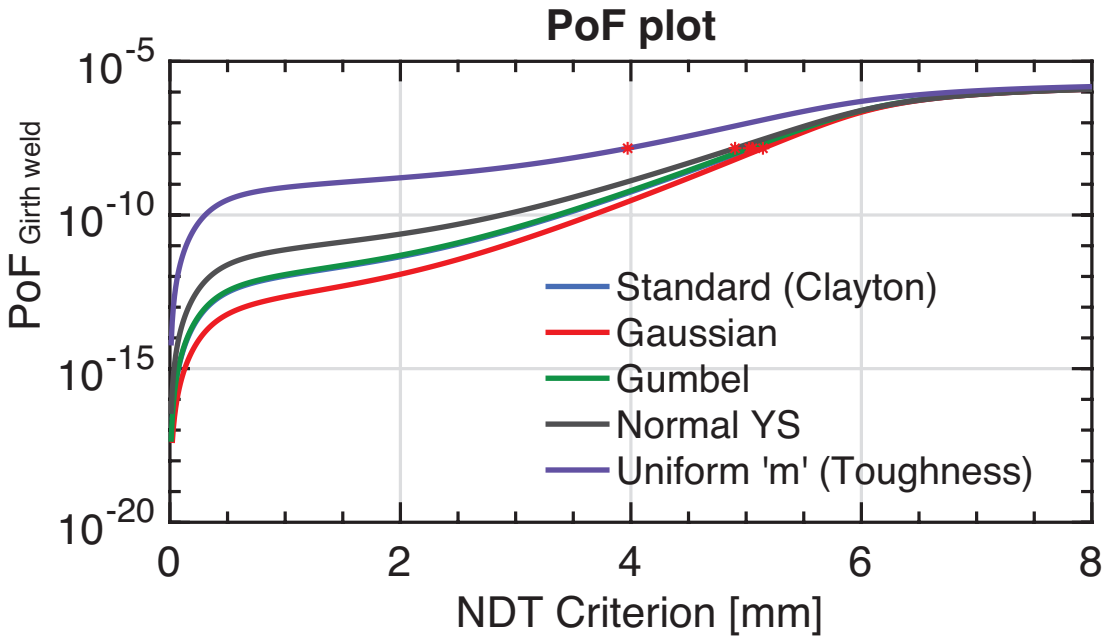

Figure 6.7: Sensitivity of the probability of failure curve vs. MAIF of a single girth weld, each MAIF distribution represented by a Logistic distribution

Sensitivity of flaw size distribution/probability of occurrence of a flaw

Since the distribution of the flaw size is a direct input of the limit state function that calculates the PoF, the shape and type of distribution will naturally have a direct impact on the PoF of a girth weld. When a distribution is chosen with a heavier right tail the failure area (enclosed area under the flaw size/MAIF distribution will increase) effectively raising the PoF.

The same goes for the probability of occurrence of a external flaw, the higher this number the higher is the probability of failure. Care should be taken to determine the distribution and probability of occurrence of the flaw as accurate as possible.

6.4. Model 2 results

This section will provide the results of the probabilistic analysis of Model 2 as discussed in section 5.2.3. The results are preliminary since the domain for importance sampling is in need of fine tuning and a suitable amount of samples has to be chosen. The results discussed in this section are based on 1,000,000 runs, in order to determine the required amount of runs it is advised to test with a varying range of samples.

6.4.1. Importance sampling domain

Importance sampling is applied to the yield strength distribution, 'm' distribution and the flaw size distribution. The ultimate tensile stress is obtained by making use of the Clayton copula again. In order to use importance sampling for all three distributions an uniform sampling distribution is applied on the area of interest (where failure is most likely to happen). The range over which the uniform distribution is applied is shown in the figures below (figure 6.8). The domains on which the uniform sampling distributions are applied needs further optimization, it is unconfirmed the domains indicated in figure 6.8 are optimal. It is challenging to determine the correct domain since many combinations may result in failure for the same flaw size (see the example below).

> ***Example:***
> A specific flaw size might fail when the pipeline material has a high toughness but also a high YS and low UTS. The opposite can be true as well, that same flaw might also fail under a low toughness and a low YS and low UTS.

In order to determine the boundaries for the uniform distribution the results of model 1 are further analyzed. The area of interest (girth weld with a pof of $10^{-}8$) is located in a domain of flaw sizes between 4.5mm and 6mm (see figure 6.2) therefore this domain is chosen for the uniform distribution during importance sampling. A consequence of using importance sampling on the flaw size is that the probability of failure curve can now only be calculated for that specific domain. When further analyzing the data that matches this flaw domain in model 1, the corresponding range of YS/UTS and 'm' values can be found. The minimum and maximum value found for YS/UTS and m are then used to define the uniform distribution.

Output

To produce the PoF Curve displayed below in figure 6.9 the input is generated from the importance sampled variables, in total 1,000,000 cycles are run in the MC which took over 10 hours of run time. By post processing the output (which are rejected flaw sizes) the PoF curve can be created just like in model 1, the PoF curves of model 1 and model 2 are both displayed in figure 6.9. In this figure it can be noticed that model 2 will produce results very much like model 1 would do when assuming the normal/rician distribution for the MAIF.

It might be to early to validate model 1 on basis of the results of model 2 since the comparison is on only one run that is based on limited data base, however the results look promising. Also on basis of the results of model 2 where the PoF curve seems to follow the Normal/Rician curve of model 1, it can be concluded that the Logistic distribution assumed for the MAIF in model 1 might be conservative and the Normal/Rician distribution should be used instead.

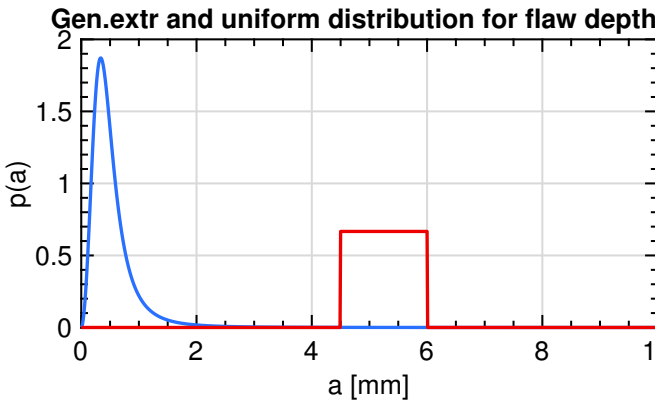

(a) Importance sampling by making use of a uniform distribution for the flaw size; domain 4.5mm-6mm

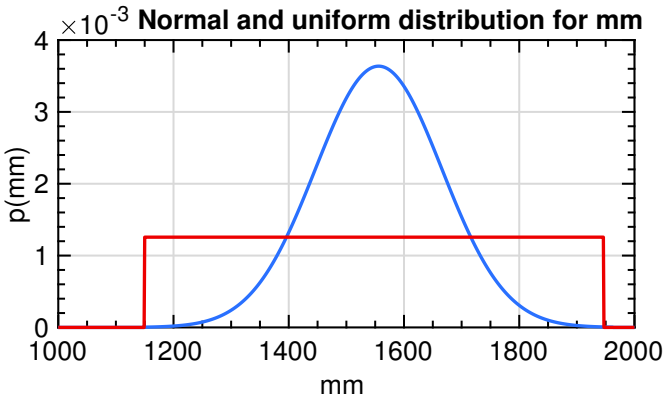

(b) Importance sampling by making use of a uniform distribution for the toughness variable 'm'; domain 1150-1946

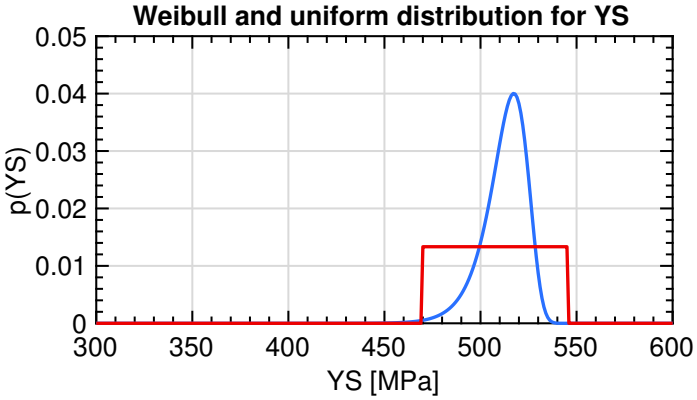

(c) Importance sampling by making use of a uniform distribution for the yield strength; domain 470MPa-545MPa

Figure 6.8: Importance sampling domains shown on the original distribution

Based on the PoF curve of model 2, the probabilistic NDT criterion is equal to 5.18mm which is 0.73mm larger than the deterministic criterion of 4.45mm.

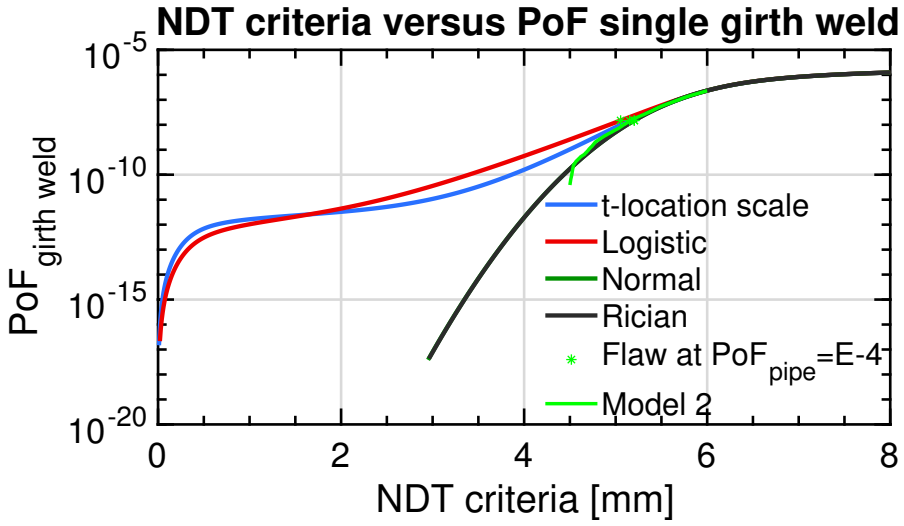

(a) The output of model 2 compared to the output of model 1

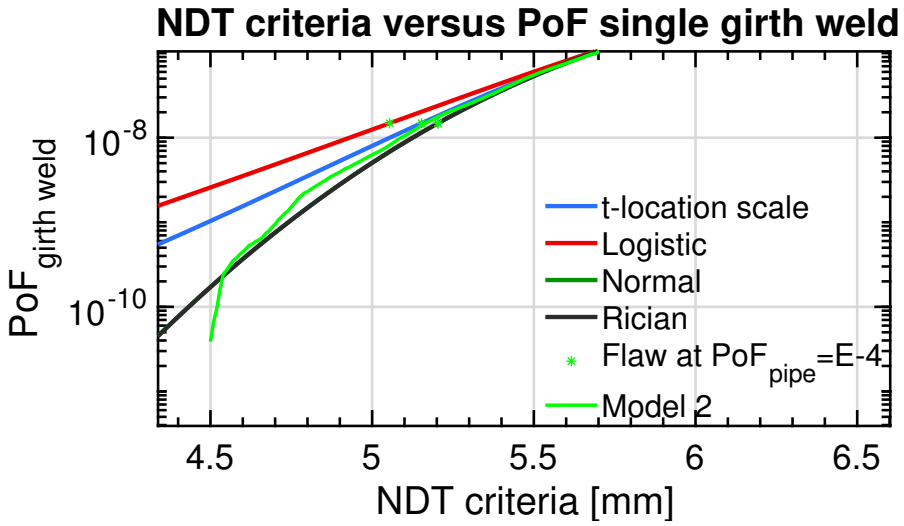

(b) Closeup of the failure curve produced by model 2 vs the failure curve of model 1

Figure 6.9: Failure curve model 2 vs failure curve model 1

6.5. Discussion of Results

The main goal of the research performed in this thesis was to develop a methodology that was able to use a reliability based computation process, in order to determine the NDT criterion of a girth weld by linking it to a required probability of failure of a complete pipe line .

The available input data for the probabilistic models is quite limited and makes it hard to determine the underlaying distribution of this data. Although literature does suggest some most probable fits, more data is needed to truly determine the real life processes of material properties and their mutual dependency. Currently the two models use a copula to provide the dependency between the material properties yield strength and ultimate tensile strength, while assuming the toughness is independent from both. The use of copula is unvalidated at this moment in time, and therefore future test should be performed to validate the use of copulas in order to expanding YS/UTS data.

Furthermore it is assumed the pipe line and its girth welds is an independent series system, with a possible flaw always located at the 12 o'clock (worst case) position while the

pipeline does not experience twist (changing the orientation of the flaw over time). These assumptions are conservative and made to simplify the model, adjusting the model to overcome these assumptions will provide a more realistic NDT criterion for a girth weld which most likely will be larger than currently computed.

Taking in to consideration the stated above the current output data of the probabilist models looks promising with respect to the output of the deterministic model. The probabilistic model 1 dictates a NDT criterion between 5.05mm-5.20mm in order to achieve a probability of failure of 10^{-4} for the complete pipeline, whilst the deterministic method dictates a NDT criterion of 4.45mm. The difference of .55mm-0.7mm in the NDT criterion is quite significant when speaking of flaw tolerances, and could benefit the welding process by relaxing NDT criteria and therefore possibly lowering unnecessary repairs of weld flaws or increasing the workability of weld equipment. The second model needs more optimization on the amount of cycles needed and the domain for importance sampling might be improved as well, however the preliminary results indicate the NDT criterion can be increased by 0.7mm. Also it seems model 2 produces a PoF curve which is closely resembles the PoF curve of model 1 when using the Normal/Rician distribution. This would imply the Logistic distribution used in the sensitivity analysis provides a conservative results.

6.5.1. Expert opinion on new NDT criterion

Since the results produced by both models follow from a mixed load case for which no in situ measurement data of the weld flaws encountered is present, an estimate on the impact of the increased NDT criteria by more than 0.5mm is provided by the experts of Heerema. In the figure below the effect of increasing the NDT criterion from 4mm to 4.5mm can be found for welds made in the tower of a vessel (see section 1.2). The increase of 0.5mm would result in three less girth welds in need of repair, this can safe up to 12 hours of repair time which is equal to one complete offshore shift, potentially saving up to hundred of thousands of Euros.

From the example above it can be concluded the increase in NDT criteria of up to 0.7mm predicted by both models can have a large impact on project durations and costs.

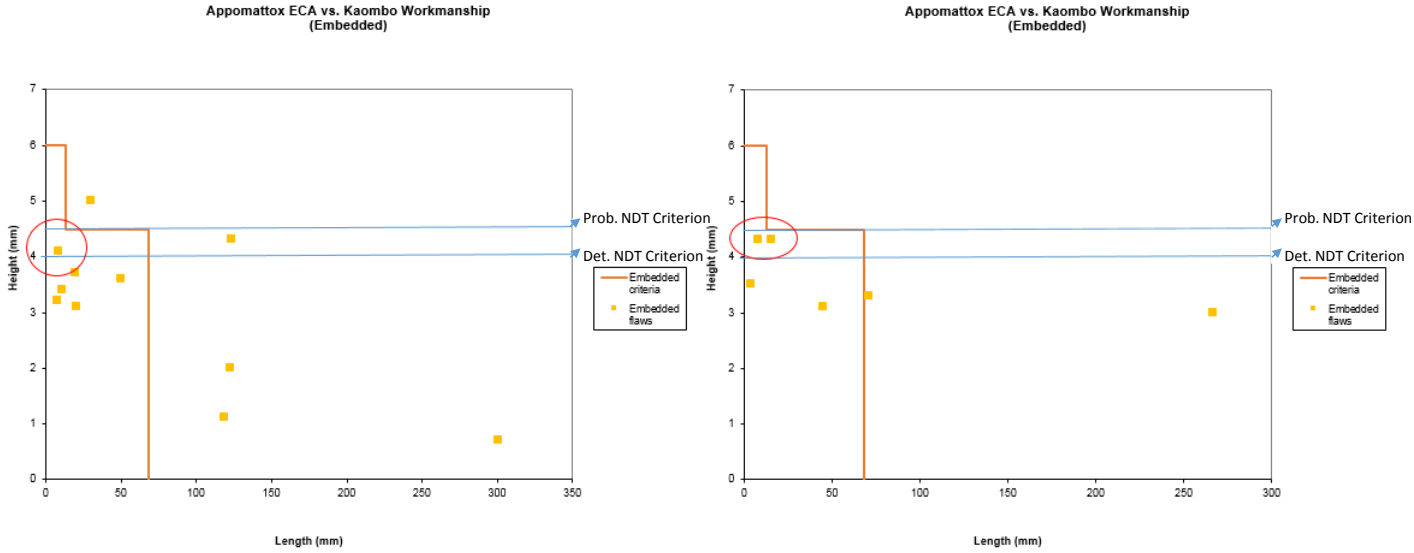

Figure 6.10: Increasing the NDT criterion by 0.5mm allows for three more flaws to be accepted

7

Conclusion and recommendations

In this chapter the final conclusions will be presented in section 7.1, in the conclusion the answers will be provided (when possible) to the research question and its support questions. The conclusion is followed by section 7.2 where recommendations on how to improve the models discussed in chapter 5 are given.

7.1. Conclusion

With pipe laying projects getting more challenging due to the increasing operational depths and more remote locations, the state-of-the art Engineering Critical Assessment methods for assessing flaws in girth weld remain manly unchanged. It is suspected that the results produced by the current ECA might be too conservative and causes too many rejected girth welds that need repairs. Sometimes criteria set by the ECA are so strict the weld equipment is not able to produce the required weld quality to guaranty the target life time to be achieved.

Therefore the main research question of this thesis was stated:

"How to determine the NDT criteria for flaws in girth welds based on a probabilistic analysis of the complete pipeline?"

An ECA consists out of a static and fatigue loading fracture mechanics , it was already found by Macia et al.,2009 and Wang et al., 2015 that the safety factor used for fatigue analysis of flaws can be substantially lowered from 5 to 1.23-1.5 (on project specific basic).

From analysis of the Ichthys project it was found 41% of total flaw growth took place in the first phase (installation) of the pipeline, where flaw growth is caused by the high strain resulting from spooling the pipe around a reel drum. Therefore also a less conservative methodology for assessing weld flaws during static ECA could benefit the first phase in the pipe laying process.

In order to create a less conservative static ECA methodology it was decided on using a level 3 reliability based computational method.In order to determine which variables should be used as stochastic input, a sensitive analysis was performed on the input of the ECA fracture mechanics formulas. From this sensitivity analysis it was found the main drivers for crack growth (and thus also the MAIF) are the yield strength, ultimate tensile strength and the toughness (JR-curve).

It was found that for both the yield strength and ultimate tensile strength the Weibull and respectively log-normal distribution where the best fit distributions. For the toughness it was decided on using a normal distribution. In order to expand the yield/ultimate tensile strength data to the required number of samples a Clayton copula was used, the expansions seems to be successful but needs conformation against more experimental data to prove reliable and fit to use for a probabilistic ECA analysis. The toughness is considered to be independent of the yield/ultimate tensile strength and random JR-curves between the upper and lower boundary can be generated.

The required probability of failure of a complete pipeline was determined to be 10^{-4} on basis of the governing offshore codes and previous research within HMC. This probability can be brought back to the individual (allowable) probability of failure of a single girth weld by (the conservative) assumption the pipeline is an independent series system. Assuming a typical reeling project consists out of three reel drums of 8 inch pipe, an average total of 6741 girth welds are produced. The allowable PoF of girth weld based on the data and assumptions above is then equal to 1.4835E-8. To increase the accuracy for the failure probability of a single girth weld more research has to be performed to their mutual dependency.

Two model have been developed in this research, the first model makes use of an iterative fracture mechanics solver that provides the Maximum Allowable Initial Flaw size as output. By solving the limit state function of this model and correcting it with the probability actually having a flaw in the girth weld the probability of failure of a girth weld versus NDT criterion could be calculated. The first model developed in this research provides good insight on the effect of the flaw distribution and MAIF distribution on the PoF of a single girth weld. Although the accuracy of the results can be doubted since the reliability of the input distributions is not to high, the model shows the NDT criteria can be set to 5mm-5.2mm in order to achieve the required PoF of the pipeline of 10^{-4}. The deterministic approach resulted in NDT criteria of 4.45mm, a difference of ~0.6mm-0.75mm with respect to the probabilistic approach.

The second model proposed in this research uses a different approach in order to determine the PoF of a girth weld. Instead of iterating to the MAIF model 2 will directly simulate the flaw size in a girth weld and calculates if tearing of the flaw will be stable and within limits. By canceling out the need of fitting/assuming a distribution of the MAIF this method possibly provides more accurate results, and can also be used in order to validate model 1. When comparing the PoF curves model 2 to model 1 it can be seen the Normal/Rician distribution is the most likely fit for the MAIF when using model 1, since the PoF curves of both model 1 and 2 are close to the same. This forms a strong indicator model 1 can be used to determine the PoF of a girth weld. Model 1 might be preferred over model 2 due to the better computational speed and the possibility of changing the flaw size curve after the model has run for fine tuning.

From the research done in this thesis it may be concluded the current ECA methodology for static loading on flaws in girth weld might indeed be conservative and a probabilistic approach is possible. The two models proposed in this thesis show a probabilistic analysis can be used in order to overcome conservatism in the current ECA methodology. Together with the earlier research conducted on the fatigue loading ECA by Marcia et al. that states the current safety factor in use for fatigue ECA is too high, it is expected the NDT criteria can be increased while complying to the safety requirements from within the industry. This can result in faster welding or less repairs of girth welds in pipeline.

7.2. Recommendations

This section will provide the recommendations to further improve the application of a probabilistic model for ECA.

1. **Collect and improve data:** In order to improve the reliability of the distributions chosen for the yield strength, ultimate tensile strength and especially the toughness, more data should be collected during test/project of these variables. Especially for the toughness more test data is required to determine the type of distribution of the variables used to construct the JR-Curve.

2. **Include the remaining cycles and phases of ECA:**The current methodology is focused on the first cycle of phase one, to confirm the feasibility of using a probabilistic approach it is advised to include the other cycles and phases in the model. Also the uncertainty of detection and measurement of a flaw by the AUT equipment should be modeled. Furthermore the required PoF of a pipeline should be investigated, at this moment the probability of failure of a complete pipeline is taken for the first reeling cycle only.

3. **Expand the probabilistic computational method by including both pipe twist,flaw location and reel layer:** The current methodology is focused on the probabilistic aspects of the input variables, however also other non material influences like pipe twist and flaw location (which in the current model is assumed to always be at the extrados) will influence the PoF of a girth weld.

4. **Verify the use of copula:** A copula is used to expand and correlate yield and ultimate tensile strength data. The use of a copula should be verified in order to increase the reliability of the model.

5. **Improve model 2:** Model two might be more suitable in further implementation of the probabilistic approach for ECA due to its (potential) faster computational speed, however to achieve these potential faster speeds the domains and the total amount of samples for importance sampling (or an other form of MC optimization) should be further optimized.

6. **Expand reliability calculation method:** Instead of determining the NDT criteria solely based on the ULS of the pipeline, the probabilistic method could be expanded towards a level 4 analysis (see chapter 4) where risk and cost of failure of the pipeline are taken in to consideration as well in order to determine the NDT criteria. Therefore it is advised to expand/develop the probabilistic model including an economic analysis of pipe laying projects to base the allowable PoF of a girth weld on.

A

Failure assessment curves

This appendix will highlight the mathematics behind the failure assessment curves.

A.1. Level 1-Failure assessment curve

$$f(L_r) = (1 + \frac{1}{2}L_r^2)^{-\frac{1}{2}}[0.3 + 0.7e^{-\mu L_r^6}] \quad for \quad L_r \leq 1 \tag{A.1}$$

$$f(L_r) = f(1)L_r^{(N-1)/(2N)} \quad for \quad 1 < L_r < L_{r,max} \tag{A.2}$$

$$f(L_r) = 0 \quad for \quad L_r > L_{r,max} \tag{A.3}$$

$$\mu = min(0.001\frac{E}{\sigma_Y}, 0.6) \tag{A.4}$$

$$N = 0.3(1 - \frac{\sigma_Y}{\sigma u}) \tag{A.5}$$

Where the parameters other than K_r and L_r are defined as:

$$E = Young's \quad modulus$$
$$\sigma_Y = Yield \quad strength$$
$$\sigma_u = Ultimate \quad tensile \quad strength$$

Note: This FAC is for materials that do not exhibit yield discontinuous yielding/Lüders plateau. If a material does show this behavior an adjusted set of FAC formula must be used. This set can be found in chapter 7 of the BS7910:2013 code [8]

A.2. Level 2-Failure assessment curve

$$F(L_r) = \left(\frac{E\epsilon_{ref}}{L_r\sigma_Y} + \frac{L_r^3\sigma_Y}{2E\epsilon_{ref}}\right)^{-1/2} \quad \text{(A.6)}$$

and

$$f(L_r) = 0 \quad for \quad L_r > L_{r,max} \quad \text{(A.7)}$$

ϵ_{ref} is the true strain at the true stress level, and can be obtained from the stress-strain data by looking up the matching σ_{ref} value.

$$\sigma_{ref} = L_r * \sigma_Y \quad \text{(A.8)}$$

Note that the FAC should minimally be evaluated at L_r=0.7,0.9,0.98,1.0,1.02 and 1.1 and then at a sufficient number of points to define the curve up to $L_{r,max}$

A.3. Level 3-Failure assessment curve

$$f(L_r = \sqrt{\frac{J_e}{J}} \quad for \quad L_r < L_{r,max} \quad \text{(A.9)}$$

$$f(L_r) = 0 \quad for \quad L_r > L_{r,max} \quad \text{(A.10)}$$

Where:

J_e: is the value from the J-integral from the elastic analysis at the load corresponding to the the Value L_r
J: is the value from the J-integral from the elastic-plastic analysis at the load corresponding to the value L_r

A.4. Flaw assessment point

$$K_r = \frac{K_I}{K_{mat}} \quad \text{(A.11)}$$

$$L_r = \frac{\sigma_{ref}}{\sigma_Y} \quad \text{(A.12)}$$

The value of K_r can be obtained through the following formula:

$$K_{mat} = \sqrt{\frac{EJ_{mat}}{1-v^2}} \quad \text{(A.13)}$$

where v is the Poisson ratio and J_{mat} is the fracture thoroughness of the material.

When the Crack Tip Opening Displacement is given as the indicator of thoughness the following formula should be used:

$$K_{mat} = \sqrt{\frac{m\sigma_Y\delta_{mat}E}{1-v^2}} \quad \text{(A.14)}$$

where:

σY is the 0.2% proof or yield strength of the material for which the CTOD has been determined.
δ_{mat} is fracture toughness in terms of CTOD
m is a coefficient given for steels by the formula A.15

$$m = 1.517(\frac{\sigma_y}{\sigma_U})^{-0.3188} \quad for \quad 0.3 < \frac{\sigma_y}{\sigma_U} < 0.98 \tag{A.15}$$

The stress intensity factor K_I can be calculated with the following formula:

$$K_I = (Y * \sigma)\sqrt{\pi a} \tag{A.16}$$

$$Y\sigma = (Y\sigma)_p + (Y\sigma)_s \tag{A.17}$$

where:
$(Y\sigma)_p$ is the contribution of the primary stresses
$(Y\sigma)_s$ is the contribution of the secondary stress

A.5. Fatigue assessment

$$\frac{da}{dN} = A(\Delta K)^m \tag{A.18}$$

Where:
A is a constant that depends on material and the applied conditions, including environment and cyclic frequency.
m is a constant that depends on material and the applied conditions, including environment and cyclic frequency.

Recommendations for A and m can be found section 8 of BS7910:2013 ([8])
For $\Delta K < \Delta K_0$, da/dN is assumed to be 0.

B

Sensitivity analysis

This appendix shows the sensitivity of various input parameters of the ECA on the failure assessment locus. The sensitivity analysis is performed with an early version of the fracture mechanics model in Matlab, conclusions on the sensitivity of each parameter will not change although the exact value Kr and Lr may be different due minor bugs which later have been corrected in the model. It was decided not to rebuild the sensitivity analysis on the last version of the Matlab model because during the research it turned out clear indeed the most sensitive parameters were found and used.

Flaw length a

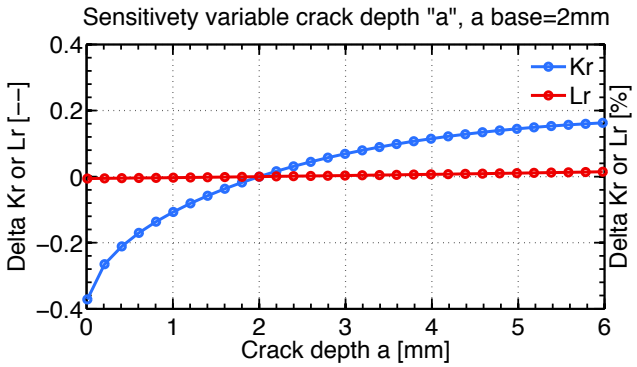

(a) On the horizontal axis the changing variable 'a', Vertical axis the changing value of Kr/Lr with respect to the base value at a=2mm

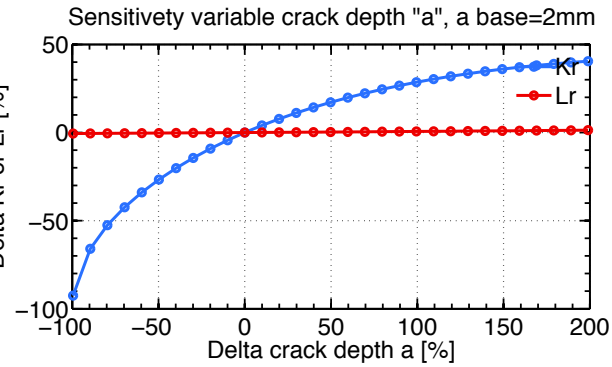

(b) On the horizontal axis the changing variable 'a' expressed in percentual change from base value; Vertical axis the changing value in percentage of Kr/Lr with respect to the base value at a=2mm

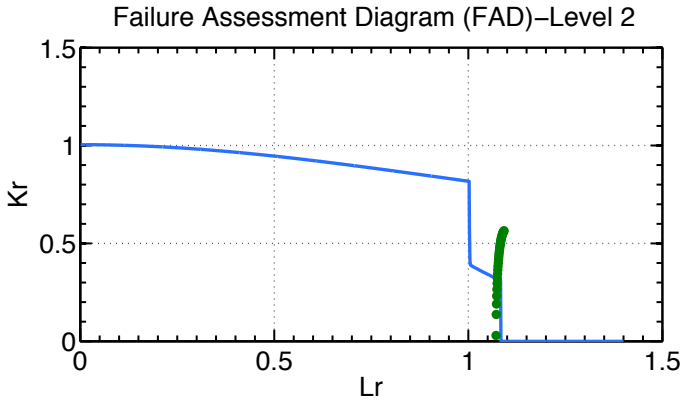

(c) Impact of changing the variable 'a' on the assessment curve (green line)

Figure B.1: Sensitivity analysis of input variable 'a'

Flaw width c

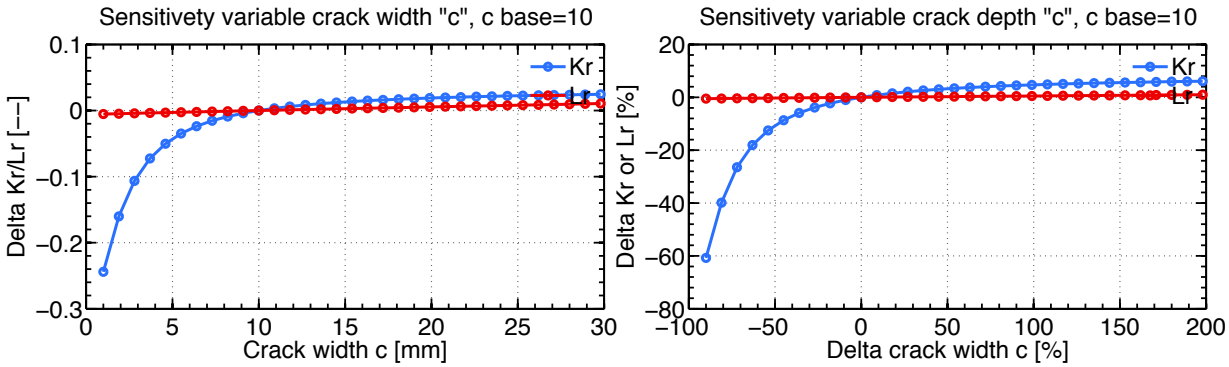

(a) On the horizontal axis the changing variable 'c', Vertical axis the changing value of Kr/Lr with respect to the base value at c=10mm

(b) On the horizontal axis the changing variable 'c' expressed in percentual change from base value; Vertical axis the changing value in percentage of Kr/Lr with respect to the base value at a=2mm

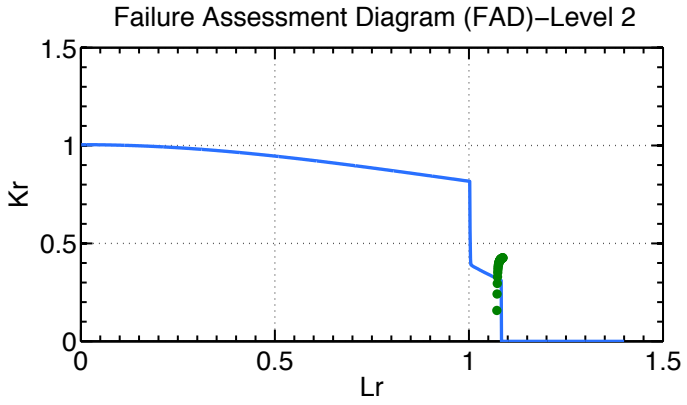

(c) Impact of changing the variable 'c' on the assessment curve (green line)

Figure B.2: Sensitivity analysis of input variable 'c'

Pipe thickness t

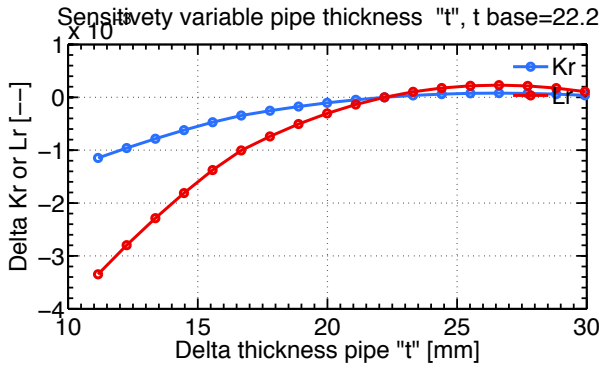

(a) On the horizontal axis the changing variable 't', Vertical axis the changing value of Kr/Lr with respect to the base value at t=22.2mm

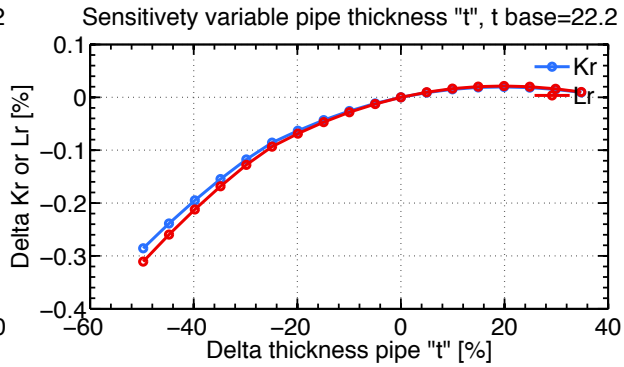

(b) On the horizontal axis the changing variable 't' expressed in percentual change from base value; Vertical axis the changing value in percentage of Kr/Lr with respect to the base value at t=22.2mm

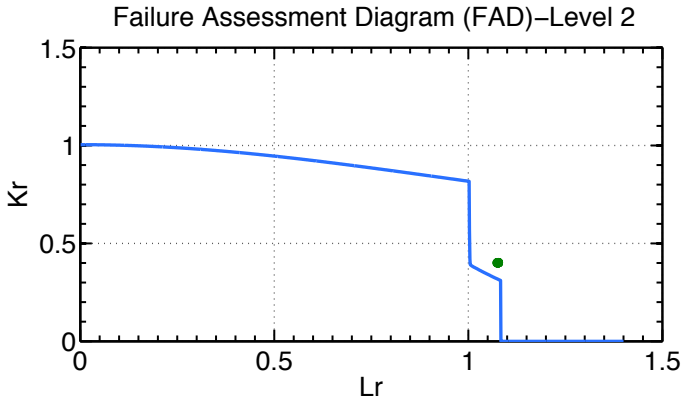

(c) Impact of changing the variable 't' on the assessment curve (green line)

Figure B.3: Sensitivity analysis of input variable 't'

Pipe outer diameter D_{outer}

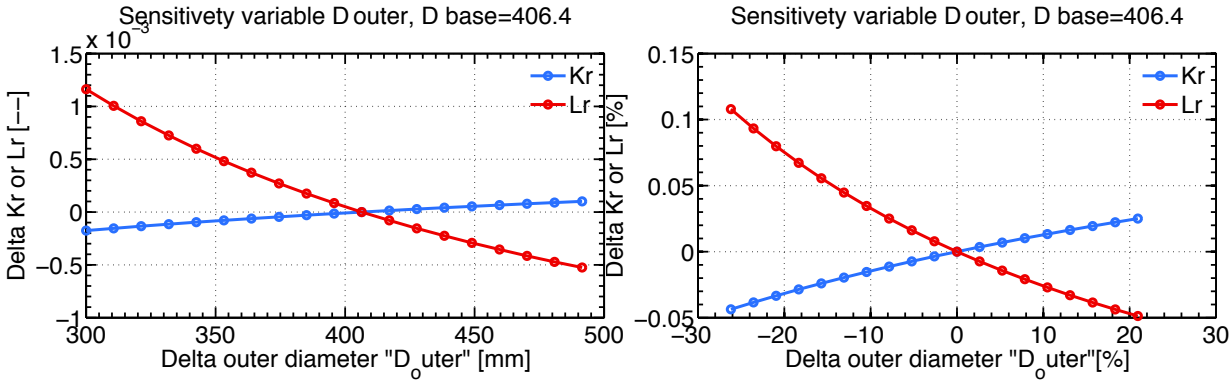

(a) On the horizontal axis the changing variable 'D_{outer}', Vertical axis the changing value of Kr/Lr with respect to the base value at D_{outer}=406.4mm

(b) On the horizontal axis the changing variable 'D_{outer}' expressed in percentual change from base value; Vertical axis the changing value in percentage of Kr/Lr with respect to the base value at D_{outer}=406.4mm

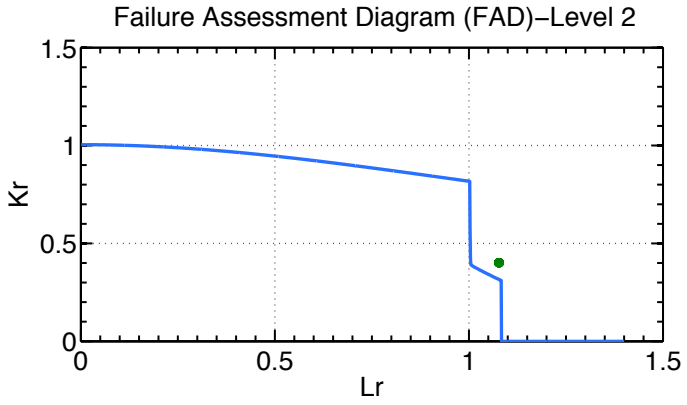

(c) Impact of changing the variable 'D_{outer}' on the assessment curve (green line)

Figure B.4: Sensitivity analysis of input variable D_{outer}'

Mismatch Hi/lo of weld cap

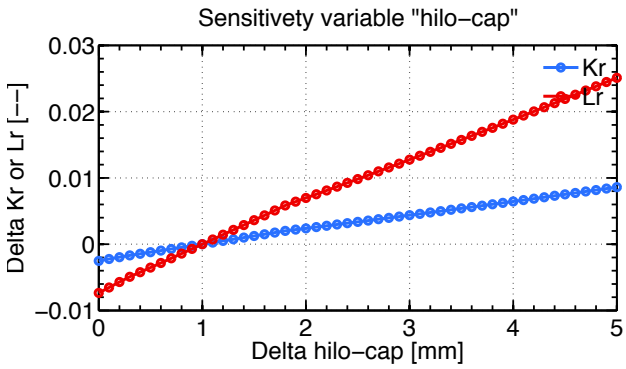

(a) On the horizontal axis the changing variable 'hilo', Vertical axis the changing value of Kr/Lr with respect to the base value at hilo=2mm

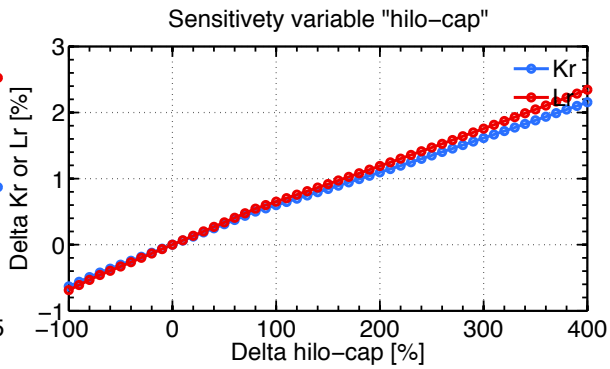

(b) On the horizontal axis the changing variable 'hilo' expressed in percentual change from base value; Vertical axis the changing value in percentage of Kr/Lr with respect to the base value at hilo=2mm

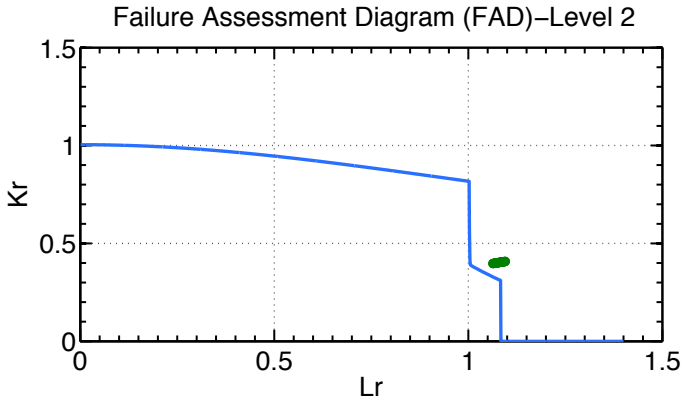

(c) Impact of changing the variable 'hilo' on the assessment curve (green line)

Figure B.5: Sensitivity analysis of input variable 'hilo'

Mismatch Hi/lo of weld root

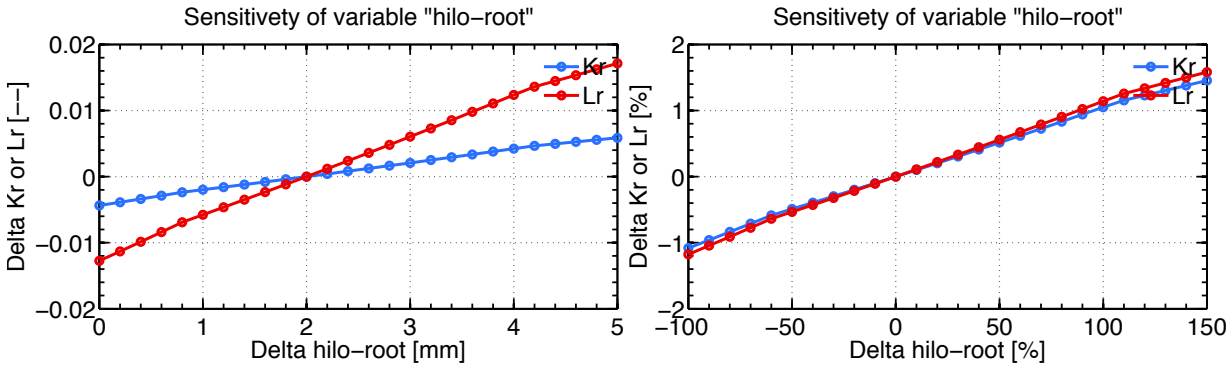

(a) On the horizontal axis the changing variable 'hilo', Vertical axis the changing value of Kr/Lr with respect to the base value at hilo=1mm

(b) On the horizontal axis the changing variable 'hilo' expressed in percentual change from base value; Vertical axis the changing value in percentage of Kr/Lr with respect to the base value at hilo=1mm

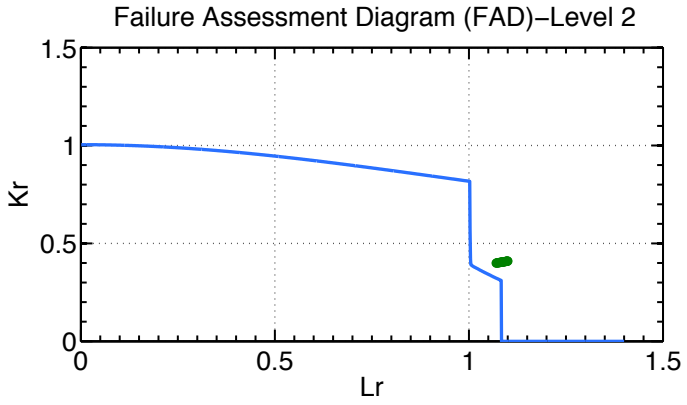

(c) Impact of changing the variable 'hilo' on the assessment curve (green line)

Figure B.6: Sensitivity analysis of input variable 'hilo'

Flaw angle theta

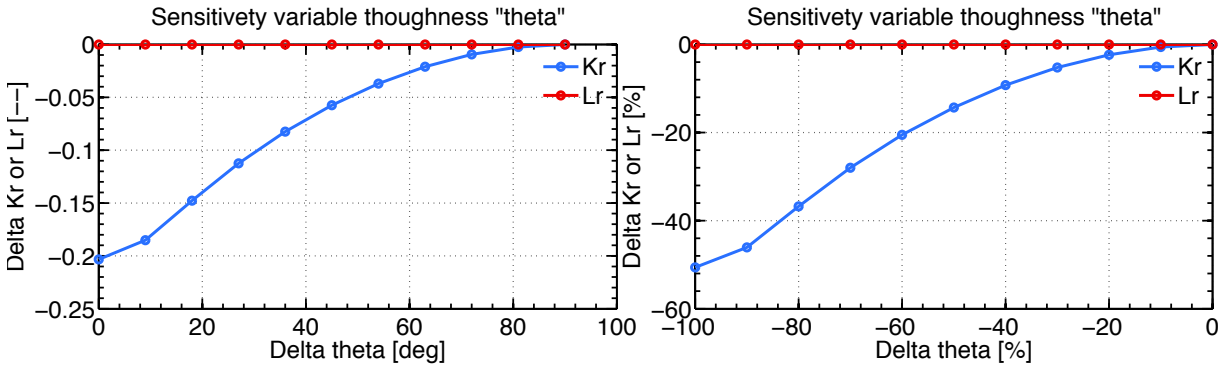

(a) On the horizontal axis the changing variable 'theta', Vertical axis the changing value of Kr/Lr with respect to the base value at theta=90 deg

(b) On the horizontal axis the changing variable 'theta' expressed in percentual change from base value; Vertical axis the changing value in percentage of Kr/Lr with respect to the base value at theta=90 deg

Figure B.7: Sensitivity analysis of input variable 'hilo'

C

Ramberg-Osgood relationship

This appendix contains the formulas of the Ramberg-Osgood method as provided in [5].

C.1. Input

The inputs of the Ramberg-Osgood method are as follows:

- Strain at yield strength ϵ_y
- Strain at Ultimate tensile strength ϵ_u
- Lüder plateau length ϵ_{lud} (only when strain hardening happens)
- True Yield strength f_y
- True Ultimate tensile strength f_u
- Young's modulus E

Where:

$$\epsilon_y = \frac{f_y}{E} \tag{C.1}$$

When a Lüder plateau is present ϵ_y=ϵ_{lud}, if the Lüder plateau is not modeled ϵ_y=0.5% is used in the formulas below.

C.2. Ramberg-Osgood relation

This section will mention how to construct a stress-strain diagram for a material without a Lüder plateau (after strain hardening) and a material with a Lüder plateau.

C.2.1. Stress-strain diagram with no Lüder plateau

$$\epsilon_{true} = \frac{\sigma_{true}}{E} + \alpha * \frac{f_y}{E} * (\frac{\sigma_{true}}{f_y})^n$$

$$where: \quad \sigma_{true} = True\ stress\ and\ running\ variable\ on\ x-axis\ of\ stress\ strain\ diagram \quad \epsilon_{true} = True\ strain\ and\ on\ y-axis\ of\ stress\ strain\ diagram \tag{C.2}$$

The formula above (formula C.2) can be directly used to construct the stress-strain diagram when no Lüder plateau is present.

C.2.2. Stress-strain diagram with Lüder plateau

When there is a plateau present the construction of the stress-strain diagram is split up in three domains:

- The elastic region where $\sigma_{true} \leq f_{true}$
- The Lüder plateau $\frac{f_y}{E} < \epsilon_{true} \leq \epsilon_{lud}$
- Non linear region where $\epsilon_{true} > \epsilon_{lud}$

And with respect to each domain the following formulas apply:

$$\epsilon_{true} = \frac{\sigma_{true}}{E} \tag{C.3}$$

$$\epsilon_{true} = \frac{f_y}{E} \tag{C.4}$$

$$\epsilon_{true} = \frac{\sigma_{true}}{E} + \alpha * \frac{f_y}{E} * (\frac{\sigma_{true}}{f_y})^n \tag{C.5}$$

D

Copulas

The Clayton copula is used in order to provide the correlation between the yield strength and ultimate tensile strength. The clayton copula formula:

$$C(u,v) = max([u^{-\alpha} + v^{-\alpha} - 1]^{-\frac{1}{\alpha}}, 0) \quad \alpha = \frac{2\tau}{1-\tau} \tag{D.1}$$

Where τ is Kendall's tau, defining the rank correlation between data.

Further more it can be seen that due to high correlation the student-t and Gaussian are the same.

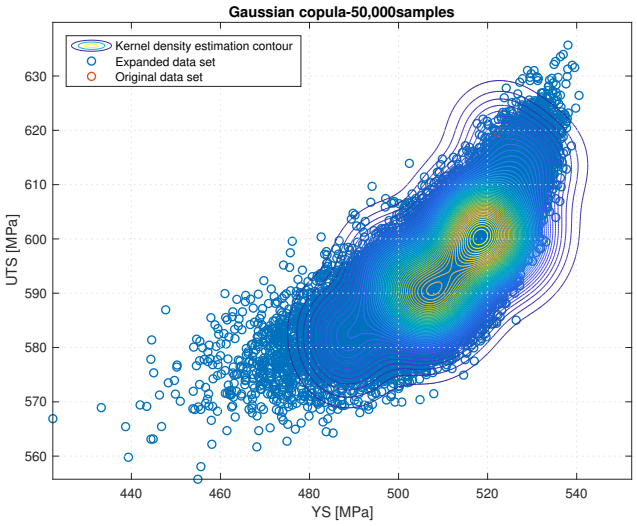

(a) Expanded data set by using a Guassian copula

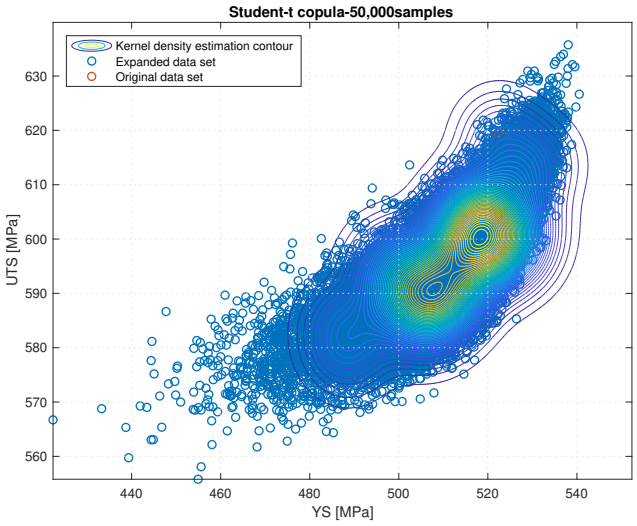

(b) Expanded data set by using a Student-t copula

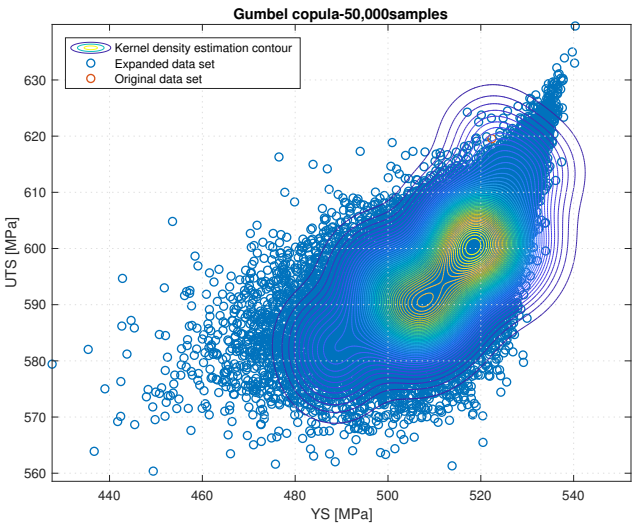

(c) Expanded data set by using a Gumbel copula

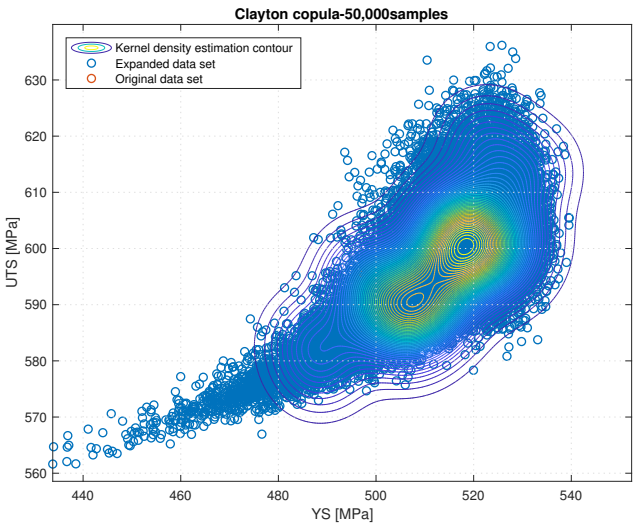

(d) Expanded data set by using a Clayton copula

Figure D.1: Different copulas used to expand the YS/UTS dataset

Bibliography

[1] Probabilistic ECA approach to fatigue - Heerema Marine Contractors-MSc thesis assignment.

[2] The World of Heerema - Session 4.

[3] DEV80074 -Reeling Knowledge Development ECA Guideline. page 84, 2011.

[4] DET NORSKE VERITAS Report HMC Guideline for Reeling Pipeline Installation Heerema Marine Contractors Nederland BV. 2012.

[5] Olav Aamlid. DET NORSKE VERITAS Report HMC Guideline for Reeling Pipeline Installation Heerema Marine Contractors Nederland BV. 2012.

[6] DNV GL As. DNVGL-RP-F108 Assessment of flaws in pipeline and riser girth welds. 2017.

[7] DNV GL As. DNVGL-ST-F101 Submarine pipeline systems. 2017.

[8] BSI — British Standards Institution. BS7910 Guide to methods for assessing the acceptability of flaws in metallic structures, 2013.

[9] Andrew Cosham and Atkins Boreas. ECAs Are they fit-for-purpose? *OPT 2008*, 2008.

[10] F. L.M. Diermanse, K. M. De Bruijn, J. V.L. Beckers, and N. L. Kramer. Importance sampling for efficient modelling of hydraulic loads in the Rhine–Meuse delta. *Stochastic Environmental Research and Risk Assessment*, 2014. ISSN 14363259. doi: 10.1007/s00477-014-0921-4.

[11] HMC. Weld-data-balder, .

[12] HMC. Welding database 1.1, .

[13] HMC. ECA_results_6_8_inch, 2014.

[14] S.N. Jonkman, R.D.J.M Steenberg, O. Morales-Nápoles, A.C.W.M. Vrouwenvelder, and J.K. Vrijling. *Probabilistic design: Risk and Reliability analysis in civil engineering*. Department of Hydraulic Engineering, Delft, third, november 2016 edition, 2016.

[15] Robert E Kass and Adrian E Raftery. Bayes Factors. *Source Journal of the American Statistical Association*, 9059124(430):773–795, 1995. URL `http://www.jstor.org/stable/2291091http://about.jstor.org/terms`.

[16] Roger T Kilgore and David B Thompson. Estimating Joint Flow Probabilities at Stream Confluences by Using Copulas. *Transportation Research Record: Journal of the Transportation Research Board*, 2262:200–206, 2011. doi: 10.3141/2262-20.

[17] Mario L Macia, Jaime Buitrago, Wan Kan, Barron Bichon, Jonathan Moody, and Stephen Hudak. RELIABILITY OF FRACTURE MECAHNICS APPROACH TO FATIGUE. 2009.

[18] McDermott Australia Pty. Ltd. and Heerema Marine Contractors Australia Pty. Ltd. INPEX Operations Australia Pty Ltd-Ichthys Gas Field Development-HMC-Flowlines Installation 6 & 8 inch-ECA. 2014.

[19] Det Norske Veritas. DNV-OS-F101 Submarine Pipeline Systems. 2013.

[20] Bruce Ratner. The correlation coefficient: Its values range between 1/1, or do they. *Journal of Targeting, Measurement and Analysis for Marketing*, 2009. ISSN 09673237. doi: 10.1057/jt.2009.5.

[21] Thorsten Schmidt. Coping with Copulas. 2006. URL http://citeseerx.ist.psu.edu/viewdoc/download?doi=10.1.1.139.888&rep=rep1&type=pdf.

[22] B W Silverman. DENSITY ESTIMATION FOR STATISTICS AND DATA ANALYSIS.

[23] Stefanie Scheid. Introduction to Kernel Smoothing Wilcoxon score, 2004. URL http://compdiag.molgen.mpg.de/docs/talk_05_01_04_stefanie.pdf.

[24] Xiangyu Wang, Guillaume Penel, Sean Swearingen, Robert Aune, Wan Kan, and Lang Fu. Reliability-Based Fracture Mechanics Approach to Fatigue Design of Julia Flowline.

[25] Brian S. Yandell, M. P. Wand, and M. C. Jones. Kernel Smoothing. *Technometrics*, 1996. ISSN 00401706. doi: 10.2307/1268906.

List of Figures

1.1 J-lay and Reel lay method in a simplified figure 5

1.2 J-Lay system on board of a vessel [2] 5

1.3 Reel lay system on board of a vessel[2] 5

1.4 Left: Detail of the bevel on two pipe ends[2]; Right: Pipe ends welded together with a mismatch (Hi/Lo present) [2] 6

1.5 Welding system [2] 7

1.6 Different types of weld flaws[8] 7

1.7 Flaw categories and definition 8

1.8 Loading on pipeline and failure scenarios 10

2.1 Clarification of loading on the pipeline and the critical loading positions 15

2.2 ECA calculations of the Ichthys 8” pipeline [13] 17

2.3 Work flow of research and model development 18

3.1 The ECA protocol as used today,[Source:Liza Lecarme, HMC] 19

3.2 ECA and the main dependent variables 20

3.3 Overview of the phases in ECA in a typical Reel lay project 21

3.4 Flow diagram of a typical ECA process [3] 22

3.5 Two stress-strain curves produced with Ramber-Osgood method 23

3.6 Neuber’s approach applied to obtain Pb 24

3.7 Clarification of assessing flaws using the FAD 26

3.8 J-R curve, on the x-axis increasing flaw depth and on thy y-axis the toughness 28

3.9 Locus on the FAD of a flaw starting at an initial flaw size of 4mmx25mm, and reaching a stable flaw size of 4.5mmx25mm 29

3.10 Paris law [8] 30

3.11 Graphical overview of the fracture mechanics fatigue approach, figure found in [17], also defining the safety factor as the ratio of design life over planned life. . 30

3.12 S-N Curve with quality categories [8] 31

3.13 Overview of the S-N approach 32

3.14 General definition of the safety factor, as the ratio between the design resistance (Rd) and design load (Sd), figure from [14] 33

4.1 SN-curve method as described in [17] 38

4.2 FM-Method as described in [17] 39

4.3 Reliability matching as described in [17] 40

5.1 Graphical overview on where in the ECA a probabilistic approach is applied . 44

5.2 Complete functionality of model 1 45

5.3 Complete functionality of model 2 45

5.4 Flow chart of the iteration process to calculate the MAIF and corresponding PoF 47

5.5 Amount of cycles on the x-axis vs NDT required on the y-axis 48

5.6 Best fit on the MAIF after 20,000 cycles 49

5.7 The separate resistance (MAIF) and load (flaw size) curves 49

5.8 Resistance and load curve and the corresponding failure area 50

5.9 Flow chart of the process to calculate maximum allowable initial flaw size and PoF 52

5.10 Left hand side of the figure graphs are presented with the actual change in size, where on the right hand side the percentual change is presented for a better comparison between the variables 56

5.11 Effect of lowering the UTS on Lr_{max} and the probability of the locus intersecting the FAC (thus providing a safe weld) 56

5.12 Distribution of the yield strength 58

5.13 Probability density function of the yield strength 59

5.14 Distribution o the ultimate tensile strength 59

5.15 Probability density function of the yield strength 60

5.16 lower,mean and upper bound JR curves 60

5.17 Linear fit and construction of new JR curves 61

5.18 Scatter plot of the measured YS and UTS point of a 8” pipeline, the linear function is the least squares linear estimator 62

5.19 From original uniform data set to expanded uniform data set by making use of the Clayton copula 63

5.20 Expanded YS and UTS data by making use of the Clayton copula (blue), orange represents the measure data set 64

5.21 Construction of a PDF using kernel density estimation with a Gaussian kernel (figure from [23]) 65

5.23 Correlation coefficient dependency on sample size and random number generator 67

5.24 Generalized Extreme Value distribution fit on the flaw sizes found in girth welds 68

5.25 Table of governing parameters in fracture mechanics calculations, no concerning difference between the model and Crackwise software is found 69

5.26 The pipeline considered as a series system; Top figure showing an unbroken system, bottom figure showing a broken system at the girth weld between pipe 1 and pipe 2. 70

5.27 Failure space of a series system, for each element in the series system the resistance (R) should be larger than the load (S) in order not to fail[14] 70

5.28 Upper(mutually exclusive) and lower(Dependent) boundary of failure of a series system [14] 70

5.29 Classification of limit states according to [7] 71

5.30 Industry standard classification for several limit states and consequence classes[19] 72

6.1 Criteria for an embedded flaw to be considered as an external surface flaw . . . 77

6.2 Probability of failure curves vs. NDT of a single girth weld 80

6.3 PDFs of the MAIF (left figure), and a close up of the density in the tail (right figure) 81

6.4 Similar results for the MAIF using the Clayton or Gumbel copula 82

6.5 Weibull distribution and normal distribution fit on the yield strength data . . . 83

6.6 Uniform distribution and normal distribution used to draw variable 'm' used for constructing the JR-curve 83

6.7 Sensitivity of the probability of failure curve vs. MAIF of a single girth weld, each MAIF distribution represented by a Logistic distribution 84

6.8 Importance sampling domains shown on the original distribution 86

6.9 Failure curve model 2 vs failure curve model 1 87

6.10 Increasing the NDT criterion by 0.5mm allows for three more flaws to be accepted 88

B.1 Sensitivity analysis of input variable 'a' 98

B.2 Sensitivity analysis of input variable 'c' 99

B.3 Sensitivity analysis of input variable 't' 100

B.4 Sensitivity analysis of input variable D_{outer}' 101

B.5 Sensitivity analysis of input variable 'hilo' 102

B.6 Sensitivity analysis of input variable 'hilo' 103

B.7 Sensitivity analysis of input variable 'hilo' 104

D.1 Different copulas used to expand the YS/UTS dataset 108

List of Tables

2.1 Reel dimensions on the Aegir (R-lay vessel of HMC) 16

5.1 Domains of N and the step size within the domain 48
5.2 Interpretation of difference in BIC score between two distributions 57
5.3 Big scores of the top four distributions tried 58
5.4 BIC scores of the top four distributions tried 59
5.5 Values 'm' and 'x' of the JR curves in figure 5.16 60
5.6 Data analysis of 100,000,000 data points generated by Clayton copula 66
5.7 y/t ratio of original and expanded data set 66
5.8 Input for validation of the model 68

6.1 Z factor depending on number of measurements n provided by [19] 76
6.2 Mean and standard deviation yield strength 76
6.3 Deterministic input for ECA 76
6.4 FAD of the deterministic case 76
6.5 Weld flaw data of quad station 77
6.6 Weld flaw data of hex station 77
6.7 Weld flaw data of tower station 77
6.8 Weld flaw data over all welding stations 78
6.9 Required NDT to achieve $PoF_{pipeline} = 10^{-4}$ 81
6.10 Required MAIF to achieve $PoF_{pipeline} = 10^{-4}$ 84